Fundamental Understanding of Sodium Citrate in Bitumen Liberation

By

Bailin Xiang

A thesis submitted in partial fulfillment of the requirements for the degree of

Doctor of Philosophy

In

Chemical Engineering

Department of Chemical and Materials Engineering

University of Alberta

Abstract

In the traditional water-based extraction process, sodium hydroxide (NaOH) is a commonly used chemical aid to improve bitumen recovery from oil sands. Recently, sodium citrate (Na_3Cit) was applied as a secondary process aid together with NaOH by Syncrude Canada Ltd. in the water-based extraction process. The combined addition of Na_3Cit and NaOH was found significantly enhanced bitumen recovery compared to applying NaOH individually. The underlying mechanism of such enhancement remains to be further understood. As one of the essential steps in the water-based extraction process, bitumen liberation is believed to be influenced by the addition of Na_3Cit, thereby contributed to the enhanced bitumen recovery. In this thesis, the roles of Na_3Cit in the bitumen liberation and its effect on solid wettability alternation were investigated. Theoretical models were applied to describe the bitumen recession process in the presence of Na_3Cit and calcium ions (Ca^{2+}) in alkaline solutions.

In contrast to the visualization techniques used in the previous research, bitumen liberation was quantified for the first time using a quartz crystal microbalance with dissipation (QCM-D). Bitumen was spin-coated on the silica sensors to simulate the oil sands and then exposed to aqueous solution for bitumen liberation. The effects of various operation conditions (such as solid wettability, solution pH, and temperature) on bitumen liberation were analyzed by QCM-D, which proved the feasibility of studying bitumen liberation

through QCM-D. The synergetic effect of Na_3Cit and NaOH on the bitumen liberation process was investigated using QCM-D in the presence of Na_3Cit and NaOH, respectively and in combination. The highest degree of bitumen liberation (DBL) was observed with the combined addition of Na_3Cit and NaOH.

Bitumen recession from quartz surfaces was studied in the presence and absence of Ca^{2+} and Na_3Cit. The dynamic displacements of bitumen from quartz surfaces were recorded by the video camera and analyzed by hydrodynamic and molecular kinetic models. At pH 8.5 and 45 ºC, the addition of Ca^{2+} slowed down the three-phase contact line (TPCL) movement. Model fittings suggested that the viscous resistance and contact line friction increased in the presence of Ca^{2+}. In contrast, the presence of Na_3Cit accelerated the bitumen displacement rate and generated smaller static water contact angles on the quartz surfaces. Both viscous resistance and contact line friction decreased with increasing the concentration of Na_3Cit.

The effect of Na_3Cit on solid wettability alternation was investigated through QCM-D and contact angle measurements. The alumina sensors were applied to simulate the alumina components contained in clay minerals from oil sands. It was found that adsorption of naphthenic acids (nature surfactants from bitumen) on alumina surfaces induced an increase of surface hydrophobicity. However, the addition of Na_3Cit prevented the adsorption of naphthenic acids in both cases with and without Ca^{2+}. Therefore, the alumina surfaces remained hydrophilic in the presence of Na_3Cit.

The benefits of Na_3Cit in the bitumen liberation process and the solid wettability were attributed to its ability to modify the interfacial properties, including zeta potential and interfacial tension in this complex system. Increased negative charges were observed not only on bitumen surfaces but also on silica and alumina surfaces in the presence of Na_3Cit under alkaline conditions, which led to stronger repulsions between bitumen and those solids. Moreover, adding Na_3Cit decreased the adhesive force between bitumen and silica, as indicated by atomic force microscope measurement. On the other hand, the bitumen-water interfacial tension was slightly reduced by Na_3Cit, which promoted the bitumen detachment processes. Due to a strong affinity of Na_3Cit to alumina surfaces, Na_3Cit preferably adsorbed on alumina surfaces and prevented the adsorption of naphthenic acids. Besides, Ca^{2+} was chelated by Na_3Cit, which reduced Ca^{2+} concentration and counterbalanced its detrimental effects on bitumen liberation.

Preface

This thesis contains published and submitted papers, as well as the article in preparation. The following is the statement of contributions to these co-authored papers presented in this thesis.

1. Chapter 1 and Chapter 2 were original work from Bailin.

2. Chapter 3 presented a published work: Bailin Xiang, Qingxia Liu, and Jun Long. "Probing Bitumen Liberation by a Quartz Crystal Microbalance with Dissipation." *Energy & Fuels* 32, no. 7 (2018): 7451-7457. Bailin Xiang performed all the experiments, the data analysis and prepared the entire manuscript. Qingxia Liu and Jun Long supervised this project and helped with editing the manuscript.

3. Chapter 4 presented a published work: Bailin Xiang, Nguyen Thuy Vu Truong, Liyuan Feng, Tianzi Bai, Chao Qi, and Qingxia Liu. "Study of the Role of Sodium Citrate in Bitumen Liberation." *Energy & Fuels* 33, no. 9 (2019): 8271-8278. Bailin Xiang was responsible for the experimental work, data analysis, and manuscript preparation. Qingxia Liu supervised this project and helped with manuscript correction. Nguyen Thuy Vu Truong provided valuable suggestions and helped with manuscript proofreading. The AFM experimental work involved Liyuan Feng and Tianzi Bai. Chao Qi helped with data interpretation and manuscript proofreading.

4. Chapter 5 presented a published work: Bailin Xiang, Rui Li, Bo Liu, Rogerio Manica, and Qingxia Liu. "Effect of Sodium Citrate and Calcium Ions on the Spontaneous Displacement of Heavy Oil from Quartz Surfaces." *The Journal of Physical Chemistry C*. Bailin Xiang was responsible for the experimental work, data analysis, and manuscript preparation. Qingxia Liu supervised this project. Rui Li greatly helped with the modeling section. Bo Liu was involved in concept development and contact angle measurements. Rogerio Manica helped with the manuscript proofreading. All the authors were involved in the discussion of the manuscript.

5. Chapter 6 presented a paper in preparation for publication: Bailin Xiang, Mahsa Nazemi Ashani, Zhiqing Zhang, Rogerio Manica, Jun Long and Qingxia Liu. "Role of Sodium Citrate in the Adsorption of Naphthenic Acids on Inorganic Mineral Surfaces." The manuscript is in preparation. Bailin Xiang was responsible for the experimental work, data analysis, and manuscript preparation. Qingxia Liu and Jun Long supervised this project. Mahsa Nazemi Ashani helped with the data analysis and mechanism development. Zhiqing Zhang was involved in zeta potential measurements. Rogerio Manica helped with the manuscript proofreading. All the authors were involved in the discussion of the manuscript.

6. Chapter 7 is the original work from Bailin Xiang.

Acknowledgements

I would like to thank all the secondary process aids (SPA) project team members for giving me proper suggestions.

Finally, my deepest gratitude goes to my family, grandparents, father, and mother, who tried their best to support me in my life and encourage me in my research.

Table of Content

List of Figures

List of Tables

Chapter 1 Introduction

1.1 Background and motivations

Bitumen is one of the major energy resources in Canada, which can be upgraded and refined to produce gasoline, diesel fuel, heating oil and so on.[1] To recover bitumen from oil sands ores, surface mining and water-based extraction process are widely applied in Canadian oil sands industries.[1-4] The water-based extraction process is originated from the Clark Hot Water Extraction (CHWE) process. The operation procedures include slurry preparation, slurry conditioning, primary separation, and secondary flotation, etc. In general, chemical aids are added along with water and mixed with oil sands to enhance the bitumen recovery. From the efficiency and economic perspectives, caustic (sodium hydroxide) has been widely applied in commercial oil sands extraction. Adding sodium hydroxide (NaOH) is capable of increasing the solution pH and promote the release of anionic natural surfactants, which benefits bitumen liberation.[5, 6] Moreover, the NaOH helps to precipitate the divalent cations from process water and alleviates the slime coating effect.[5] However, the long-term and high dosage use of NaOH creates undesired consequences due to its corrosivity. Additionally, the recovery of poor-processing ores is rarely improved by NaOH even with a high dosage.[6] Therefore, it is necessary to reduce the amount of caustic or replace it with alternative chemical aids. Plenty of chemical aids have been tested for decades, either in the laboratory extraction or industrial production.[7-10] However, none of them has been commercialized or applied in industrial production until

a novel secondary process aid, sodium citrate (Na₃Cit), has been discovered. It was found that the combined addition of Na$_3$Cit with NaOH significantly improved the bitumen recovery in oil sands extraction compare to using NaOH alone.[11] Such innovation reduced the usage of NaOH and solved the poor-processability problem of low-grade ore. Unlike NaOH, Na$_3$Cit showed a negligible influence on the solution pH, which has been recognized as a pH buffer and chelating agent in the daily life and cleaning industry. The underlying mechanisms of how sodium citrate enhances the bitumen recovery in the water-based extraction process remains unclear.

In the water-based extraction processes, the bitumen liberation process and the hetero-coagulation between bitumen and solids are highly important to bitumen extraction.[12] Under the effects of temperature and shear action from the surrounding aqueous phase, the thinning of the bitumen film on sand grains results in a pin-hole and then gradually forming a three-phase contact line (TPCL). Later, the bitumen phase recedes from the solid surface due to the advance of the aqueous phase.[2, 13] The detachment of bitumen from solid surfaces is the last step of bitumen liberation, which generally requires hydrodynamic forces such as the fluid drag force, shear force, and buoyance force. The successfully detached bitumen can then be collected by air bubbles or engulfed on air bubbles to form bitumen froth. However, suppose the mineral solids (sands and clay particles) become hydrophobic during the extraction process, which depresses the liberation efficiency and induces a re-coagulation of bitumen and solids. Therefore, it is highly important to investigate the role of Na$_3$Cit on the bitumen liberation process and the solid wettability alternation.

The traditional methods of studying bitumen liberation rely on the techniques of image analysis and video recording. Through microscopes and cameras, the liberation process of the individual oil sand and the model oil sands were observed under various conditions.[14-17] To our best knowledge, little research has been done to precisely quantify the bitumen liberation. The quartz crystal microbalance with dissipation (QCM-D) is a powerful tool that has been widely applied for real-time surface characterization. By recording the resonance frequencies of the sensor, the adsorption and desorption processes on the sensor surface can be determined, while the dissipation signal provides the viscoelasticity information of the adsorbed layer.[18-20] In the petroleum industry, QCM-D has been applied to study the adsorption of crude oil and its major components on different mineral surfaces.[21, 22] In this study, QCM-D was first-time used in quantifying the detachment process of bitumen from silica surfaces. Meanwhile, the role of Na_3Cit on the adsorption of naphthenic acids (NAs) on alumina surfaces was also investigated by QCM-D. The hydrodynamic (HD) model and the molecular kinetic (MK) model were applied to describe the wetting dynamics of the bitumen-solid-water system. With the application of these two models, the underlying physics of Na_3Cit on enhancing bitumen displacement can be determined.[23]

1.2 Research objectives

This study aims at developing a new method to quantify the bitumen liberation process and fundamentally understand the roles of Na_3Cit as a secondary process aid in bitumen liberation and solid wettability alternation. The main objectives are listed below:

1. To develop a new method of quantifying the bitumen liberation process using QCM-D. Such methodology enables us to quantify the bitumen liberation at various chemical and physical conditions.

2. To investigate the effects of Na_3Cit on bitumen liberation and solid wettability alternation, including the liberation kinetics, degree of bitumen liberation (DBL), dynamics of bitumen displacement and wetting transition on solid surfaces induced by NAs adsorption.

3. To reveal the mechanism of how Na_3Cit benefits the above processes through studying the interfacial properties of bitumen-water and solid-water interfaces and measuring the intermolecular forces.

In the first part of this thesis (Chapter 3), a method was developed to study the bitumen liberation process using QCM-D. The mechanisms of bitumen film detaching from the silica sensor surfaces were illustrated by analyzing the frequency and dissipation changes. The effects of different conditions, including solid wettability, solution pH, and operation temperature, on bitumen liberation efficiency were investigated. The successful application of QCM-D provided a unique way to examine the effect of various conditions in bitumen liberation.

The second part of this thesis (Chapter 4) investigates the synergetic effect of Na_3Cit and NaOH on the bitumen liberation from the silica sensor by QCM-D. The DBL was calculated based on the mass ratio of detached bitumen and coated bitumen. To fundamentally understand the results, the colloidal interactions between bitumen and silica

surfaces were determined by the atomic force microscope (AFM). Meanwhile, the zeta potential of both bitumen and silica suspensions was measured, and a possible mechanism of how Na_3Cit manipulates the surface charges of bitumen and silica surfaces was proposed.

The third part of this thesis (Chapter 5) focuses on the dynamic displacement of bitumen from quartz surfaces under the effect of Na_3Cit and calcium ions (Ca^{2+}). At a controlled temperature and solution pH, the dynamic contact angles and the TPCL motion were captured under different chemical additions and theoretically analyzed by the hydrodynamic and molecular kinetic models. The interfacial properties (including zeta potential and interfacial tension) were measured to explain the effects of Na_3Cit and Ca^{2+} on the dynamics of bitumen displacement. Meanwhile, the relationship between interfacial properties and the static contact angles were discussed.

The last part of this thesis (Chapter 6) investigates the effect of Na_3Cit on solid wettability alternation induced by the NAs adsorption. The alumina surfaces and mica basal cleavages were applied to mimic the clay minerals from oil sands ores. The adsorption of NAs on alumina surfaces was investigated in the presence and absence of Na_3Cit using QCM-D. Zeta potentials of alumina particles were measured at various conditions to explain the mechanism of NAs and Na_3Cit adsorption. The wetting transition on mica surfaces induced by NAs adsorption was measured to illustrate the effect of Na_3Cit in bitumen recovery.

1.3 Thesis outline

This thesis consists of 7 chapters. Chapters 3, 4 and 5 are published research papers, and Chapter 6 contains a paper in preparation. The content of each chapter is summarized below:

Chapter 1 introduces the background and motivations of the research objectives and the structure of this thesis.

Chapter 2 provides a review of elementary steps involved in the water-based extraction process and the previously applied chemical aids. The experimental and theoretical methods related to the current study were also reviewed.

Chapter 3 introduces the application of a novel technique, the QCM-D, which can quantitatively study the bitumen liberation process under various conditions. The detailed methods of preparing bitumen coated sensors and the experimental procedure for bitumen liberation are illustrated. The mechanisms of bitumen film detaching from sensor surfaces under aqueous flow are well explained. This chapter has been published:

Bailin Xiang, Qingxia Liu, and Jun Long. "Probing Bitumen Liberation by a Quartz Crystal Microbalance with Dissipation." *Energy & Fuels* 32, no. 7 (2018): 7451-7457.

Chapter 4 discusses the synergetic role of Na_3Cit and $NaOH$ on bitumen liberation by using QCM-D. The DBL was compared between Na_3Cit, $NaOH$ and their combinations. The adhesion forces between bitumen and silica surfaces, and their zeta potentials are measured to support the liberation results. A mechanism of Na_3Cit modifying the electrical properties and the consequent influences on the DBL is proposed. A version of this chapter has been published:

Bailin Xiang, Nguyen Thuy Vu Truong, Liyuan Feng, Tianzi Bai, Chao Qi, and Qingxia Liu. "Study of the Role of Sodium Citrate in Bitumen Liberation." *Energy & Fuels* 33, no. 9 (2019): 8271-8278.

Chapter 5 illustrates the influence of Na_3Cit and Ca^{2+} on the sub-step of bitumen liberation, the oil-water displacement process. The receding of bitumen on a quartz surface in ambient water is recorded, and the dynamic contact angles are extracted from captured images. Theoretical models are applied to describe the dynamics of bitumen receding. Meanwhile, the interfacial properties of bitumen and quartz under different water chemistries and their relationship to the static contact angle are discussed. A version of this chapter has been published:

Bailin Xiang, Rui Li, Bo Liu, Rogerio Manica and Qingxia Liu. "Effect of Sodium Citrate and Calcium Ions on the Spontaneous Displacement of Heavy Oil from Quartz Surfaces." *The Journal of Physical Chemistry C* (2020).

Chapter 6 discusses the effect of Na_3Cit on the solid wettability alternation of alumina and mica surfaces induced by NAs adsorption. The competitive adsorption between Na_3Cit and naphthenic acids was measured by QCM-D under two scenarios with and without Ca^{2+} ions. The adsorbed layer conformation and the zeta potential of alumina surfaces are analyzed to illustrate the competitive adsorption mechanisms. The wetting transition of mica surfaces is measured to demonstrate the role of solid wettability in bitumen liberation.

Bailin Xiang, Mahsa Nazemi Ashani, Zhiqing Zhang, Rogerio Manica, Jun Long and Qingxia Liu. "Role of Sodium Citrate in the Adsorption of Naphthenic Acids on Inorganic Mineral Surfaces." In preparation.

Chapter 7 summarizes the conclusions from this research and presents future research plans.

Appendix provides additional results for this thesis.

Chapter 2 Literature Review

2.1 Alberta oil sands

Oil sands, tar sands, and bituminous sands are a type of non-conventional petroleum deposit. The high molar mass and extremely viscous form of petroleum in the oil sands ore is technically referred to as bitumen. After upgrading and refining, the bitumen can be used to produce gasoline, diesel fuel, and so on.[2] Natural oil sand deposits are widely distributed throughout the world. In particular, Canada has substantial quantities of oil sands reserves, which ranks third after Saudi Arabia and Venezuela. The bitumen resources from Canada are mainly located in the Athabasca, Cold Lake, and Peace River within the province of Alberta.[24] The bitumen from these deposits can be recovered by two approaches, open-pit mining and in-situ drilling.[1] The first method is also referred to as surface mining, which is suitable for the oil sands deposit close to the surface. Vegetation and surface covers need to be removed before mining, and the mined oil sands ores are further treated with the water-based extraction process to recover bitumen.[12] However, this method becomes uneconomic when the depth of the ore exceeds 75 m; thus, the second method is applied instead for the deeper deposits. For example, Steam-assisted gravity drainage (SAGD) is one of the representatives of in situ production. In SAGD, steam is introduced to the horizontal well to heat the ores, which reduces bitumen's viscosity, and then the liquefied bitumen is collected and pumped to the surface.[25] According to the report in 2013,

approximate half of the bitumen production was contributed from the surface mining and water-based extraction process.[26]
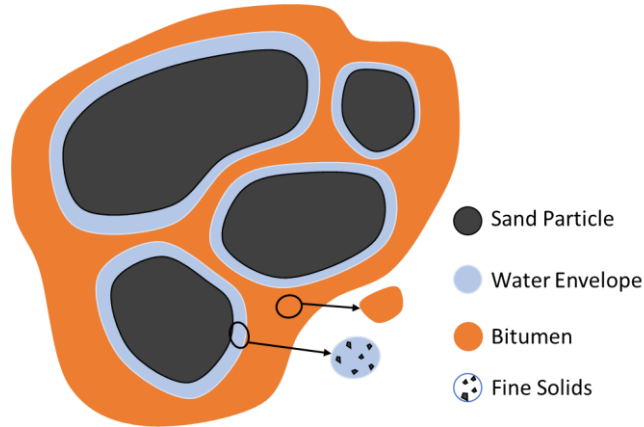
Figure 2.1. The Schematic Structure and Composition of Athabasca Oil Sands.

The Athabasca area is the largest oil sands deposit in the world.[27] A schematic structure of the Athabasca oil sands is illustrated in Figure 2.1. The hydrophilic nature of the solids ensures Athabasca oil sands to be successfully processed by the water-based extraction method. Precisely, a thin layer of water film (~10 nm) is sandwiched between bitumen and sand grain.[28-30] In general, the oil sands consist of 7 - 13 wt. % of bitumen, 3 - 7 wt. % of water and 80 - 85 wt. % of solids (including minerals and clays). In the oil sands industry, fines are defined as the mineral solid with a size less than 44 μm, and high fine content usually indicates solids in oil sands containing more than 20 wt. % of fines. Based on the different content of bitumen and fines, the oil sands ore can be categorized into several grades. In order to reach the required bitumen recovery with economic value, the mined oil sands should contain a minimum of 7 wt. % of bitumen (cutoff grade). Good oil sands ores typically contain more than 11 wt. % of bitumen, while the low-grade ores contain less

bitumen (< 9 wt. %) with high fines content.[1] It is necessary to note that the processability

is highly dependent on the quality of oil sands ores.

2.2 Water-based extraction process
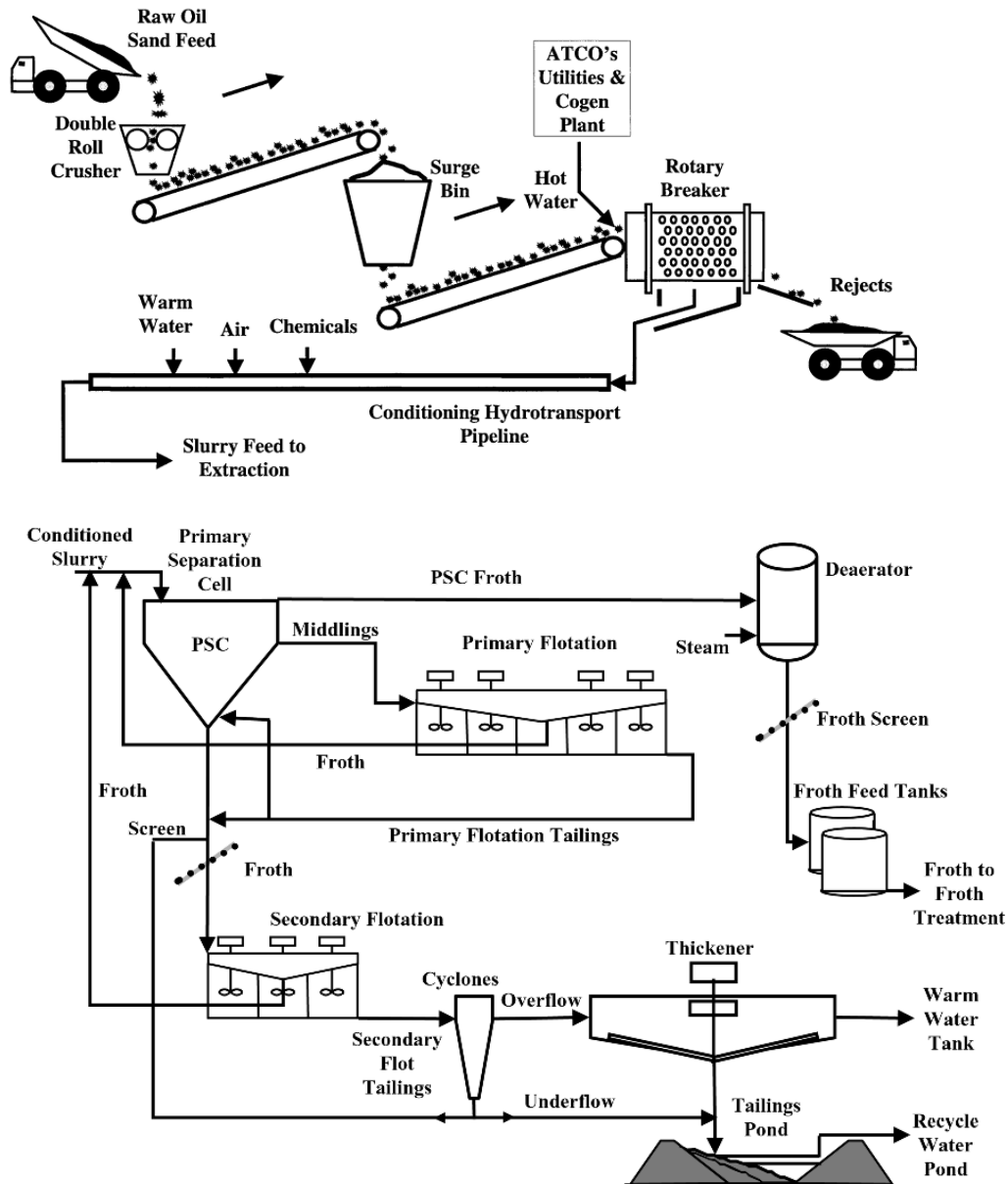
Figure 2.2. Schematic of oil sands processing using water-based extraction process.

The Clark Hot Water Extraction (CHWE) process was originated by Clark in 1923, which is the first bitumen extraction method applied in commercial oil sands industry.[3, 4, 12] CHWE is the foundation for the current water-based oil sands extraction technology. To save energy, hot water used in oil sands industries had been replaced by warm water[31,32]. The typical operating procedure for the water-based extraction process is shown in Figure 2.2.[1]

First, the oil sands are mined from open-pit mine with shovels and trucks, generally referred to as the truck-and-shovel method.[1] Before mixing the oil sands with the recycled process water, the oil sands lumps need to be crushed for size reduction. Process aids are usually introduced together with process water to prepare the slurry. Slurry conditioning happens at the hydrotransport pipeline, where bitumen liberation and aeration take place. Then, the conditioned slurry is transferred to a large primary separation vessel/cell (PSV/PSC) for gravity separation. The operation temperature ranges from 35 ºC to 75 ºC in different extraction plants, while 40 - 55 ºC slurry temperatures have been widely applied in the current operation. It is believed that bitumen becomes fluid-like at 40 ºC[31]; therefore, the oil sands lumps can be easily ablated with the size reduction under the effect of both warm water and mechanical shear.

The aerated bitumen froth has a lower density than water, which floats to the top and can be skimmed off from the slurry. The tailing at the bottom of the PSV is discharged to tailing ponds for solid separation and water recycling. Middling usually contains a small amount of bitumen, which is further processed by flotation. The collected bitumen froth usually

contains approximately 60% of bitumen, 30% of water and 10% of solids, which is de-aerated and sent to the froth treatment unit. The overall efficiency from the elementary steps involved in the water-based extraction process, such as bitumen liberation, aeration, the coalescence of bitumen droplets, determines bitumen recovery.

2.3 Bitumen liberation

Bitumen liberation includes the recession and detachment of bitumen from the solid surfaces, which is the primary step in the water-based extraction process. Surrounding by the warm aqueous environment, the bitumen film starts thinning and forms pin-holes. Then, the ruptured bitumen film results in a three-phase contact line (TPCL), as shown in Figure 2.3. The release of natural surfactants from bitumen changes the interfacial tension (IFT) of the bitumen-water interface, promoting the movement of the TPCL until it reaches equilibrium, and this step is referred to bitumen recession.[15, 33] Eventually, the bitumen forms droplets on the solid surfaces, and subsequently, these droplets detach from the solid surfaces under the assistance of aeration and hydrodynamic forces during the extraction process.
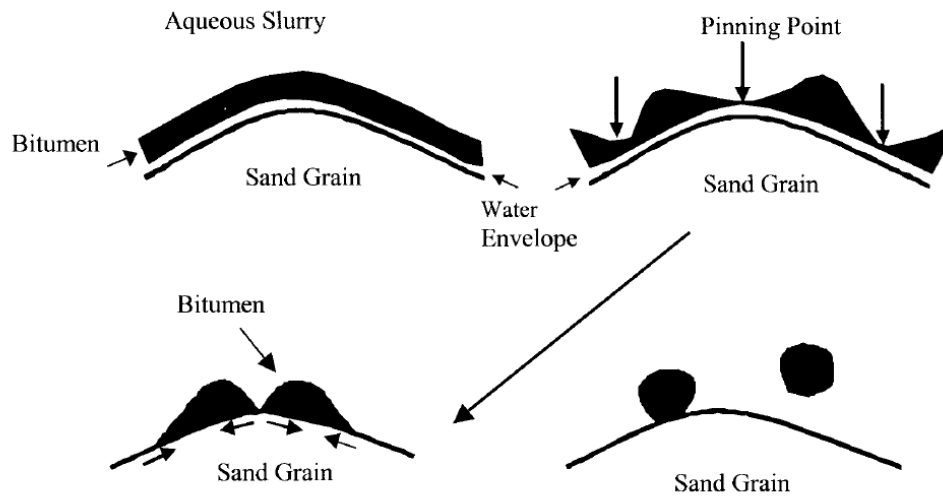
Figure 2.3. Conceptual steps for bitumen liberation.[13]

2.3.1 Interfacial energies

Once the oil sands are exposed to the water phase, the bitumen-water, solid-bitumen and solid-water interfaces are formed. Interfacial tension and zeta potential of those interfaces play significant roles in the bitumen liberation process.[34]
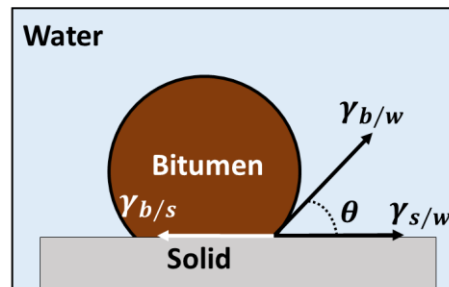
Figure 2.4. Schematic of bitumen-water-solid system and the interfacial energies.

Figure 2.4 illustrates a typical bitumen-water-solid system in bitumen liberation process, where $\gamma_{b/s}$, $\gamma_{b/w}$ and $\gamma_{s/w}$ indicate the interfacial energies of bitumen-solid, bitumen-water and solid-water interfaces, respectively, and θ is the contact angle. Initially, bitumen is

spread on the solid surface. After it contacts with water, the TPCL starts moving due to the imbalanced surface tension force. In the bitumen recession process, the bitumen-solid interface is gradually replaced by the solid-water interface, and the required energy per unit area can be simply expressed by the following equation.

$$\frac{\Delta G}{\Delta A} = \gamma_{s/w} - \gamma_{b/s} \tag{2.1}$$

where ΔG and ΔA represent the change of Gibbs free energy and interfacial area. With the application of Young's equation (Eq. 2.2)[35],

$$\cos(\theta) = \frac{\gamma_{b/s} - \gamma_{s/w}}{\gamma_{b/w}} \tag{2.2}$$

Eq. 2.1 can be simplified into Eq. 2.3,

$$\frac{\Delta G}{\Delta A} = -\gamma_{b/w} \cos\theta \tag{2.3}$$

when θ is less than 90° (the substrate is hydrophilic), this process is thermodynamically favourable and the smaller the θ the more benefits for bitumen recession. On the contrary, when θ is higher than 90° (hydrophobic substrate), this process is thermodynamically unfavorable. In this condition, a lower $\gamma_{b/w}$ favours bitumen recession.

In addition, the interfacial energy for the bitumen droplets to detach from the solid surfaces is described with Eq. 2.4,

$$\frac{\Delta G}{\Delta A} = \gamma_{s/w} + \gamma_{b/w} - \gamma_{b/s} \tag{2.4}$$

which indicates that the bitumen-solid interface is replaced by the bitumen-water and solid water interface. By inserting Young's equation, it reduces to Eq. 2.5.[1]

$$\frac{\Delta G}{\Delta A} = \gamma_{b/w} \ (1 - \cos\theta) \tag{2.5}$$

According to Eqs. 2.4 and 2.5, it is evident that the bitumen detachment process is thermodynamically unfavorable. Additional energies such as fluid drag force and buoyancy force are necessary for the complete detachment of bitumen droplets. Also, the smaller the $\gamma_{b/w}$ the less energy is required for bitumen detachment. The decrease of $\gamma_{b/w}$ can be achieved by increasing the slurry pH, which results in more natural surfactants released from bitumen.[36, 37]

2.3.2 Zeta potential

The zeta potential is an essential interfacial property in the colloidal system. In aqueous solution, the charged surface generates an electric field that attracts the counterions to the surfaces. The surface charges and the counterions form an electric double layer (EDL), as shown in Figure 2.5.[38] The zeta potential is a measurable potential at the slipping plane, which can be used to predict the surface potential. Studying the zeta potentials of bitumen-water and solid-water interfaces help explain the electrostatic interaction between bitumen and solids during the liberation process.
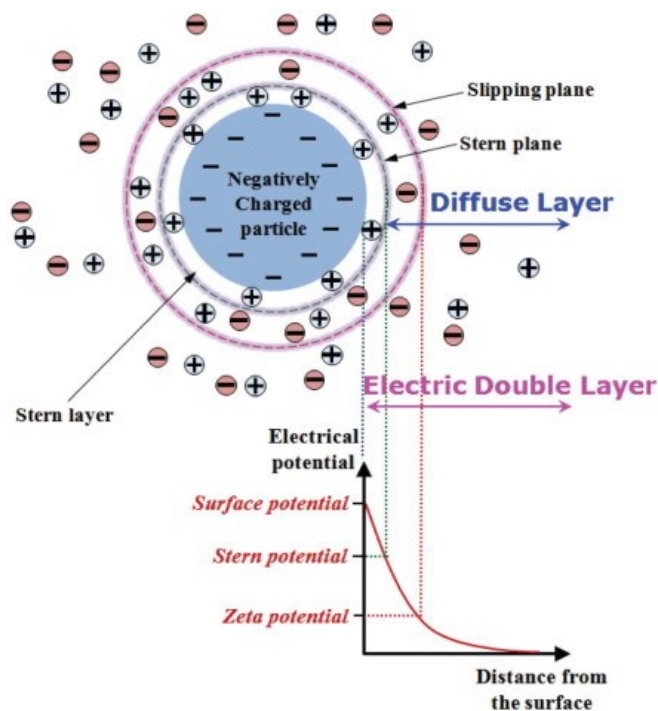
Figure 2.5. Schematic illustration of zeta potential and electric double layer.[38]

The bitumen surface's charging mechanism is mainly governed by the interactions of polar compounds contained in bitumen and chemical species from the aqueous phase. It was observed that the zeta potential of bitumen depended strongly on the solution pH due to the protonation and deprotonation of the natural surfactants (sulphonate, carboxylate and amines) from bitumen.[39] Previous studies concluded that the bitumen surface is dominated by the positively charged surfactants and exhibits positive zeta potential at very low pH range (< 3), while it becomes increasingly negative with increasing the solution pH.[39, 40] Besides, the divalent cations such as calcium (Ca^{2+}) and magnesium ions (Mg^{2+}) from the process water are able to shift the bitumen surface to a less negatively charged state.[41-43]

On the other hand, the quartz sands (silica) is the major composition of solids in oil sands. The origin of electric charges on the sand-water interface is mainly attributed to the

deprotonation of hydrolyzed sand surfaces and the adsorption of charged molecules onto the surfaces. Similar to bitumen, the quartz surface becomes more negatively charged with increasing solution pH and less negatively charged with the presence of divalent cations.[42, 44]

The zeta potential variation not only determines the electrostatic interactions between bitumen and silica, but also influences the interfacial energy of solid-water and bitumen-solid interfaces. It was shown that the energy of the formation of an electric double layer on the solid-water interface is capable of varying the solid-water interfacial energy. This energy can be influenced by the surface charges and the surface reactions, thereby altering $\gamma_{s/w}$ and the solid wettability.[45]

The $\gamma_{b/s}$ can be modified by the interactions between bitumen and solid at the TPCL. It was experimentally proved that a thin layer of water film (nanometer thickness) is sandwiched between the oil and solid surfaces at the TPCL. The disjoining pressure from this thin film consists of the DLVO (Derjaguin–Landau–Verwey–Overbeek) interactions and the non-DLVO interactions.[46, 47] Evidently, the electrostatic interaction is considered. Therefore, the surface charges of bitumen and solids are highly related to the $\gamma_{b/s}$, which consequently influences the bitumen recession and detachment processes.

2.4 Quantification Methods for bitumen liberation

Various techniques have been developed to study the bitumen liberation process, a primary step in the bitumen extraction. The following content summarizes the most commonly applied methods.

2.4.1 Optical methods for model oil sands system

Bitumen film thinning, rupture and recession on the solid surfaces can be captured by microscopic video recording using a model system. The bitumen film is generally coated on glass and silica surfaces to simulate the oil sands. Basu et al. studied the effect of solution pHs and operation temperature on bitumen displacement using bitumen coated glass slides.[15, 16] With camera recording, the displacement rate of bitumen from solid surfaces and the static contact angle at the end of receding can be analyzed. Later, a CCD camera with macro-lens was positioned to study the bitumen displacement by the aqueous phase on a glass surface, the negative impact of calcium ions and montmorillonite clay on the bitumen recession process were confirmed at different pHs and temperatures.[48]

The micro-pipette development enabled us to study the bitumen liberation from the micro-spherical surface (the curved surface), which is closer to the morphology of the real oil sands. The dynamic contact angle and TPCL motion were captured using such technique, and the data were analyzed by theoretical models to explain the wetting behavior under the effect of substrate wettability and water chemistry.[23]

2.4.2 Optical methods for real oil sands system

Using oil sands ore to study the liberation process is more related to real industrial operations. The current technologies of measuring the degree of bitumen liberation (DBL) were originated from Luthra's work, who introduced an alternative method to estimate the bitumen recovery from analyzing the greyscale variation of captured images.[49] Based on the same principle, the laboratory hydrotransport extraction system (LHES) was developed, which was able to study the bitumen liberation and recovery kinetics independently. The images of the slurry conditioning process were captured by the camera, the black pixels of captured images decreased overtime, and the DBL was calculated by the decreased black pixels at a given time divided by the black pixels at the beginning of the recording. Also, a custom programmed software was designed to quantify the pixels and greyscale values, which could calculate the DBL in real-time.[13]

Later on, the development of the bitumen liberation flow visualization cell (BLFVC) by Srinivasa et al. allowed an online visualization of bitumen recession from real oil sands ore under different industrial operation conditions.[17] Figure 2.6[17]illustrates the bitumen receding on the oil sand grains over time captured by their equipment. The effect from temperature, solution pH, salinity and the weathering of oil sands were studied, which confirmed the reliability of this BLFVC in understanding the critical process conditions on bitumen liberation.[17]
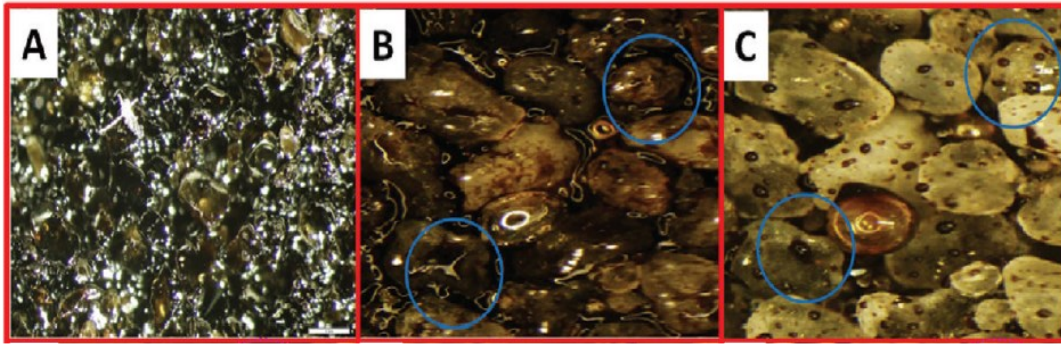
Figure 2.6. Bitumen receding from sand grains over time.

2.4.3 Interactions between bitumen and solids

In addition to the methods built on visualization techniques, a fundamental understanding of the bitumen liberation process was conducted by measuring the interactions between bitumen and solid surfaces. By analyzing the pickup time of solids by bitumen, the interactions between bitumen and solids were investigated by the induction time apparatus.[40] The detachment of sands from bitumen can be achieved using a high pH solution and a high operating temperature; and the mechanisms were explained by the increased electrostatic repulsion and confirmed by the DLVO theory.[40] The atomic force microscope (AFM) is one of the most commonly used techniques to determine the colloidal interactions. The bitumen surface can be prepared by either spin-coating diluted bitumen on the substrates or dip coating on the AFM tips. The effects of salinity, divalent cations, temperature and solution pH on the long-range repulsive force and adhesion force can be measured by AFM.[42] In addition, Long et al. modified the AFM cantilever with the real sand particles and clay particles from oil sands tailing stream, and measured the

interactions between the bitumen and minerals in the process water to simulate the industrial conditions.[50]

2.5 Control factors for bitumen liberation

The efficiency of bitumen liberation is highly important to the bitumen recovery, which can be influenced by physical, chemical and hydrodynamic conditions. Because the detachment process of bitumen from the sand surface is thermodynamically unfavorable, the hydrodynamic energies are necessary for a successful liberation.[1] Therefore, static contact angles at the end of bitumen liberation are highly important for a successful bitumen liberation. The bitumen recession process determines not only the static contact angle but also the efficiency of bitumen liberation, which is controlled by the solution chemistry, solid wettability and operation temperature etc.

2.5.1 Physical factors

Physical parameters such as the operation temperature and oil sands ore weathering are essential to bitumen liberation efficiency. It was revealed that the bitumen recession process was significantly accelerated at a higher temperature, due to the decreased viscosity of the bitumen.[15] Although the equilibrium contact angle of bitumen recession is insensitive to the temperature, the bitumen recession rate is highly dependent on the temperature.[15] A critical temperature of 35 °C is necessary to ensure proper liberation behavior.[31] In addition to increasing the temperature, the reduction of bitumen viscosity can be achieved by adding the solvent such as naphtha and toluene. It was found a lower IFT or a smaller bitumen

viscosity benefits the DBL. However, the bitumen displacement dynamics were found linearly correlated to the IFT/viscosity ratio according to the study of Lin et al. .[51] As for the weathering effect, the loss of formation water promotes the adsorption of organic materials onto the mineral surfaces, resulting in a hydrophobic solid surface.[52, 53] Therefore, poor liberation kinetics and low DBL was found with the weathered oil sands ores even when high temperature and a high pH were applied.[17, 54]

2.5.2 Solution pH

It is well known that high pH is favorable for bitumen liberation. The underlying mechanisms rely on the adsorption of deprotonated natural surfactants from bitumen on the interfaces, which modifies the interfacial properties of bitumen-water and solid water interfaces.[9, 17, 34, 55] The addition of sodium hydroxide (NaOH) during bitumen extraction is one of the methods to adjust the operation pH. The increased alkalinity promotes the deprotonation of anionic natural surfactants from bitumen.[6, 36, 56] The ionized surfactants, such as carboxylates and sulfonates[6], prefer to adsorb on the bitumen-water interface, which not only reduces the IFT of the bitumen-water interface but also increases the negative charges on this interface (Figure 2.7).[37, 57] In addition, the hydrolyzed sand surface tends to deprotonate under a high pH environment, becoming more negatively charged and hydrophilic.[58] Therefore, the increased solution pH benefits bitumen liberation through increasing the electrostatic repulsion between bitumen and solid.[42] Moreover, due to a faster bitumen displacement rate at a low pH (< 7) and a high static contact angle of

bitumen droplet at high pH (>7), a concept of pH cycle was introduced to improve the industrial operation in the hydrotransport pipeline.[16]
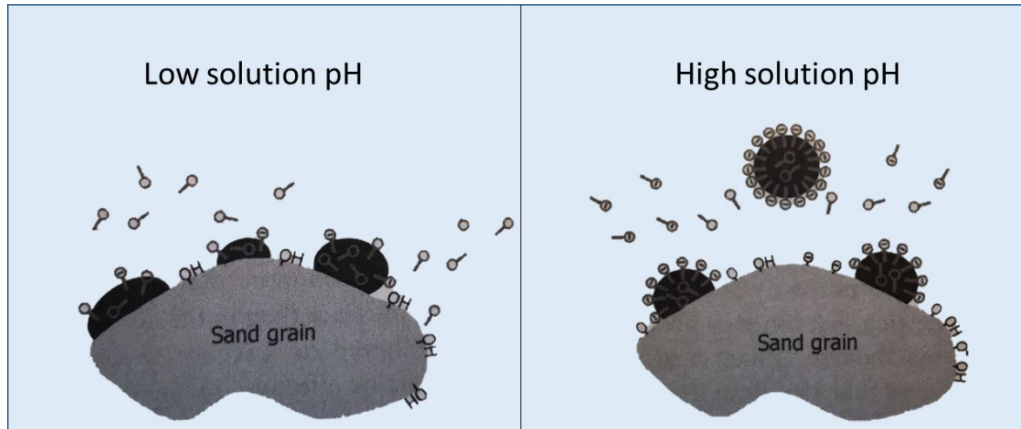
Figure 2.7. Effect of solution pH on bitumen liberation from sand surfaces.[1]

2.5.3 Metal cations

The major inorganic components in the process water are metal cations, such as sodium ions (Na^+), Ca^{2+} and Mg^{2+} ions range from tens to hundreds of parts-per-million (ppm).[59, 60] The effect of salinity on bitumen liberation was investigated by Chen et al. .[61] with the BLFVC. At pH 8.5, only a marginal depression of the DBL was found with the increased salinity (up to 4000 ppm Na^+). However, increasing the salinity at a high pH (11.2) resulted in a drastic decrease of bitumen liberation kinetics and the DBL.

The interfacial properties of bitumen-water and solid-water interface can be altered in the presence of divalent cations, thereby changing the bitumen liberation. The natural surfactants from bitumen can be precipitated by Ca^{2+}, which reduces the activity of surfactants and results in a less negatively charged bitumen-water interface.[1, 62] In addition, the adsorption of divalent cations on the sand and clay surfaces reduces their negative

charges.[41] Therefore, an increase in the adhesion force and a decrease in the long-range repulsive force between bitumen and solid surfaces were observed in the presence of Ca^{2+}.[63] A poor bitumen displacement dynamics were found in the presence of divalent cations due to an increased attraction between bitumen and solid surfaces .[23, 48]

2.5.4 Chemical aids

Chemical process aids are usually applied in the oil sands extraction to enhance bitumen recovery. Over the past decades, the most commonly used chemical aid in the water-based bitumen extraction is caustic, specifically sodium hydroxide. It has been proven that adding NaOH significantly enhanced the bitumen recovery and froth quality, in which the optimal dosage of NaOH for oil sands processing is determined by both the ore grade and fines content.[4, 56] However, the corrosivity of caustic causes concerns on the long-term application of NaOH. Besides, minor enhancement was found on the processing performance of poor ores with the addition of NaOH.[6, 56] In order to make the oil sands extraction industry more efficient and environmentally friendly, engineers and scientists devoted significant efforts to minimize the application of caustic or find an alternative chemical.

Several chemical aids, such as demulsifier, dispersant, and chemicals for pH adjustment and flocculation, have been tested in industrial or laboratory-scale oil sands processing. For example, the addition of hydrolyzed polyacrylamide (HPAM) reduced the adhesive force between bitumen and silica, while increasing adhesion between clay and silica. These results indicate that adding HPAM is beneficial to bitumen liberation and tailing settling.[7]

25

Meanwhile, the DBL was improved by adding sodium silicates, a dispersant/depressant of clays. It was found that the divalent cations were precipitated by sodium silicate during bitumen extraction, which prevented slime coating and enhanced bitumen recovery.[8] Flury et al.[9] pointed out that ammonium hydroxide (NH$_4$OH) is a suitable replacement for NaOH. Their results showed a shorter induction time of bitumen-bubble attachment in the presence of NH$_4$OH, although similar enhancement in bitumen liberation was observed between NH$_4$OH and NaOH. It was indicated that NH$_4$OH is a viable alternative to NaOH because it helped bitumen aeration at high pH (11.3) when comparing to NaOH.[9] In addition to the general water-based extraction, diluents such as kerosene and naphtha were added upfront to mix the oil sands ore with water, which can reduce the bitumen viscosity and increase the accumulation of surfactants at the bitumen-water interface.[64] Meanwhile, ethyl cellulose (demulsifier) added together with a solvent which is beneficial to the bitumen liberation rate and DBL.[65]

2.6 Sodium citrate

The application of chemical aids has a long history in the oil sands industry; however, there is no clear conclusion on the most effective chemical additives. The application of a secondary process aid, sodium citrate (Na$_3$Cit), significantly enhanced the processability of oil sands ores. Compared to applying NaOH alone, the combined addition of Na$_3$Cit improved not only the bitumen recovery but also the froth quality on both good ores and poor ores.[11]

Sodium citrate is a sodium salt with three carboxyl groups, which has been widely applied in our daily life. Most of the applications are based on the chelating and buffering ability of citrate. For example, Na₃Cit is used to remove the limescale from boilers or as a builder with detergents.[66] The reactions of citric acid deprotonation are listed in Eq. 2.6 to Eq. 2.8[67], where the L indicates the ligand (citrate anion in this study). According to the equations, these pK_a values suggest that citric acid has the buffering capacity between pH 3 to around 6.3. In an industrial process at operation pH around 8.5, Na₃Cit dissociates to $C_3H_5O(COO)_3^{3-}$ carrying three negative charges.

$$H_3L = H^+ + H_2L^- \qquad pK_{a1} = 3.128 \qquad (2.6)$$

$$H_2L^- = H^+ + HL^{2-} \qquad pK_{a2} = 4.761 \qquad (2.7)$$

$$HL^{2-} = H^+ + HL^{3-} \qquad pK_{a3} = 6.396 \qquad (2.8)$$
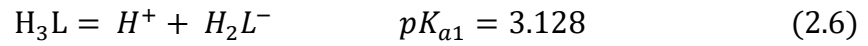
In addition, sodium citrate is well known as a commercial builder. It serves to counterbalance the detrimental effects of polyvalent cations to increase the effectiveness of surfactants.[68] Divalent cations such as Ca^{2+} and Mg^{2+} in the process water show adverse effects on bitumen recovery. The presence of divalent cations is expected to increase the adhesion between bitumen and solid, which reduces the efficiency of bitumen liberation. Moreover, the cation bridge formed between bitumen and clay particles results in slime coating, which reduces the flotation efficiency and froth quality. The application of Na₃Cit is capable of reducing the concentration of free divalent cations in a wide pH range. Figure 2.8 illustrates the chelation ability of citric acid of different cations.[44] At the industrial operation pH 8.5, most of the cations exist as complexes with citrate. Therefore, the

effectiveness of natural surfactants can be recovered by Na₃Cit, and the slime coating can be prevented.[44, 62]
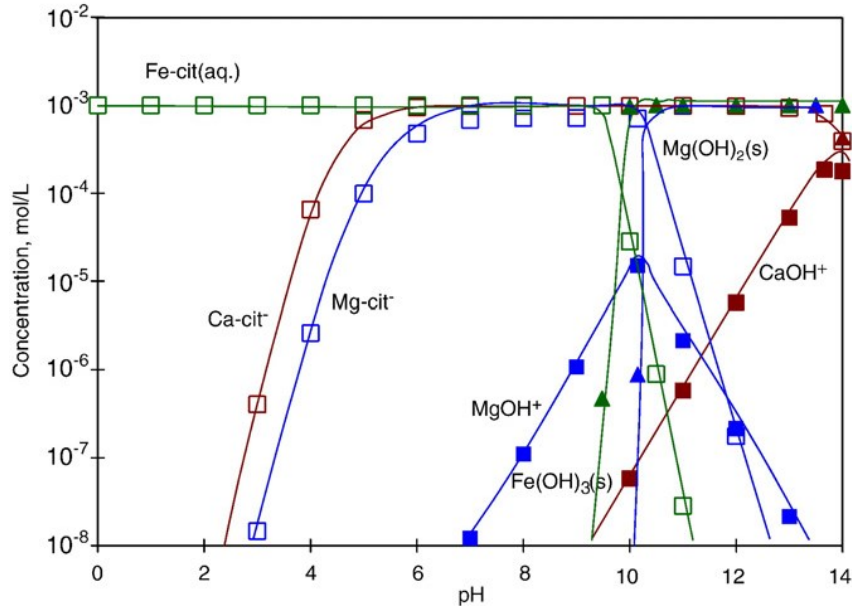
Figure 2.8. Speciation diagram of different cations versus pH. The aqueous solution contains 10^{-3} mol/L of Ca^{2+}, Mg^{2+} or Fe^{3+} and 2×10^{-3} mol/L citric acid.[44]

2.7 Surfactant adsorption and solid wettability

The successful application of the water-based extraction process on the Athabasca oil sands relies on the hydrophilic nature of most of the mineral solid contained in oil sands. However, the adsorption of organic polar components changes the water-wet mineral solids to the oil-wet solids.[69-71] Naphthenic acids (NAs) are a group of cyclopentyl and cyclohexyl carboxylic acids, which are known as the natural surfactants contained in bitumen. During bitumen extraction, they partition to the water phase and deprotonates to carry negative charges at alkaline conditions.[72] Since the water used for processing oil sands are recycled

process water, the concentration of NAs can increase to 100 ppm.[73, 74] The carboxyl groups from NAs are expected to coordinate with metal ions and metal oxides, which consequently modifies the wettability of mineral solids. There are two possible mechanisms for the adsorption of naphthenic acids on mineral solids[1]: (1) NAs adsorb on the negatively charged solid surfaces through cation bridge; (2) NAs directly adsorb on the positively charged solid surfaces. The adsorbed NAs expose their hydrophobic tails to the aqueous phase and induces coagulation between free bitumen droplets and the mineral solids, as proposed in Figure 2.9.
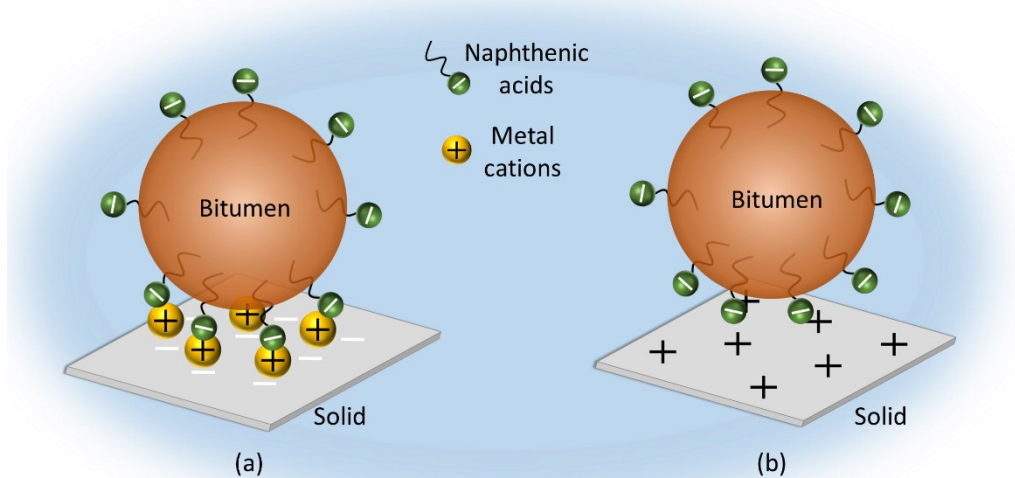
Figure 2.9. Mechanisms of surfactant induced solid wettability alternation: (a) anionic surfactants on bitumen-water interfaces adsorb on the negatively charged solid surface through cation bridge; (b) anionic surfactants on bitumen-water interfaces adsorb on the positively charged solid surface.

According to the study from Jiang et al., the kaolinite particles were mixed with toluene and synthetic brine in the presence and absence of sodium naphthenates (NaN). The fraction of water-wet kaolinite particles decreased from 96% to only 18% when 100 ppm of NaN was added into the brine-toluene mixture.[70] In addition, the wettability of fine silica changed when both palmitic acid (mimic naphthenic acid) and Ca^{2+} were present in the solution.[43] It was found that NAs with unsaturated aromatic rings were irreversibly adsorbed on calcite and mica surfaces, which modified them to the oil-wet state.[75] Obviously, the adsorption of NAs on mineral solids alters the wettability of the surfaces, and the hydrophobic solid surfaces are expected to hinder bitumen recession and detachment process.[17, 76] Moreover, the hetero-coagulation between the bitumen droplets and hydrophobic clay particles depresses froth quality in bitumen extraction.

2.8 Common methods for wetting dynamics

Bitumen liberation is an essential step in the water-based extraction process. Once the oil sands ores mix with water, the hydrodynamic forces from the surrounding aqueous solution lead to the thinning and rupture of the bitumen covered on the solid surface, and a bitumen-water-solid TPCL is formed at the pin-hole. The bitumen recession during the liberation process is a displacement of bitumen by water on the solid surface. To fully understand such a process, the TPCL velocity and the dynamic contact angle need to be quantified.[77] In general, there are two commonly used approaches to study the dynamic wetting processes, which are defined according to their different energy dissipation mechanisms. One of them is the hydrodynamic (HD) model, which highlights that the energy dissipation

is caused by the viscous shear within the liquid bulk near the three-phase contact line.[78] Another one emphasizes that the friction in the immediate vicinity of the TPCL is the dominant dissipation mechanism, and known as the molecular kinetic (MK) model.[79] Although these approaches rely on different mechanisms, they have been frequently applied to study the relationship between the dynamic contact angle and the wetting line velocity either individually or in combination. Interestingly, two distinct dynamic regions were observed according to the paper of Fetzer and Ralston. The initial stage with fast TPCL motion could be well described by the HD model, while MK model successfully captured the final stage with slow velocity.[80]

Applying these two models, the underlying physics of the effect of fluid viscosity, droplet size, solid wettability and liquid chemistry on the dynamic wetting process have been well understood. The effect of viscosity on the dynamic wetting process was usually studied using polymer melts or heavy oil. Increasing the viscosity was believed to hinder the TPCL motion. Specifically, the contact line friction became larger, whereas the displacement frequency decreased with increasing viscosity.[81-83] Moreover, the displacement dynamics exhibited a strong dependence on the substrate wettability. For example, it was shown that increasing the hydrophobicity of the substrate increased the contact line friction using the MK model.[83, 84] Meanwhile, the viscous resistance parameters from the HD model was increased with a more hydrophobic solid surface.[85] Also, the solution pH was found to play an important role in the dynamic displacement of bitumen. Results indicated that increasing the solution pH accelerated the displacement rate of bitumen.[23]

2.8.1 Hydrodynamic model

Although various calculations were proposed for the HD model analysis, the most frequently used calculation is Cox's solution.[86] According to his analysis, the interface of the advancing and receding phases can be divided into three hypothetic regions.[77] The outer region can be experimentally observed, which has a macroscopic length scale. The interface at the outer region is assumed to be static and form a macroscopic contact angle with solid surfaces. This contact angle is considered as the dynamic contact angle (θ_d) in the HD model. The intermediate region has a scale smaller than the macroscopic region, which is also referred as mesoscopic region. The significant viscous dissipation arises from this region, and the viscous bending usually happens at the interface. As for the inner region, the scale is at a microscopic length. In order to characterize the size of this region, the cut-off length (L_S) has been introduced. The microscopic contact angle (θ_m) in the inner region is suggested to be governed by the intermolecular forces such as van der Waals and electric double layer forces.[77] In addition, the fitted θ_m is supposed to reflect the static contact angle (θ_s).

According to the simplest form of the Cox's solution, the relationship between the macroscopic contact angle (θ_d) captured at the outer region and the microscopic contact angle (θ_m) at the inner region is proposed as follows,

$$g\left(\theta_d, \frac{\mu_1}{\mu_2}\right) - g\left(\theta_m, \frac{\mu_1}{\mu_2}\right) = \pm Ca \ ln\frac{L}{L_s} \qquad (2.9)$$

where the capillary number expressed as $Ca = U\mu/\gamma$, and U, μ and γ are the velocity of the TPCL, the viscosity of the fluid under consideration, and the IFT between advancing

and receding fluids. The plus and minus sign before the Ca denotes the case of advancing or receding a three-phase contact line. The L characterizes a typical macroscopic length, such as the size of the droplet. In Eq. 2.9, the function $g(\theta_d, \mu_1/\mu_2)$ is defined as

$$g\left(\theta, \frac{\mu_1}{\mu_2}\right) = \int_0^\theta \frac{d\epsilon}{f\left(\epsilon, \frac{\mu_1}{\mu_2}\right)} \qquad (2.10)$$

where the $f(\epsilon, \mu_1/\mu_2)$ is given by

$$
f\left(\epsilon, \frac{\mu_1}{\mu_2}\right)
$$
$$
= \frac{2 \sin \epsilon \left[\left(\frac{\mu_1}{\mu_2}\right)^2 (\epsilon^2 - \sin^2 \epsilon) + 2\frac{\mu_1}{\mu_2}\{\epsilon(\pi - \epsilon) + \sin^2\epsilon\} + \{(\pi - \epsilon)^2 - \sin^2 \epsilon\}\right]}{\left(\frac{\mu_1}{\mu_2}\right)^2 (\epsilon^2 - \sin^2 \epsilon)\{\epsilon(\pi - \epsilon) + \sin \epsilon \cos \epsilon\} + \{(\pi - \epsilon)^2 - \sin^2 \epsilon\}(\epsilon - \sin \epsilon \cos \epsilon)}
$$

$$(2.11)$$

The term μ_1/μ_2 represents the viscosity ratio of the two liquids, and μ_2 is the viscosity of the liquid under consideration in the modelling. When the viscosity of the dominant liquid is much higher than another liquid, μ_1/μ_2 approaches zero. Consequently, $g(\theta_d, \mu_1/\mu_2)$ can be simplified to

$$g(\theta, 0) = \int_0^\theta \frac{\epsilon - \sin \epsilon \cos \epsilon}{2 \sin \epsilon} d\epsilon \qquad (2.12)$$

Additionally, when θ is in the range between 30° and 135°, the g(θ, 0) can be approximated by $\theta^3/9$ according to Voinov's approximation.[87] Thus, Eq. 2.10 can be reduced to

$$\theta_d^3 - \theta_m^3 = \pm 9 \, Ca \, \ln \frac{L}{L_s} \qquad (2.13)$$

Two free fitting parameters from the HD model are the microscopic contact angle (θ_m) and the logarithmic ratio of two length scales, ln (L/L_S).

2.8.2 Molecular kinetic model

The MK model was initially proposed by Blake and Haynes.[79] In this model, the motion of the TPCL is determined by the thermally activated attachment and detachment process of the microscopic elements at the immediate TPCL.[79] At the equilibrium state, the frequency of the random microscopic elements displacement at the TPCL is denoted as K_0, which can be expressed as the following equation based on the theory of activated rate process.[88]

$$K_0 = \frac{k_B T}{h} \exp\left(\frac{-\triangle G_0}{N_A k_B T}\right) \tag{2.14}$$

where k_B is the Boltzmann constant, T is the absolute temperature, and h is the Planck constant. N_A is Avogadro's number, and ΔG_0 the activated free energy of displacement at equilibrium. During the dynamic wetting process, the thermal energy barrier of this displacement is considered to be overcome by the unbalanced interfacial tension force (F_d), $F_d = \gamma(\cos\theta_s - \cos\theta_d)$, where γ is the interfacial tension of the advancing and receding phases. Therefore, the displacement frequency of forward motion K^+ and backward motion K^- can be expressed as follows with the consideration of interfacial tension force.

$$K^+ = \frac{k_B T}{h} \exp\left(\frac{-\triangle G_0/N_A + F_d\lambda^2/2}{k_B T}\right) \tag{2.15}$$

$$K^- = \frac{k_B T}{h} \exp\left(\frac{-\triangle G_0/N_A - F_d\lambda^2/2}{k_B T}\right) \tag{2.16}$$

Here, λ is the average distance between two adsorption sites. The overall velocity (U) of the TPCL can be calculated based on the net frequency of forward (K^+) and backward (K^-) motion by

$$U = \lambda \, (K^+ - K^-) \tag{2.17}$$

Combining Eq. 2.14 with Eq. 2.17, the relationship between contact line velocity and dynamic contact angle is calculated as

$$U = 2K_0\lambda \sinh \left[\frac{\gamma(\cos\theta_s - \cos\theta_d)\lambda^2}{2k_BT} \right] \tag{2.18}$$

The above equation is the full version of the MK model, containing two microscopic fitting parameters, K_0 and λ. In Eq. 2.18, if the argument of the hyperbolic sine function is small enough, it can be reduced to the linear form.

$$U = \frac{\gamma}{\xi} \, (\cos\theta_s - \cos\theta_d) \tag{2.19}$$

where ξ is the contact line friction coefficient, given by $\xi = \frac{k_BT}{K_0\lambda^3}$, which quantifies the energy dissipation at the immediate three-phase contact zone.

2.9 Crude oil desorption process by QCM-D

The quartz crystal microbalance with dissipation (QCM-D) has been widely applied to quantify the adsorption and desorption processes at different surfaces. The working principle of QCM-D relies on monitoring the frequency and dissipation changes on a quartz crystal sensor, which allows a determination of mass variation on the sensor surfaces.[20, 89] Recently, the desorption of the crude oil and its fractions from mineral surfaces raises increasing attention since this process is related to the recovery of crude oil. There are two

widely applied methods to pre-adsorb the crude oil on the sensor surface before the detachment experiments. The first one is injecting solvent diluted crude oil and its fractions into the QCM-D chamber, and the crude oil adsorbs on sensors from the solvent. Then, the desorption process is directly performed with the injection of the aqueous solution. Using such a method, Farooq et al. investigated the desorption of asphaltene from the silica sensor under different salt concentrations and cations valency.[90] Similarly, the effect of low-salinity and surfactant solution on the desorption of crude oil components from silica and aluminosilicate surfaces was studied through QCM-D.[91] Later, to obtain a uniform surface on the QCM-D sensor and to avoid the influence from the solvent, the spin-coating method was applied to pre-adsorb bitumen and its fractions on the mineral surfaces.[60] The desorption behavior of resins, asphaltenes, saturates, and aromatics under alkaline solution and surfactants solution were compared on different mineral coated sensors by QCM-D. Strong polar interactions between asphaltenes and mineral surfaces were predicted to be the reason of less desorption of asphaltenes compared to other crude oil fractions.[92] Based on these studies, QCM-D is expected to be an alternative method to quantify the kinetics and DBL of bitumen liberation under various conditions.

Chapter 3

Probing Bitumen Liberation by Quartz Crystal Microbalance with Dissipation

Abstract

The detachment of bitumen from sand grains in oil sands processing is known as bitumen liberation. In this study, a quartz crystal microbalance with dissipation (QCM-D) was applied to study the bitumen liberation process under various process conditions. Bitumen was coated on the surface of silica sensors to simulate the oil sands ore. By recording the change of frequency and dissipation of the coated sensor, QCM-D allows a real-time quantitative analysis of the bitumen detachment process. The effects of solid wettability, solution pH, and operation temperature on bitumen liberation were investigated using QCM-D. The effects of different solution pHs and temperature on bitumen liberation were conducted with untreated hydrophilic silica sensors. It was found that the degree of bitumen liberation (DBL) was improved from 32% to 98% when the solution pH was increased from 7.8 to 11, indicating the importance of solution pH in the water-based bitumen extraction process. Increasing temperature enhanced not only the DBL but also the rate of bitumen detachment. The DBL from a hydrophobic silica surface was about 1.2% at pH 11.5 and 22 ºC, which is much lower than the hydrophilic one. QCM-D is a powerful tool in studying the bitumen liberation from both hydrophobic and hydrophilic surfaces.

3.1 Introduction

Oil sands ore is a type of non-conventional petroleum deposit. It impregnates with high molar mass and extremely viscous form of petroleum, which is technically referred to as bitumen.[2] Natural oil sands deposits are widely distributed throughout the world. In particular, Canada has extremely large quantities of bitumen resource, which is mainly located in Athabasca, Cold Lake and Peace River in the province of Alberta. In general, oil sands consist of 7 - 13 wt. % bitumen (oil), 3 - 7 wt. % water and 80 - 85 wt. % solids (clays and minerals). Bitumen is covered on the solid surface, forming the oil sands lump. Due to the high viscosity of bitumen, it is difficult for bitumen to detach from oil sand grains. Innovative technologies and methods were developed in order to efficiently recover the bitumen from oil sands ores. As a result of the hydrophilic nature of solids contained in Athabasca oil sands (Alberta, Canada), the water-based extraction processes originated from the Clark Hot Water Extraction (CHWE) process are widely used in the oil sands industry for bitumen recovery.[2, 3] The general operation procedures of the water-based extraction process include slurry preparation, slurry conditioning, primary separation, and secondary flotation etc. Water along with process aids is mixed with mined oil sands ores to form a slurry, and the slurry is further conditioned in hydrotransport pipelines. During conditioning, bitumen recesses from the sand grains to form small droplets on the sand surfaces. These droplets eventually detach from the sand grains and then attach to the air bubbles to form the bitumen froth. These two steps are known as bitumen liberation and aeration.

Bitumen liberation is an essential step in the water-based bitumen extraction process and generally includes the bitumen recession and separation from the sand grains. This process is controlled by the interactions between bitumen and the sand grains, which can be influenced by the physical and chemical conditions, such as the temperature, solution pH, chemical additives, solid type and wettability. In the early stage, lab-scale investigations of bitumen liberation were mostly conducted with home-built apparatus by microscope. Takamura et al.[14] studied the bitumen disintegration process of individual oil sands in different aqueous solutions by microscope video recording. An immediate migration of bitumen was observed when immersing the oil sand in a sodium hydroxide (NaOH) solution with pH 11.8 at 70 ºC. Basu et al. [15, 16] simulated the bitumen liberation process with a model system by coating bitumen on a glass plate and a polytetrafluoroethylene plates (PTFE). The bitumen film thinning, rupture, and displacement processes on a glass surface under different solution pHs and temperatures were clearly visualized and measured by a microscope, whereas such a process did not occur on PTFE. Their results indicated high-pH water enhanced bitumen film thinning and rupture processes, and the water temperature significantly influenced the bitumen displacement rate. The development of a novel bitumen liberation flow visualization cell (BLFVC) by Srinivasa and Flury et al.[17] allowed a real-time study of bitumen liberation of real oil sands ores. Images of bitumen recession from the sand grains were captured at different time intervals, and the greyscale of those images was then analyzed to calculate the degree of bitumen liberation. In their studies, the effects of temperature and pH on bitumen liberation were consistent with previous findings. In addition, they indicated that the weathering of ores,

the presence of fines in oil sands and the increase of salt concentration in aqueous phase were detrimental for bitumen liberation.

In addition to the methods based on visualization by microscope, other researchers studied bitumen liberation through the investigation of bitumen-solid interactions. For example, Dai and Chung[40] studied the bitumen-sand interactions at different pHs, particle sizes, temperatures and solvent additions in bitumen using an induction timer. The pickup time of sands by bitumen was recorded. Their results indicated that increasing pH is favorable for bitumen liberation due to the increase in electrostatic repulsive forces between bitumen and sand. Considering that liberation process is dominated by the interfacial interactions between the bitumen and sand grains, the colloidal forces between the bitumen surface and the silica sphere were measured with atomic force microscopy (AFM). It was found that increasing pH and temperature reduced the adhesion force between silica and bitumen due to increased long-range repulsive force, whereas the opposite effects were found with divalent cations addition.[55, 63] However, up to date, the bitumen liberation has never been accurately quantified by QCM-D.

In this study, a quartz crystal microbalance with dissipation (QCM-D) was applied for the first time to investigate the fundamentals of bitumen liberation. QCM-D is a powerful instrument for real-time surface characterization. It monitors the frequency and dissipation changes of a sensor, allowing a quantitative investigation of the bitumen detachment process. QCM-D has been widely applied in various research areas, such as studying biological materials interactions, adsorption and desorption phenomena of surfactants and

polymers, as well as their viscoelastic properties.[20, 93-95] Recently, some researchers in the petroleum industry had applied QCM-D to determine the adsorption and desorption of crude oil from a solid surface.[96] The effect of low salinity brine on desorption of crude oil had been investigated, and the heavy oil recovery kinetics and mechanisms have also been studied under a surfactant flood condition by a QCM-D.[91, 97-99] The current study was inspired by these previous work of investigating the desorption of heavy oil by QCM-D. The objective of this study is to explore the feasibility of using QCM-D to study the bitumen liberation process in order to better understand the kinetics and mechanisms of bitumen liberation under different operation conditions. Bitumen was coated on silica sensors to simulate the oil sands, and the bitumen detachment process was measured by QCM-D. The effects of solid wettability, solution pH, and operation temperature on bitumen detachment from silica surface were studied.

3.2 Experimental

3.2.1 Materials

SiO_2 (QSX 303, Q-Sense) sensors were used to simulate the sand surfaces. The bitumen used in this study was the vacuum distillation unit (VDU) feed bitumen provided by Syncrude Canada Ltd. The 1N sodium hydroxide solution, toluene (99.5% purity), ethanol (91% purity) were purchased from Fisher Scientific. Octadecyltrichlorosilane (OTS) and sodium dodecyl sulfate (SDS, 99% purity) were purchased from Sigma Aldrich. The Milli-Q water with a resistivity of 18.2 MΩ·cm was used throughout this study.

3.2.2 QCM-D

3.2.2.1 Principle of QCM-D

The quartz crystal microbalance with dissipation (QCM-D) is well-known for quantifying the adsorption and desorption processes due to the nano-gram sensitivity and easy operation feature. The QCM sensor generally consists of a quartz disk sandwiched by a pair of gold electrodes. When the AC voltage is applied cross the electrodes, shear stress is generated due to the piezoelectric property of quartz and results in oscillation of the crystal at its resonance frequency. By recording the shifts in resonance frequency, the mass changes on sensor surface can be calculated. If the attached film on the crystal surface is rigid and firmly distributed, and much smaller than the crystal, the resonance frequency changes linearly with the added mass according to the Sauerbrey relation, which described in Eq. 3.1,[100] where n is the harmonic number, f_0 is the fundamental resonance frequency, t_q and ρ_q represents the thickness and the specific density of quartz crystal sensor. C is the sensitivity constant, which equals to 17.7 ng Hz^{-1} cm^{-2} for a 5 MHz crystal.

$$-\Delta f = \frac{nf_0}{t_q\rho_q} \times \Delta m = \frac{n\times\Delta m}{C} \qquad (3.1)$$

When the loaded mass on the crystal exhibits viscoelasticity or slip at the interface, the frequency shift (Δf) is also influenced by the mechanical properties of the adsorbed film.[101] In this case, the dissipation of a sensor's energy (ΔD) needs to be involved, which is given by Eq. 3.2, and the mass variation is calculated based on both Δf and ΔD.

$$D = \frac{E_D}{2\pi \times \Delta E_S} \qquad (3.2)$$

Where E_D is the total loss of energy during one oscillation period, and E_S is the total energy stored in the oscillation system. In some circumstances, the change in dissipation is substantial (> 5% of the frequency change), indicating a significant impact from the viscoelasticity of the loaded film. The Voinova -Voigt model should be applied instead of the Sauerbrey relationship.[19, 102] In this study, some of the results exhibited significant influence from viscoelasticity of the bitumen film, and the dissipation shift is much higher than 5% of the frequency change, we used the Voigt model in the Q-Tools software to calculate the mass variations.

3.2.2.2 Cleaning procedure of QCM-D sensors and flow modules

Prior to each experiment, the quartz crystal sensors were rinsed with toluene and ethanol to remove organic contaminants, followed with a rinse by Milli-Q water and blow-dried with nitrogen gas. Afterwards, the sensors were cleaned by immersing in a 2 wt. % SDS solution for 30 minutes, and dried with pure nitrogen after rinsing with Milli-Q water. The dried sensors were further cleaned with UV/ozone treatment for 10 minutes. The QCM-D flow modules and connecting tubes also need to be cleaned before each experiment, by following a similar procedure but without UV/ozone treatment.

3.2.2.3 Preparation and characterization of the QCM-D sensor surface

The hydrophobized sensor surfaces were prepared by immersing the silica sensor into octadecyltrichlorosilane (OTS) /Toluene (0.1 vol. %) solution for 30 sec. Then, the treated sensors were rinsed with toluene and dried with nitrogen gas. The bitumen films on both hydrophilic and hydrophobic sensor surfaces were prepared with a spin-coater (Laurell

WS-400A-6NPP/Lite). In order to obtain a smooth bitumen film, diluted bitumen (5 wt. % of bitumen in toluene) used for spin coating was centrifuged and filtered to remove fines and aggregates. The toluene was considered to be an excellent solvent for bitumen due to the high solubility of asphaltene, therefore it was frequently applied in the model system for preparing bitumen surface.[42, 60, 103] Five drops of the diluted bitumen were added on the sensor under rotation at 2500 rpm in a period of 40 sec. Any excess solvent was removed by spinning at 4500 rpm for an additional period of 50 sec. In order to remove a trace amount of solvent, coated sensors were placed in an oven at 50 ºC for 30 minutes and dried in a dust-free chamber for 24 hours. Therefore, only bitumen was left on the silica surfaces, which simulates the bitumen covers on the sand surfaces in oil sands ore. By measuring the resonance frequencies of the bare silica sensor and bitumen coated sensor with QCM-D, the thickness of the coated bitumen layer can be determined.

3.2.2.4 Bitumen liberation by QCM-D

The detachment of bitumen from sensors was studied at various wettability of the solid surface, solution pH, and operation temperature. Figure 3.1 illustrates the steps involved in bitumen liberation experiments. A bare silica sensor was used to mimic the solids (sands) contained in oil sands. The mass and thickness of coated bitumen films were estimated by comparing the resonance frequency between bare silica sensor and bitumen coated one by QCM-D under 22 ºC in air. For all experiments, the fluid flow rate was set at 0.1 mL/min by using a peristaltic pump. A series of solutions with different pHs prepared with NaOH dissolved in Milli-Q water were used in this study, and the operation temperature was set

from 35 ºC to 45 ºC to investigate the effect of temperature on bitumen liberation. A 10 minutes baseline was established by Milli-Q water. Then, the prepared test solution was injected into the system for bitumen liberation.
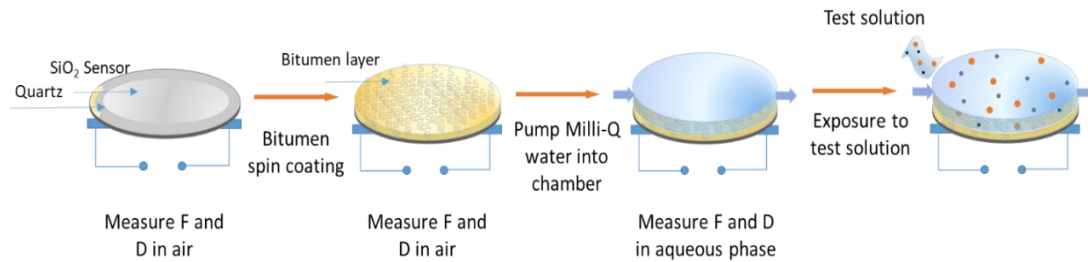
Figure 3.1. Schematic of QCM-D experimental procedures for the effect of different pH on bitumen liberation.

3.2.3 Surface characterization

In order to investigate the morphology changes of sensor surface during QCM-D experiments, the sensors of selected experiments were observed in a Zeiss axioskop 40 polarization microscope. The micrographs of bitumen on the sensor surfaces were obtained using a digital camera. The contact angles of different sensor surfaces were measured with the sessile drop method by using an Attension Optical Tensiometer.

3.3 Results and discussion

3.3.1 Surface characteristics of spin-coated sensors

The spin coating method led to a uniform and fairly smooth bitumen layer on the silica sensor. The contact angle of a DI water droplet on the sensor surface was determined to be

~ 2° and ~ 96° before and after bitumen coating, as shown in Figure 3.2a and Figure 3.2c. After hydrophobizing the silica sensors, the sensor surface looked similar to the untreated sensors but had a contact angle at approximately 66° (Figure 3.2b). The thickness and mass of the bitumen film coated on the sensor were measured based on the steps listed above, and the average thickness was 150 nm. The mass of the coated bitumen was determined before each individual experiment, and used for the liberation efficiency calculation. Due to the limitation of the QCM-D instrument, the thickness of spin-coated bitumen film in this study unable to quantitively simulates the real oil sands ore, but it can qualitatively represent the bitumen covered sand surface.
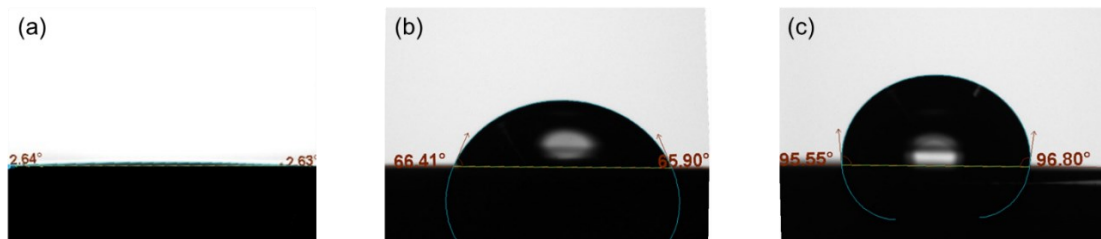
Figure 3.2. Contact angles of a DI water droplet on (a) untreated clean silica sensor (b) hydrophobized silica sensor and (c) bitumen coated silica sensor in air.

3.3.2 Effects of solid wettability on bitumen liberation

The reason that the Athabasca oil sands can be successfully processed by the water-based extraction process is the hydrophilic nature of the solids in the oil sands.[104] However, the wettability of the solids varies largely in oil sands ore, thus resulting in different bitumen recovery efficiency.[53, 105] In order to investigate the impact of solid wettability on bitumen liberation, the hydrophobized silica sensors were applied. The effects of solid wettability

on bitumen liberation were tested at pH 11.5 and 22 °C, and the examples of frequency and dissipation changes with time were shown in Figure 3.3.

When the sensors were exposed to Milli-Q water, two opposite trends of frequency shifts were observed with the hydrophilic (untreated) sensor (Figure 3.3a) and hydrophobized (treated) sensor (Figure 3.3b) respectively. After the injection of NaOH at pH 11.5, a sharp decrease followed with an immediate increase in frequency was found for the untreated sensor, as seen in Figure 3.3a. On the other hand, a slight increase in frequency coupled with a negligible shift in dissipation indicates that only a trace amount of bitumen was detached from the treated (hydrophobized) sensor surface. In the case of the untreated (or hydrophilic) sensor, the drastic change in the corresponding dissipation indicates that the coated bitumen layer was first softened by a mass loading process, and then the surface rigidity was restored due to bitumen detachment. In Figure 3.3b, the negligible shift in dissipation suggests that the sensor surface remained stiff during the entire experiment.
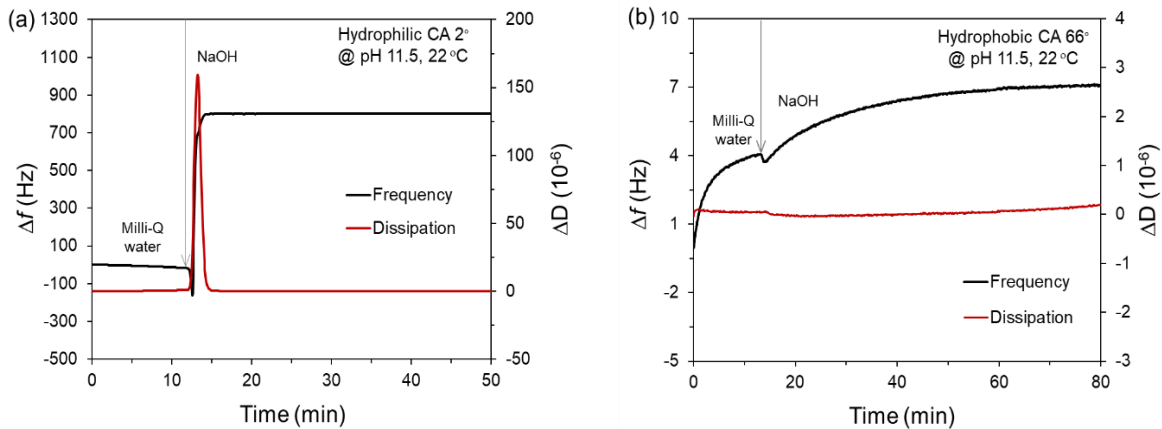
Figure 3.3. Frequency and dissipation changes as a function of time for bitumen detachment from (a) hydrophilic (untreated) and (b) hydrophobic (treated) sensors.

Since the Milli-Q water was used to establish the baseline before injecting NaOH, the liquid loading effects can be neglected. For a fair comparison, the degree of bitumen liberation (DBL), defined as the mass ratio of the removed bitumen to initially coated bitumen in this study, was used to illustrate the effects of different conditions on bitumen liberation. The DBL for the untreated sensor was around 95%, resulting in a nearly clean silica surface after the liberation experiment. However, only 1.2% of the coated bitumen was detached from the hydrophobized silica sensor. The bitumen layer still stayed on the sensor surface after being taken out from the QCM-D module.

Such differences in frequency and dissipation changes between the treated and untreated sensors were caused by their different surface wettability. From this observation, the mechanism of bitumen liberating from the silica sensor was proposed as follows. After the bitumen surface was exposed to the aqueous phase, the dissolution of water-soluble species and the release of natural surfactants from bitumen lowered the bitumen/water (b/w) interfacial tension and altered the distribution of bitumen on the silica surface (Figure 3.4a – 3.4b). Water molecules diffused and penetrated through the b/w interface to form water channels in the bitumen layer. It was believed that the adsorption of surfactants on b/w interface and the wetting of water molecules on silica surface were the driving factors of water channels formation.[98, 106, 107] The expansion of water channels and the deformation of the bitumen layer resulted in a porous structure of bitumen (Figure 3.4c), which was responsible for the decrease in frequency (mass loading) and increase in dissipation (surface softening) in Figure 3.3a. The untreated silica sensor has a hydrophilic (water-

loving) surface, favorable for water penetration and wetting of the silica surface. Because of the hydrogen bonding interactions between water molecules and silica surface, more water molecules were adsorbed on the silica surface over time. The bitumen started shrinking from the solid and forming micro-droplets with the adsorption of natural surfactants on b/w interface (Figure 3.4c – 3.4d).[97, 106-108] A high pH promoted anionic natural surfactants releasing and increased the repulsive force between bitumen and silica (Figure 3.4c). Similarly, increasing temperature reduces the viscosity of bitumen; and the fluid-like bitumen is easier to be deformed to allow more surfactants migrate to the b/w interface (Figure 3.4b, 3.4d), which facilitates the detachment of the bitumen droplets from the sensor surface. Both pH and temperature play significant roles in bitumen detachment from the coated sensor surface.
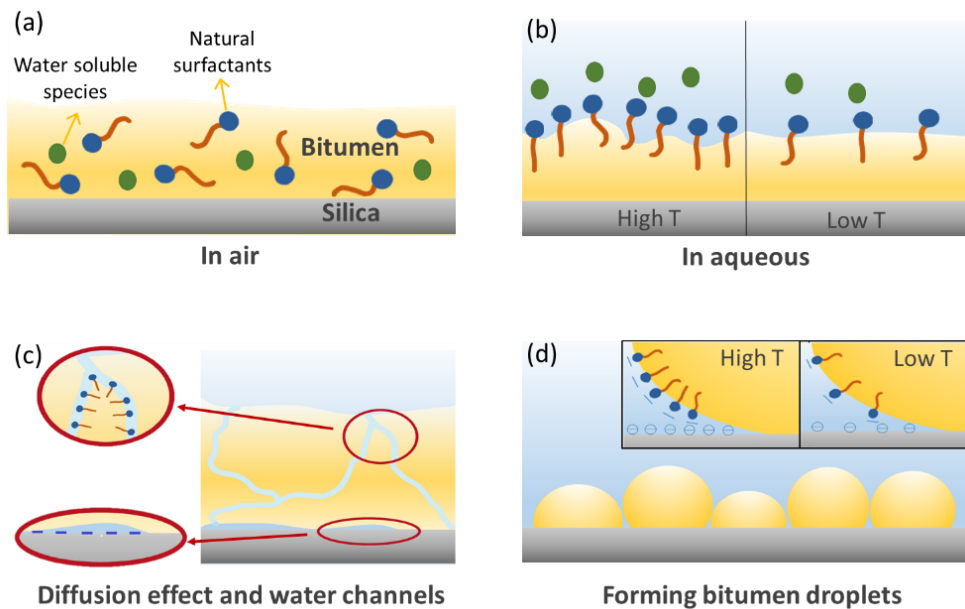
Figure 3.4. Possible mechanism of bitumen detachment from coated sensor surface. (a) The natural surfactants and water-soluble species in bitumen. (b) When the system is

exposed to aqueous, the water-soluble species are dissolved into the aqueous phase, and natural surfactants are migrated to the b/w interface. Increasing temperature and pH facilitates this process. (c) Water penetrates into bitumen film and forms water channels. At a high pH, both silica and bitumen surfaces carry negative charges. (d) Due to the hydrophilic nature of silica, the three-phase contact line (bitumen, water, silica) shrinks. Water gradually occupies the silica surface, and bitumen detachment occurs.

Previous studies on the effect of solid wettability on oil sands processability indicated that hydrophobic solids in oil sands ore deteriorate bitumen recovery. Also, a weak repulsive and strong adhesion forces between bitumen and solids were observed through an atomic force microscope when the solid surface is less hydrophilic.[53, 109] In contrast to the untreated sensor, the treated sensor had a hydrophobic silica surface that was unfavorable for bitumen liberation. The dissolution of water soluble species, or a small amount of bitumen detached could account for the increase in frequency at the beginning. However, it is difficult to form water channels inside the bitumen layer because the hydrophobized silica surface was easier to be wetted by bitumen than by water. The negligible dissipation signal in Figure 3.3b further confirmed this hypothesis. As a result, the coated bitumen layer would stay on the hydrophobic silica surface, rather than detaching from it.

3.3.3 Effects of solution pH on bitumen liberation

Caustic (NaOH) has been widely used as a process aid in the oil sands industry to enhance bitumen recovery. One of the most important reasons is that adding NaOH can adjust the

slurry pH, thus affecting the bitumen liberation process. Figure 3.5 shows the degree of bitumen liberation under different solution pHs at 35 °C by QCM-D.
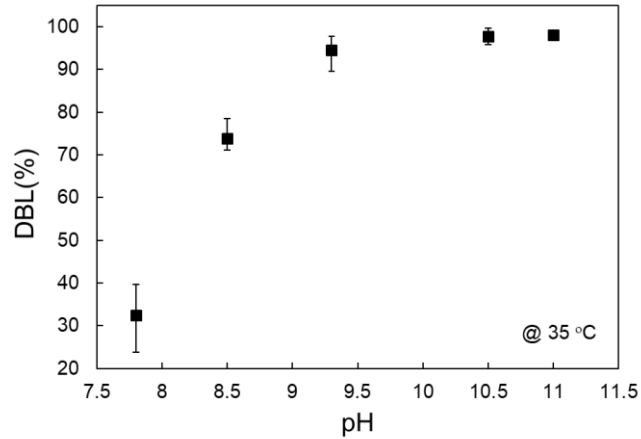
Figure 3.5. Effect of solution pH on bitumen liberation.

The lowest DBL was observed at pH 7.8 at around 32%, while a slight increase in the NaOH dosage from pH 7.8 to pH 8.5 significantly improved DBL. However, the increase in liberation efficiency became insignificant when the pH was higher than 9. Similar enhancement in DBL with an increase in solution pH was reported in previous researches.[2, 15-17, 40, 110] Srinivasa and Flury et al. studied the DBL of the high-grade oil sands ore at various pHs under the temperature of 30 °C. They found that the equilibrium DBL was increased from approximately 30% to 95% with the increase of solution pH from 7.8 to 11.3.[17] In addition, Flury et al. compared the effects of different caustics on the bitumen liberation process. They confirmed that the bitumen liberation was increased with the pH or the concentration of hydroxide ions, but not influenced by the type of caustics.[9] A high pH is more favorable for the ionization and the release of the natural surfactants from the bitumen. Anionic surfactants are easier to be generated in an alkaline condition, and they

migrate to the b/w interface, which consequently decreases the interfacial tension and changes the surface charge[37]. Additionally, increasing pH hydrolyzes the sand grains and makes the sand surface more hydrophilic and more negatively charged, leading to a repulsive interaction between bitumen and silica surfaces.[57, 58] Therefore, it facilitates the formation of water channels and shrinking of the three-phase contact line, and promotes bitumen liberation.
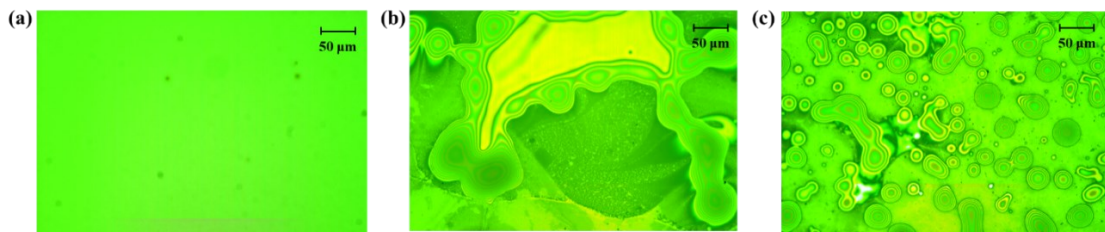
Figure 3.6. Microscopic view of bitumen film on silica surface (a) before liquid flooding, after 30 minutes of NaOH flooding treatment at (b) pH 7.8 and (c) pH 9.3.

The morphology changes of bitumen film with pH are shown in Figure 3.6. Figure 3.6a was obtained before liquid flooding, suggested a clean and smooth bitumen film coated on the silica sensor surface. After QCM-D treatment for 30 minutes under 35 ºC, different morphologies of bitumen surfaces were captured at pH 7.8 (Figure 3.6b) and pH 9.3 (Figure 3.6c). During the first 30 minutes of treatment, water channels started forming and distorted the bitumen film. The shrinking of bitumen film led to the formation of micro-droplets on silica surfaces. At a high pH, bitumen droplets were easily formed on the silica sensor (Figure 3.6c). However, several patches of bitumen film were observed in Figure 3.6b, showing that a lower solution pH is unfavorable for bitumen detachment. This observation

is consistent with the proposed bitumen detachment mechanism and confirmed that a higher pH promotes bitumen detachment.

3.3.4 Effects of temperature on bitumen liberation
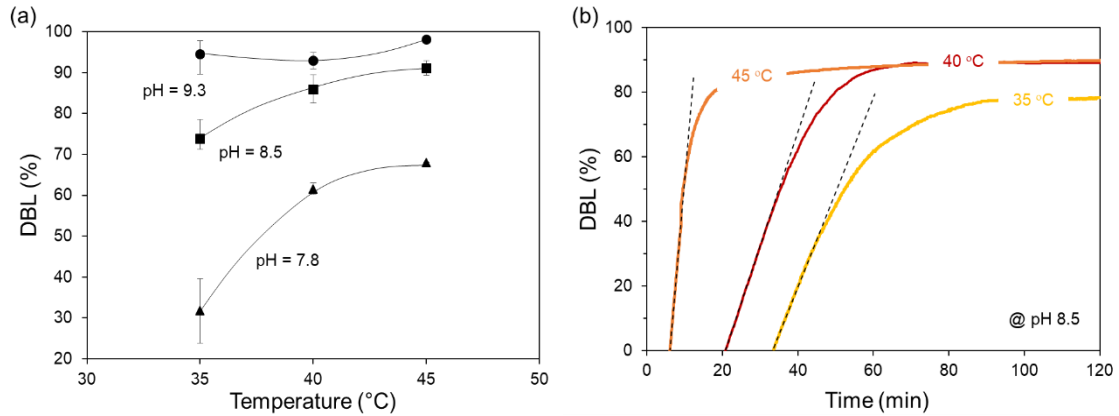
Figure 3.7. Effect of temperature on bitumen liberation by QCM-D. (a) Bitumen detachment efficiency and (b) bitumen detachment kinetics at pH 8.5.

The effects of temperature on bitumen liberation have been widely investigated with both real and model oil sands. Here, three different temperatures of 35 ºC, 40 ºC, and 45 ºC were used to study the effect of temperature on bitumen liberation under different pH conditions. At pH 7.8 and 8.5, increasing temperature significantly promoted the detachment of bitumen from the silica surface. Especially at pH 7.8, the DBL increased from 32% to 61% when increasing temperature from 35 ºC to 40 ºC. This finding was consistent with the previous bitumen liberation results with BLFVC, where a significant improvement in bitumen liberation behavior was observed when increasing temperature from 30 ºC to 46 ºC under pH 7.8.[17] It is not surprising to observe that the DBL does not sensitively respond to temperature variation at a high pH level (pH 9.3), since such high pH is sufficient for

almost all the bitumen to be liberated from the sensor surface. The rates of bitumen liberation curve of selected points at pH 8.5 were plotted in Figure 3.7b, which shows the effect of temperature on bitumen detachment kinetics. The DBL at the highest temperature required the least time to reach the equilibrium. Moreover, the initial slope of bitumen liberation kinetics increased with increasing temperature. By investigating the effects of temperature on bitumen liberation, Wallwork et al. found that the bitumen liberation rate was accelerated by increasing temperature for both high fines and low fines ores.[13] It is well-known that increasing temperature enhances both the DBL and liberation kinetics, which relies on the significant reduction in bitumen viscosity and the change of interfacial interactions between bitumen and solid.[31, 40, 111] The viscosity of Athabasca bitumen decreases in the order of magnitude with the increase in temperature, and the fluid-like bitumen at a high temperature is easier to be rolled up.[112] It is believed that increasing temperature not only reduces the viscosity of bitumen but also enhances the repulsive forces between bitumen and silica.[40] Similarly, Long et al. reported the adhesion force between bitumen and solid surface decreased, and the long-range repulsive force increased with increasing temperature, leading to an enhancement in bitumen liberation.[111] A high temperature promotes the surfactants releasing from bitumen, which results in a strong repulsive force between bitumen and silica surface.

It is worth noting here that the DBL value of bitumen coated silica sensor cannot be identical with those real oil sands ores since the real oil sands ores are complex mixtures containing unexpected variables. However, the trend of bitumen liberation was the same

as comparing with real oil sands ores under different conditions. The QCM-D method is capable of accurately quantifying the bitumen liberation process and verifying the effects of process variables from real oil sands ores (i.e. different solid wettability, clay types, and processing aids) on bitumen liberation, which makes the QCM-D a powerful tool for the fundamental understanding of bitumen liberation.

3.4 Conclusions

In this study, the QCM-D was used to study bitumen liberation under different process conditions. By comparing the frequency and dissipation changes between the untreated sensor and the hydrophobized sensor, a mechanism of bitumen detachment from the silica surface was proposed. A hydrophobic solid surface is unfavorable for bitumen detachment from the solids under the normal water-based extraction process conditions because water channels were unable to form between bitumen and hydrophobic silica. Increasing pH is beneficial for bitumen liberation. A higher temperature led to faster liberation kinetics and a better DBL due to a decrease in bitumen viscosity. QCM-D is a powerful tool for investigating the fundamental mechanism of bitumen liberation, which provides an unprecedented opportunity to study the effect of various process aids, the solid types (different clays) on bitumen liberation in the future research.

Chapter 4

Study of the Role of Sodium Citrate in Bitumen Liberation

Abstract

A novel secondary process aids (SPA), sodium citrate (Na_3Cit), recently has been applied in oil sand extraction industries. It was discovered that adding sodium citrate as a secondary process aid with sodium hydroxide (NaOH) enhanced the bitumen recovery of both good and poor processing ores. In this study, we investigated the synergetic effect of sodium citrate and sodium hydroxide on the bitumen liberation. A quartz crystal microbalance with dissipation (QCM-D) was applied to estimate the bitumen liberation from silica surface in the presence of NaOH only, Na_3Cit only, and their mixture (1:1 molar ratio). It was observed that the degree of bitumen liberation (DBL) increased when the concentration of chemical aids increased. More importantly, the combination of sodium citrate with sodium hydroxide showed the highest DBL. The colloidal interactions between bitumen and silica measured with an atomic force microscope (AFM) indicated that adding Na_3Cit into the solution reduced the adhesive force between bitumen and silica. Meanwhile, the adhesive forces became negligible with the addition of NaOH and the 1:1 mixture of NaOH and Na_3Cit. Zeta potential results indicated that the combined addition of NaOH and Na_3Cit led to a more negatively charged surface of both bitumen and silica. A stronger repulsive force between bitumen and silica surfaces resulted in a weaker adhesion between bitumen and silica, leading to the efficient detachment of bitumen from silica surfaces, which in turn increased the degree of bitumen liberation. The possible mechanism of the synergistic effect of NaOH and Na_3Cit on modifying the surface properties of bitumen and silica is elucidated in this study.

4.1 Introduction

The depletion of high-grade minable oil sands deposits and the increase in the demand for fossil fuel resources stimulated the recent development of new technologies on the oil sands extraction process. Increasing the processability of oil sands ore and minimizing the harmful impact on the environment becomes the priority to oil sands industries. The current commercial technology to extract bitumen from Athabasca minable oil sands is known as the warm-water-based extraction process.[2, 113] Chemical aids are usually introduced in this process for the purpose of enhancing bitumen extraction performance. For example, caustic (normally sodium hydroxide) is the most commonly used process aids in oil sands industries, due to its low cost and high efficiency in bitumen extraction. Over the past decades, numerous studies have been focused on investigating the roles of sodium hydroxide (NaOH) in the bitumen extraction process. These studies showed that adding sodium hydroxide increased the slurry pH and altered the surface properties of both bitumen and sands. It was proposed that surface-active components contained in bitumen were released in an alkaline condition, which decreased the interfacial tension of bitumen/water (b/w) and allowed the bitumen surface to carry more negative charges.[6, 37, 57] On the other hand, sand grains were hydrolyzed at a high pH condition, leading to a hydrophilic and negatively charged sand surfaces.[58] As a result, a stronger repulsion between bitumen and sand grains is generated, which benefits bitumen liberation.[42] Moreover, the addition of NaOH was reported to reduce the concentration of divalent cations, which potentially reduced the slime coatings and increased bitumen recovery.[5]

It was also found in literatures that addition of NaOH showed a limited enhancement in bitumen extraction on poor-processing ore. Schramm et al. compared the processability of three different grades of oil sands ores and concluded that the bitumen recovery only reached an average level for the poor-processing ore even when a high dosage of NaOH was applied.[6] Therefore, the researchers have been devoted to reduce the usage of caustic and to find alternative chemicals that not only increase the bitumen extraction from poor-processing ore but also have no negative impacts on the environment. Several other chemical aids have been tested in industries and laboratory-scale extraction experiments for many years. For example, in 1983, kerosene was added as a diluent in the hot water digestion flotation test of oil sands by Hupka et al..[114] Later, Schramm et al. applied kerosene and methyl isobutyl carbinol (MIBC) in oil sands extraction.[115] These researches pointed out that the addition of diluent reduced the viscosity of bitumen, which promoted the detachment of bitumen from solid and significantly improved the bitumen recovery.[114-116] Later on, Li et al. reported that direct addition of hydrolyzed polyacrylamide (HPAM) not only increased the bitumen recovery but also facilitated the settling of tailings.[7] Their AFM results indicated a decrease in the adhesion between silica and bitumen, and an increase in the adhesion between silica and clay in the presence of HPAM, which proved the selective flotation of bitumen using HPAM.[7] Meanwhile, the acidified sodium silicate was applied in extracting poor-processing oil sands ore; and the better bitumen liberation performance and faster flotation rate were achieved as compared to the traditional caustic (sodium hydroxide).[8] Additionally, Flury et al. reported the effect of various caustics on bitumen extraction performance in order to discover a substitute for NaOH.[9] However,

there was no clear conclusion in these studies regarding to the best chemical aids for oil sands extraction, and none of such chemicals was applied in oil sands industries.

Recently, a novel secondary process aids, sodium citrate (Na_3Cit), was discovered and applied in combination with NaOH to oil sands extraction industries. Sodium citrate is a non-toxic and eco-friendly chemical, which has been widely applied as food additives or to soften drinking water. Compared to the traditional caustic, the combined addition of Na_3Cit with NaOH significantly enhanced the oil sands processability of both good ores and poor ores, leading to higher bitumen recovery and better froth quality.[11] To our best knowledge, this is the first time that Na_3Cit together with NaOH, has been successfully applied in oil sands industries. Such an innovation not only reduces the usage of caustic but also enhances the bitumen extraction from the poor ores. However, the fundamental mechanism of how Na_3Cit enhances the oil sands extraction performance remains unclear. Bitumen liberation represents the displacement of bitumen from sand grains. As one of the essential steps in the warm-water-based extraction process, the mechanism and method of bitumen liberation had been well developed. By video recording, both the bitumen film displacement from a glass surface and the dynamic liberation of bitumen from real oil sands can be investigated.[15, 17] However, in the present study, a quartz crystal microbalance with dissipation (QCM-D) was applied to quantitatively study the liberation process instead of the traditional methods. The purpose of this study is to investigate the effect of Na_3Cit in combination with NaOH on the bitumen liberation and on the surface properties of bitumen and sand grains.

4.2 Materials and methods

4.2.1 Materials and chemicals

Silica sensors (QSX 303, Q-Sense) were used for bitumen liberation experiments by QCM-D, and the - 15 μm silica particles (U.S. Silica) with a median diameter (d_{50}) of 6.2 μm were applied for zeta potential measurements. The AFM probes with silica sphere (d = 6.62 μm) at the end of the cantilever were purchased from NanoAndMore (USA), and the substrates were prepared by octadecyltrichlorosilane (OTS) (≥ 96% purity, Sigma Aldrich) treated silicon wafers (NanoFAB, CA). The vacuum distillation unit (VDU) feed bitumen used in this study was provided by Syncrude Canada Ltd. The 1N sodium hydroxide solution, 1N hydrochloride acid, ethanol (91% purity) and potassium chloride (≥ 99% purity) were purchased from Fisher Scientific. Sodium citrate dihydrate (≥ 99% purity), sodium dodecyl sulphate (SDS, 99% purity), heptane (≥ 99% purity) and toluene (99.8% purity) were purchased from Sigma Aldrich. The Milli-Q water with a resistivity of 18.2 MΩ·cm was used throughout this study.

4.2.2 Bitumen liberation by quartz crystal microbalance with dissipation

4.2.2.1 Preparation of bitumen film

The bitumen liberation efficiency can be significantly influenced by the states of the solid surface, such as the extent of hydration and the surface wettability.[117] In order to eliminate the influence of silica surface properties, the cleaning procedures for the silica sensor maintained the same for all experiments. Prior to each experiment, the silica sensor was

rinsed with toluene and ethanol to clean the organic residuals, followed by sonication in 2 wt. % of SDS for 30 mins. After rinsing with Milli-Q water, the sensor was dried with pure nitrogen gas and treated with UV/ozone for 10 mins. The contact angle of a water droplet on the cleaned silica sensor was determined at 0°, indicating a clean and fully hydrophilic silica surface. 5 wt. % of bitumen in the toluene solution was centrifuged at 20,000 × g for 15 mins and filtered to remove the fines and aggregates. The bitumen film was prepared by using a spin coater (Laurell WS-400A-6NPP/Lite). Five drops of the diluted bitumen were added on the clean silica sensor at a rotation speed of 2,500 rpm within 40 s, and then the excess solvent was removed by spinning at 4,500 rpm for an additional 50 s. In order to further remove the trace amount of solvent, the bitumen coated sensor was transferred into an oven at 50 ºC for 30 mins and dried in a dust-free chamber for 24 hrs. The details of preparing bitumen film and the bitumen surface characterization results were reported in our previous study.[76]

4.2.2.2 Bitumen liberation measurements

To estimate the effect of secondary processing aids on the degree of bitumen liberation (DBL), QCM-D was applied to monitoring the detachment of bitumen from a silica sensor under the flooding condition. The QCM-D measurement is able to detect the frequency and dissipation variation of a piezoelectric sensor, thereby estimating the mass changes by Sauerbrey equation.[100] The principle of QCM-D was well-described in many studies.[19, 101, 118] The clean procedures for the flow modules and tubings were the same as described in the cleaning silica sensor, excludes the UV/ozone treatment. Three series of solutions

(NaOH, Na₃Cit and the 1:1 mole ratio mixture of them) were prepared at the concentration of 0.1 mM, 0.2 mM and 0.5 mM. The resonance frequency of the sensor before and after coating was measured in air in order to calculate the thickness and mass of the coated bitumen layer, and the thickness of the bitumen film was ranged from 145 nm to 168 nm. The details of the thickness calculation can be found in our previous study[14]. The liberation tests were carried out at 30 °C under a flow rate at 0.1 mL/min for all experiments. The Milli-Q water was used to establish the baseline for 10 mins, then switched to the prepared sample solutions. Frequencies and dissipations were recorded for data analysis with Q-tool software. Sauerbrey relation and the Voinova−Voigt model (when dissipation > 5% of the frequency change) were applied to estimate the mass variation on the sensor. The degree of bitumen liberation was calculated as the mass ratio of the removed bitumen to initially coated bitumen (Eq. 4.1).

$$DBL\ (\%) = \frac{Mass\ of\ removed\ bitumen}{Mass\ of\ coated\ bitumen\ layer} \tag{4.1}$$

4.2.3 Surface force measurement

4.2.3.1 Substrate preparation

The silicon wafer was cut into 15×15 mm square pieces and use as the substrate for the bitumen film. Before experiments, the silicon wafers were first cleaned by a heated piranha solution ($V_{98\%\ H2SO4}$:$V_{30\%\ H2O2}$ = 3:1) for 30 mins at 90 °C, and rinsed with Milli-Q water. Then, the silica wafers were further treated by UV/ozone for 10 mins and blow-dried by the ultrapure nitrogen gas. In order to ensure the bitumen layer tightly staying on the substrate, those cleaned silicon wafers were hydrophobized by immersing them into the

0.1 wt. % of OTS in toluene solution for 2 mins and rinsed with toluene. After hydrophobized, the average contact angle of water droplets is 83°. The diluted bitumen was prepared at a concentration of 2.5 mg bitumen per ml toluene. The same procedures were applied here to remove the fine solids in diluted bitumen and to coat the bitumen on hydrophobized substrates as described in preparation of bitumen film for QCMD.

4.2.3.2 Force measurements

AFM has been widely applied in studying the interactions between different phases in oil sands extraction, and the principle and operations were well described in many other published works[42, 55, 119-122]. In this study, interaction forces between silica and bitumen in aqueous solutions were measured by using the colloidal probe technique on an MFP-3D AFM system (Asylum Research, Santa Barbara, CA). Rectangular silicon cantilever with a 6.62 µm diameter SiO_2 sphere attached at the end and bitumen coated wafers were employed for force measurements. To produce a clean sphere, the AFM cantilever was rinsed with toluene and acetone and dried with high-purity nitrogen, followed by 1 min of UV/ozone treatment. The spring constants of the cantilever were determined to be in the range of 0.3 - 0.4 N/m by Hutter and Bechhoefer method. Prior to each experiment, the target solution was slowly injected onto the bitumen coated wafers to avoid trapping air bubbles. Both the probe and surfaces were immersed in the solution for 30 mins for equilibrium. The cantilever was driven toward the bitumen coated wafer at a velocity of 1 µm/s until an applied force of 20 nN was detected. The force - separation curves were taken at more than 50 positions of two wafers with freshly prepared AFM cantilevers to ensure

reproducibility. For clarity, only one representative force curve was shown in this work. The so-called adhesion force required to separate the silica sphere from the bitumen coated wafer was calculated and statistically evaluated. All the force curves have been normalized by the radius of the silica sphere (3.31 µm).

4.2.4 Zeta potential measurement

4.2.4.1 Preparation of stock suspensions

A solvent-diluted bitumen was prepared at a mass ratio of bitumen:heptane:toluene = 1:3:1, then centrifuged at $10,000 \times g$ for 20 mins to remove any solids contained in bitumen. 1 mL of solid-free diluted bitumen was added into 40 mL of 1 mM KCl solution, and heated to 85 °C for 15 mins to evaporate the organic solvent. The bitumen stock emulsion was then generated by a Model 550 sonic dismembrator (Fisher) for 10 mins, and the bitumen emulsion was considered as free of solids and solvent. The emulsified bitumen suspension had an effective diameter of 1.68 µm which increased to 1.72 µm after 6 hrs creaming (measured by Brookhaven ZetaPALS). Therefore, the prepared bitumen emulsion was considered to be stable during the zeta potential measurements. The stock suspension of silica was prepared by mixing 1 g of silica particles into 1 L of 1 mM KCl solution in a volumetric flask.

4.2.4.2 Zeta potential measurements

Sample solutions were prepared by adding different amounts of interested chemical aids into 1 mM KCl solution. For each zeta potential measurement, 5 mL of the stock bitumen or silica suspension was added into 100 mL of prepared sample solutions and stirred by a

magnetic mixer for 10 mins. The conditioned sample was then transferred into a sample cuvette for measurement. A Brookhaven ZetaPALS was used for measuring the zeta potential of silica particles and bitumen droplets, and the temperature was set at 22 ºC. Each sample was measured with 10 runs (5 cycles for each run), and the average value of these 10 runs was recorded. According to the results, the standard deviation for 10 runs was within ± 5 mV.

4.3 Results and discussion

4.3.1 Effect of different chemical aids on bitumen liberation by QCM-D

4.3.1.1 Bitumen liberation with QCM-D

To explain the liberation mechanism, the schematic view of the bitumen liberation from a silica sensor surface and the corresponding QCM-D raw data are shown in Figure 4.1. During the experiment, the Milli-Q water was first pumped into the QCM-D flow module to establish a baseline, followed by the injection of sample solutions. Later, the Milli-Q water was switched back into the system in order to wash off the adsorbed chemical aids. When Milli-Q water was firstly injected, the surfactants contained in bitumen migrated to the bitumen/water (b/w) interface, which lowered the interfacial tension of b/w interface and altered the distribution of the bitumen layer on the silica surface. The water channels started forming and led to a slight decrease of frequency. This process was suddenly facilitated by the injection of interested chemical aids solutions, and resulted in an expansion of water channels inside the bitumen layer.[76, 97] Thereby, a sharp decrease in the

frequency and an increase in the dissipation can be found in Figure 4.1 after injecting sample solutions into the system. Then, the bitumen layer started shrinking from the silica surface and forming bitumen droplets, which reflected by a continuous increase in the dissipation signal. Finally, those droplets detached from the sensor surface and resulted in an increase in the frequency and a decrease in the dissipation, which is referred to the bitumen liberation process. Since the bitumen detachment levelled off at its maximum and the rigidity of the sensor surface was recovered, the shifts of both frequency and dissipation reached the equilibrium.
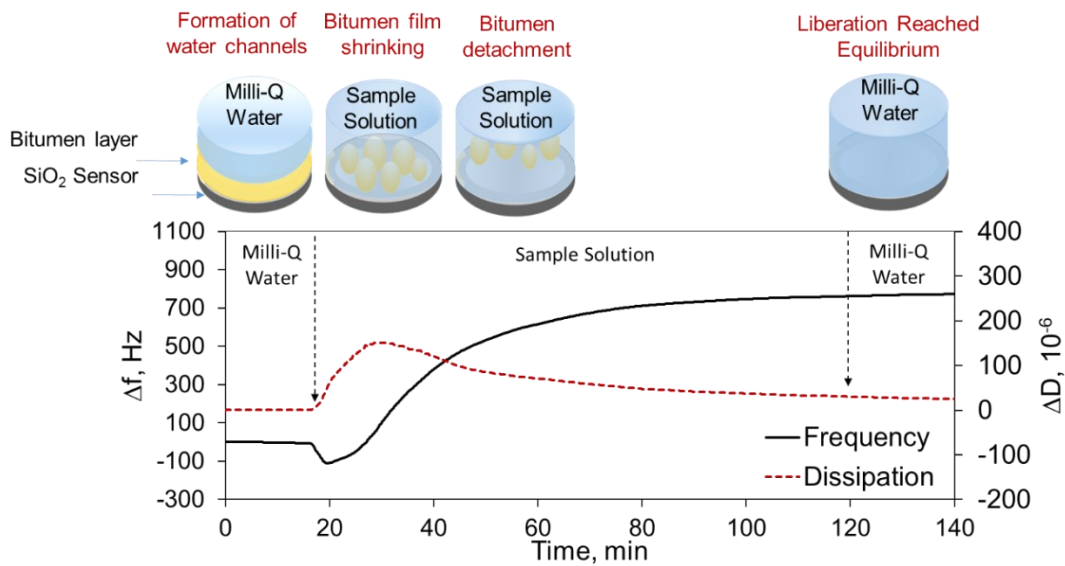
Figure 4.1. Schematic view of bitumen liberation by QCM-D.

4.3.1.2 Effect of chemical aids on bitumen liberation.

As one of the critical steps in the water-based bitumen extraction process, bitumen liberation plays an important role in manipulating bitumen recovery. Applying chemical process aids could potentially improve the efficiency of bitumen liberation, thus increasing

the bitumen extraction. The effects of NaOH and Na_3Cit on bitumen liberation were investigated in this study. For a fair comparison, the total chemical dosage was controlled at 0.1, 0.2 and 0.5 mM for all three conditions, i.e., NaOH, Na_3Cit and the 1:1 mole ratio for the mixture. The pH of each solution was measured before QCM-D tests and plotted in Figure 4.2. It was found that adding NaOH into Milli-Q water drastically increased the solution pH, while sodium citrate showed a moderate effect on pH. Applying Na_3Cit as a SPA with NaOH (a mixture of them at 1:1 mole ratio) results in a slightly lower pH value than applying sodium hydroxide alone.
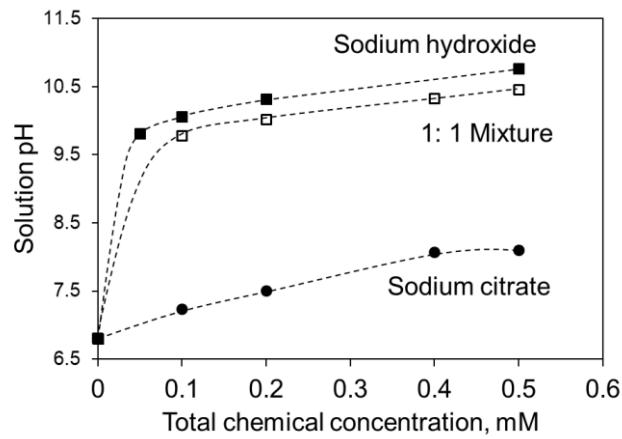
Figure 4.2. Effect of chemical aids dosage on solution pH.
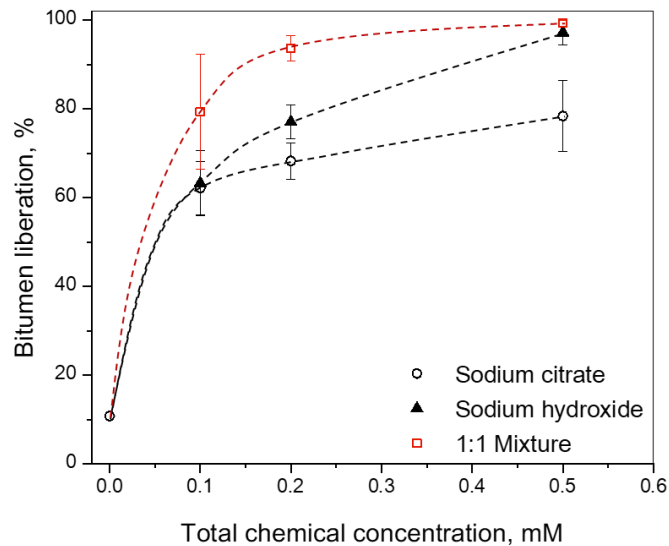
Figure 4.3. Bitumen liberation with different chemical aids.

The liberation results are shown in Figure 4.3. The degree of bitumen liberation increased with increasing the chemical dosage at all three testing conditions. Applying NaOH alone, the DBL raised to 93.6% at the concentration of 0.5 mM. Sodium citrate showed less enhancement in DBL as compared to NaOH, although it still increased DBL approximately from 10% to 80%. The reason that sodium hydroxide had a much higher DBL than sodium citrate possibly relies on their different solution pHs. However, it was surprisingly observed that the mixture produced the highest DBL for all testing concentrations, indicating a synergistic effect between NaOH and Na_3Cit on bitumen liberation. This observation explained the oil sands extraction results reported by Long et al.[11], since a good performance in bitumen liberation could be the reason for a higher bitumen recovery and better froth quality. At a low concentration (0.1 mM and 0.2 mM), the combined addition of chemical process aids generated a quite high level of DBL, roughly 15% and 25% higher

than applying NaOH or Na$_3$Cit separately. Increasing the concentration to 0.5 mM, the DBL of both sodium hydroxide and the mixture reached > 90%, but the mixture showed a fast liberation.

4.3.2 Colloidal interactions studied by AFM
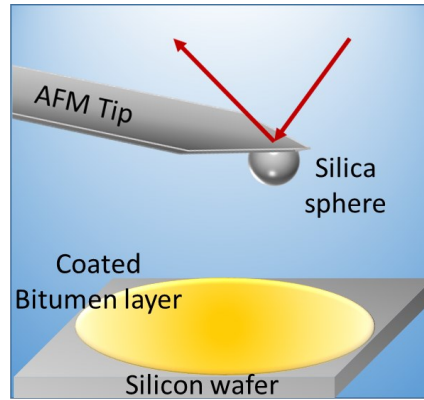
Figure 4.4. Schematic view of the AFM experimental setup.

Bitumen liberation is largely controlled by the interaction forces between bitumen and sand. Therefore, measuring the adhesion between bitumen and silica is critically important to understand the fundamentals of bitumen liberation[42]. The total chemical concentration of 0.2 mM was selected to investigate the interactions between bitumen and silica surfaces, and all the chemical aids were prepared in 1 mM of KCl solution. The schematic force measurement setup was illustrated in Figure 4.4, and the representative force-distance curves with summarized adhesive forces were plotted in Figure 4.5. The adhesion distributions and the long-range interaction forces for bitumen and silica in 1mM of KCl (Figure 4.5a) were agreed well with the previously published work by Liu. et al[42] and Hogshead. et al[122], with the value of the adhesion forces in a range of 1 to 4 mN/m. It can

71

be noticed that the adhesive forces reduced and the long-range repulsive forces increased after the addition of chemical aids. Comparing the 0.2 mM of Na_3Cit in 1mm of KCl solution with the 1 mM KCl solution, a slight increase in long-range repulsion force was observed in Na_3Cit solution, and the adhesion forces decreased to less than 2 mN/m for Na_3Cit (Figure 4.5b). Figure 4.5c and 4.5d showed the bitumen-silica interaction forces in NaOH and the 1: 1 mixture of NaOH and Na_3Cit, respectively. The two approach curves are similar to each other, suggesting the similar repulsive forces between bitumen and silica under these two conditions, even though the 0.2 mM of NaOH has a higher solution pH than 0.2 mM of mixture. Moreover, the normalized adhesive forces between bitumen and silica for these two conditions were found negligible (less than 0.1 mN/m) for all the tests. These results indicated that the bitumen substrate was unable to wet the silica tip under these two conditions, which is beneficial for the bitumen liberation process.
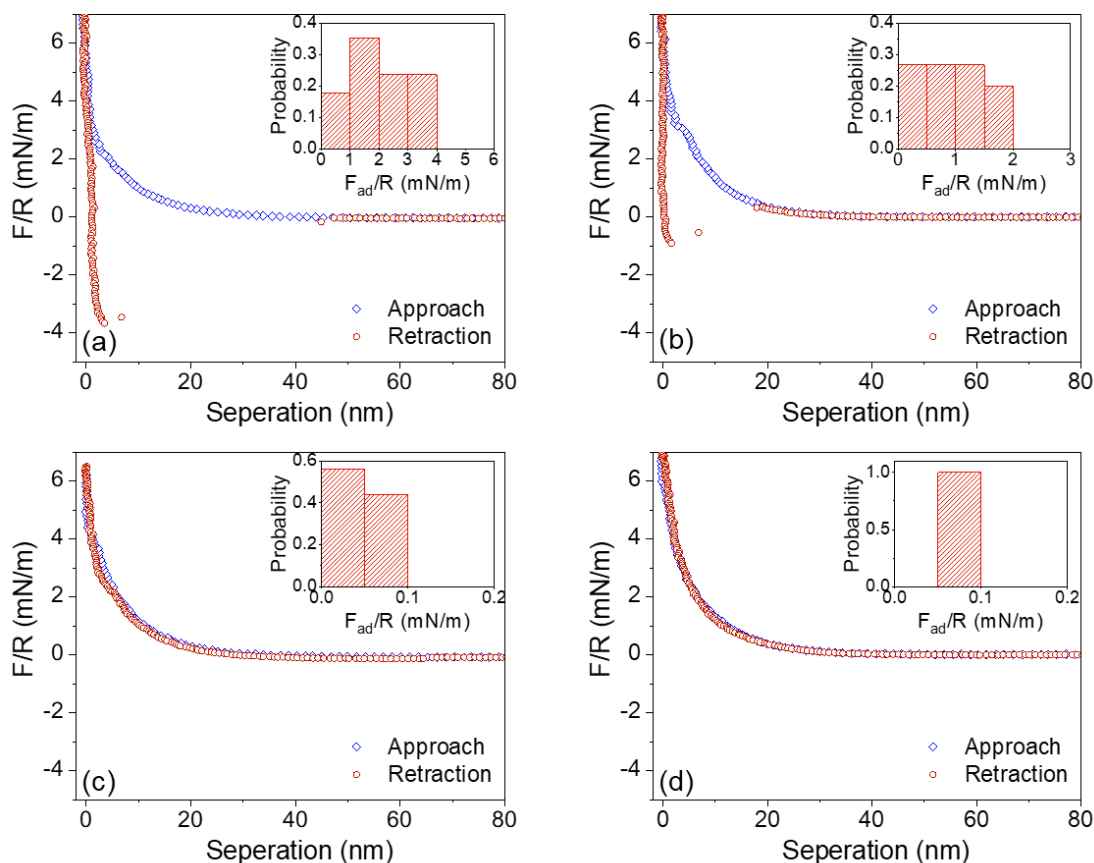
Figure 4.5. Representative force (F/R) – distance approach (blue) and retraction (red) for the silica-bitumen interactions in (a) 1 mM of KCl, (b) 0.2 mM of Na_3Cit + 1 mM of KCl, (c) 0.2 mM of NaOH + 1 mM of KCl, (d) 0.2 mM of mixture + 1 mM of KCl.

4.3.3 Results of zeta potential measurements

Based on our bitumen liberation data, the combination of NaOH and Na_3Cit has been proven to effectively increase the bitumen detachment from a silica surface. To better understand the fundamental science underpinning the bitumen liberation, zeta potentials of bitumen and silica were measured in different chemical aids concentrations (0.2 to 2 mM). The pH values of sample solutions were measured before mixing with the prepared stock

suspensions, and results are summarized in Figure 4.6. Due to the addition of 1 mM KCl in the sample solutions, the pH values were slightly lower than those applied in QCM-D experiments. However, the trend was the same, that NaOH generated the highest alkaline solution.
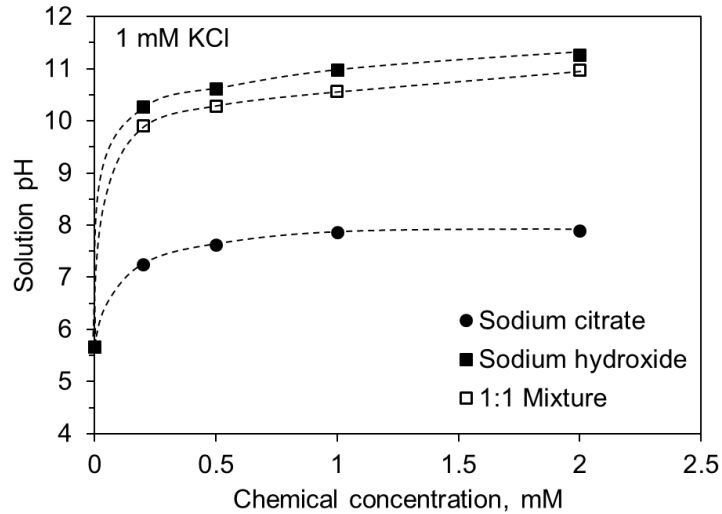
Figure 4.6. Effect of chemical aids dosage on pH of 1 mM KCl solution

4.3.2.1 Effects of chemical process aids on the zeta potentials of bitumen

The zeta potentials of bitumen droplets with various chemical process aids are shown in Figure 4.7. As can be seen from the results, bitumen carried negative charges for all three conditions, and the zeta potential became more negative with increasing chemical dosages. The addition of sodium hydroxide drastically increased the solution pH from a moderate value to 11, and decreased the zeta potential of bitumen suspension from -45 mV to around -120 mV. This agreed well with the value reported by Gan and Liu, that the zeta potential of bitumen levelled off at -120 mV when the pH increased above 8.[62] Apparently, adding Na₃Cit also increased the negative charges on bitumen surfaces, with a less negative value

than that of sodium hydroxide. The most effective condition is the combination of NaOH

and Na₃Cit, which decreased the zeta potential to around -140 mV.
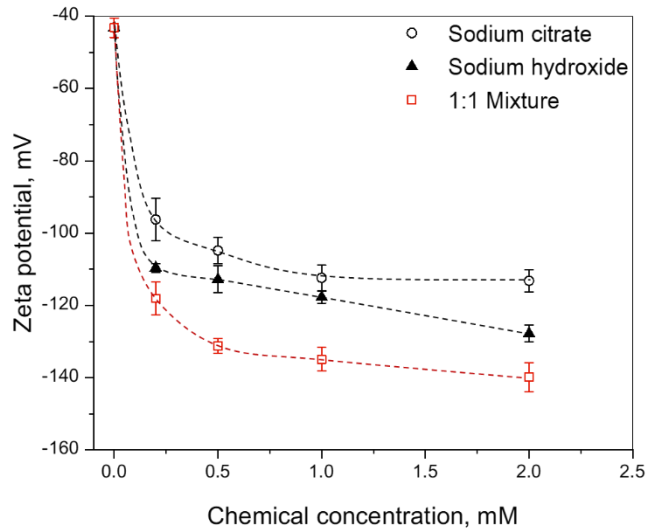
Figure 4.7. Zeta potential of bitumen droplet as a function of chemical aids addition.

4.3.2.2 Effects of chemical process aids on the zeta potentials of silica
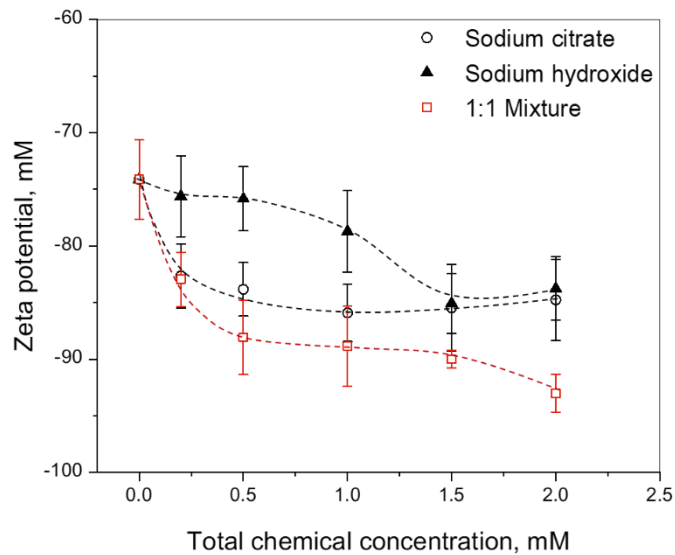
Figure 4.8. Zeta potential of silica suspensions as a function of chemical aids addition.

Similarly, the silica surface was negatively charged during the entire experiment. However, chemical aids showed different trends of silica zeta potentials as a function of concentrations when compared with the zeta potentials of bitumen (Figure 4.8). Unlike bitumen, the addition of sodium hydroxide showed negligible effects on the zeta-potential of silica at low concentrations. The zeta potential was stabilized around -75 mV when the concentration was lower than 0.5 mM. With increasing the sodium hydroxide concentration, the zeta potential of silica particle dropped to around -85 mV. According to the literature, the zeta potential of silica is sensitive to the solution pH at a low pH range, particularly carrying a positive value when the pH below the isoelectric point (normally pH ~2.1).[42, 44] In general, the decrease of silica zeta potential will reach the equilibrium at a high pH.[123] With the addition of sodium citrate, the zeta potential of silica suspension decreased to around -85 mV at a concentration of 1.0 mM, and stabilized around this value. More interestingly, the most negatively charged silica surfaces were observed in the presence of both sodium citrate and sodium hydroxide at 1: 1 molar ratio mixture. The zeta potential decreased from -75 to approximately -95 mV with increasing the total chemical concentration, indicating a more negatively charged silica surface than applying sodium hydroxide or sodium citrate alone. The results of zeta potential measurements suggest that the addition of sodium citrate and sodium hydroxide together made the surface of both bitumen and silica more negatively charged.

4.3.4 Discussion

4.3.4.1 Effects of zeta-potential and interaction force on bitumen liberation

The detachment of bitumen from the silica (sand) surface is directly related to the adhesion forces between them. The increase in the negative surface charges of both bitumen and silica enhances the electrical repulsive forces, leading to less adhesion forces between them and results in a better bitumen liberation.[2, 40] Apparently, one of the most important effect of adding sodium hydroxide in the bitumen liberation process is to modify the solution pH, as shown in Figure 4.2 and Figure 4.6. A high pH environment promotes the ionization of anionic surfactants that naturally contained in bitumen, and their migration to b/w interface.[6, 9, 34, 40] This explained why the zeta potential of bitumen decreased after adding sodium hydroxide (Figure 4.7). Additionally, silica surfaces carried negative charges at all the tested concentrations of sodium hydroxide (Figure 4.8) because of the deprotonation of the silanol group.[42, 58] Therefore, through increasing the solution pH, two surfaces were more repulsive to each other, which can be observed from the increase in the long-range repulsive forces between bitumen and silica. Meanwhile, the negligible adhesion between bitumen and silica resulted in an enhancement in the bitumen liberation.

In Figures 4.7 and 4.8, adding sodium citrate also decreased the zeta potential of both bitumen and silica, with a smaller extent when compared to sodium hydroxide. A similar trend was found in the AFM results; a small reduction of adhesion forces led to a marginal enhancement in DBL. However, the mechanism for Na_3Cit modifying the bitumen–silica interactions is different from NaOH. In Figure 4.2, increasing the concentration of Na_3Cit only slightly modified the solution pH in a range from 7 to 8. However, a similar DBL (~76%) was achieved by the 0.5 mM Na_3Cit with a low pH ~ 8 as compared to 0.2 mM

NaOH with a high pH ~ 10.3, indicating that bitumen liberation was not only attributed to solution pH.

In the experiments of 1:1 molar mixture, a less amount of NaOH was used, and the pH value of the mixture was slightly lower than applying sodium hydroxide alone. However, the adhesion forces between bitumen and silica are similar to those by adding NaOH alone. One of the possible reasons is that the solution pHs for both NaOH and mixture are high enough to eliminate the adhesion forces. Surprisingly, the mixture of Na_3Cit and NaOH led to the most negatively charged surfaces of both bitumen and silica as compared to applying them individually (Figure 4.7 and 4.8). Also, the use of mixture generated the highest DBL, indicating a synergetic effect between NaOH and Na_3Cit in bitumen liberation.

4.3.4.2 Possible mechanisms on how sodium citrate modifies the surface properties of bitumen and silica.

In order to understand the mechanism behind the synergistic effect of the mixture, zeta potentials of bitumen droplets as a function of pH in the absence and presence of 1 mM sodium citrate were measured and shown in Figure 4.9a. In the absence of sodium citrate, the bitumen sample had an isoelectric point (IEP) at pH 4.5. After adding sodium citrate, the IEP of bitumen only slightly moved towards an acidic direction, suggesting the marginal adsorption of sodium citrate on bitumen surfaces. However, the zeta potentials of bitumen became more negative in the presence of sodium citrate at a wide pH range. Compared with the value of -110 mV in the absence of sodium citrate, the zeta potential of bitumen droplets decreased rapidly to -140 mV with the addition of sodium citrate when

the solution pH was higher than 10. The speciation diagram of 1 mM citric acid in 1 mM KCl aqueous solution is constructed by using data from literature[67] and is shown in Figure 4.9b. The concentration of citric acid (acid form) decreased with increasing solution pH and vanished after pH 6. Simultaneously, the deprotonation of carboxyl groups from sodium citrate led to more negatively charged species with rising pH. From the speciation diagram and the zeta potential results, it was found that the decrease in the zeta potential of bitumen in the presence of sodium citrate was attributed to the deprotonation of carboxyl groups of citrate at a high pH value. The difference in zeta potentials between two curves in Figure 4.9a becomes more apparent after pH 5 and then stabilized after pH 9 due to the complete dissociation of citrate ions (Figure 4.9b).

(a)

(b)
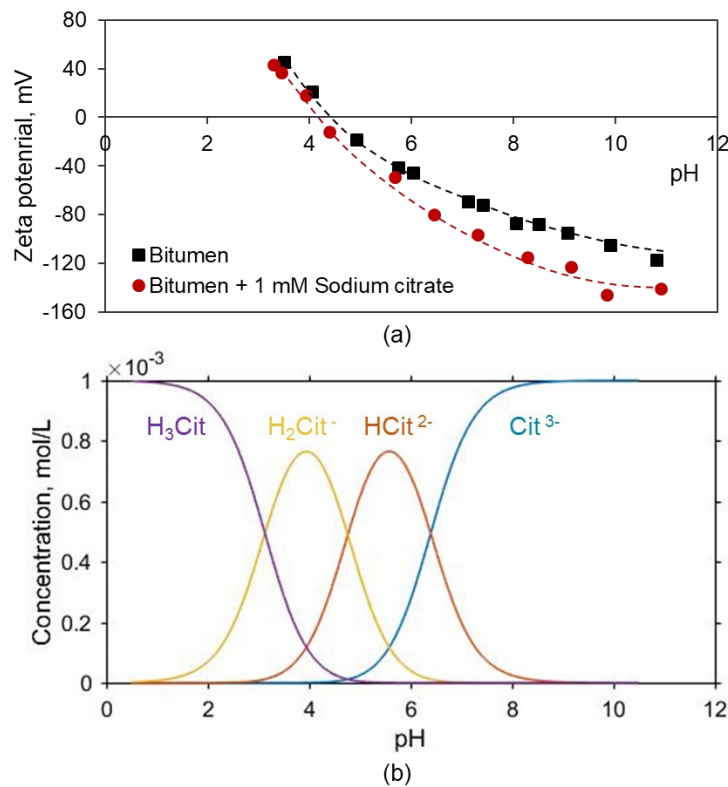
Figure 4.9. (a) Zeta potential of bitumen droplets as a function of pH in the absence and presence of sodium citrate. (b) Citric acid speciation at different bulk pH. The aqueous solution contains 1mM KCl and 1mM citric acid.

Based on the discussion above, the possible mechanism of the synergistic effect of sodium citrate and sodium hydroxide on the zeta potential of bitumen and silica droplets is proposed in Figure 4.10.
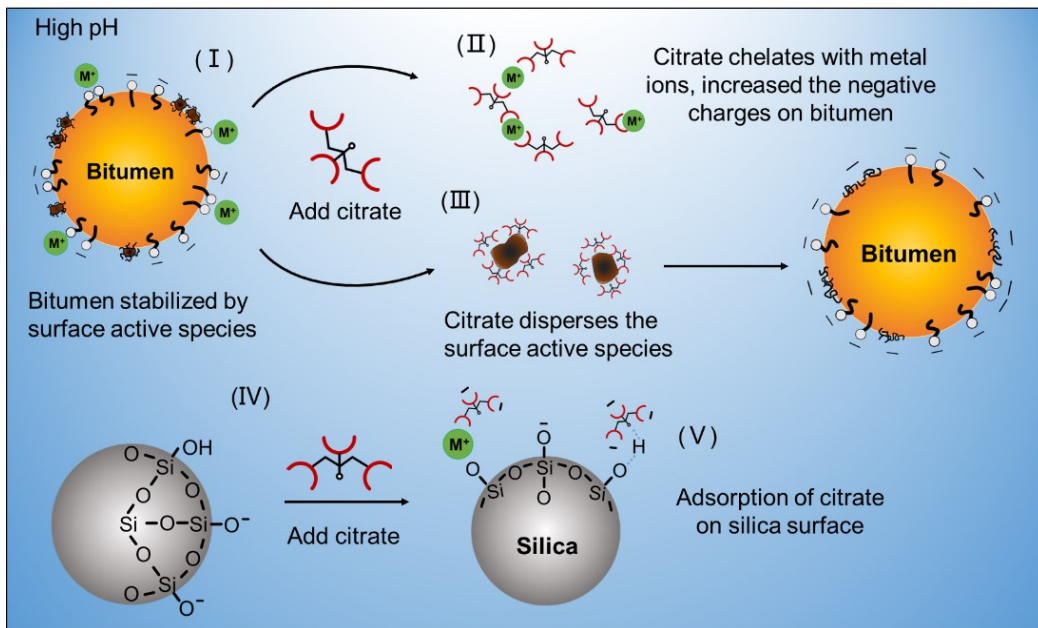
Figure 4.10. Possible mechanism of the synergistic effect of sodium citrate and sodium hydroxide.

With the addition of sodium hydroxide, the natural surfactants have been ionized and migrated to the bitumen/water interface. Additionally, bitumen from oil sands contains metal components such as Ca, Mg, Si, Al, Fe, V, and so on[124, 125], which probably de-activate the surfactants and reduce the zeta potential of bitumen droplets, causing a strong adhesion between bitumen and silica as shown at stage I in Figure 4.10. Meanwhile,

previous studies indicated the existence of the surface-active ultra-fines (< 200 nm) components inside the bitumen.[126-128] Those ultra-fines components may be organic-rich solids, with aromatic, polar components adsorbed on the surfaces such as humic substance and asphaltene-like materials.[127, 129] Therefore, it is possible that the ultra-fines are stabilized on the bitumen surfaces as shown in Figure 4.10 stage I. With the addition of caustic, sodium citrate is dissociated to the anionic carboxylate form with three deprotonated carboxyl groups (Figure 4.9b), which can serve as a builder to interact with cations, thus increasing the effectiveness of surfactant adsorption on bitumen.[66, 130] The possible formation of chelating complexes between citrate and metal cations as described in stage II could lead to the removal of such metal cations from the bitumen, resulting in a more negatively charged surface. On the other hand, due to the strong chelation ability between citrate and the solid composition of ultra-fines, the organic matters could be released and then adsorbed on the bitumen surfaces (stage III).[131] The hypothesis is that the organic matters removed from the solids are surface-active or carrying negative charges, which adsorbed at the bitumen/water interfaces and are contributed to the increase of negative charges on bitumen surfaces, thus enhancing the bitumen detachment from silica surface.

The surface charge of silica particles are not only dependent on the dissociation of silanol group but also can originate from the adsorption of charged ions and dissolution process.[132, 133] Based on the literature review, the possible mechanism of the synergistic effect of sodium citrate and sodium hydroxide on the zeta potential of silica particles is presented in

Figure 4.10. At a high pH environment, the silica surface carries negative charges due to the deprotonation of the silanol group (stage IV). The proposed mechanism is based on the evidence that the hydrogen bonding is formed between the citrate and the silanol group, which was reported in previous studies on the fabrication of porous silica materials by using citric acid.[134-136] Also, the positively charged sodium ions can form a complex with citrate groups, and possibly adsorbed together on silica surfaces. Thus, the decrease of zeta potential of silica surface probably can be attributed to the adsorption of citrate groups, which carries more negative charges than the original silanol group, as described in stage V. Meanwhile, sodium citrate was reported to possibly break the silica surface and its Si-O-Si structures.[137] Bennett et al. compared the dissolution of quartz in the presence of different organic acid anions, and found that citrate ion showed the strongest effect on the dissolution of quartz.[138] The reaction between ligand and metal oxides and the formation of weak organic complexes could facilitate the silicon dissolution process and increase the negative charges on the silica surfaces.[139, 140] However, the exact mechanism still needs to be investigated in future research.

4.4 Conclusion

The role of sodium citrate as a secondary process aid in bitumen liberation was investigated in this study, and the conclusions are listed below.

1. The combined addition of sodium citrate with sodium hydroxide significantly enhanced the degree of bitumen liberation via QCM-D experiments.

2. A reduction in adhesive force and increase in long-range repulsive force between bitumen and silica were observed using AFM with the addition of Na_3Cit, NaOH and the mixture of them. Negligible adhesion forces were found in both NaOH and mixture solution, which is agreed well with the high bitumen liberation.

3. Zeta potential results supported the bitumen liberation data. Compared to applying sodium hydroxide and sodium citrate individually, a more negatively charged surface of both bitumen and silica was found with the addition of the mixture. As a result, a stronger electrostatic repulsion between bitumen and silica formed.

4. The addition of sodium hydroxide leads to the dissociation of sodium citrate and the formation of negatively charged carboxyl groups, which is probably related to the synergistic effect from NaOH and Na_3Cit on bitumen liberation.

Chapter 5

Effect of Sodium Citrate and Calcium Ions on the Spontaneous Displacement of Heavy Oil from Quartz Surfaces

Abstract

The dynamic displacement of heavy oil from solid surfaces by water plays a significant role in the oil recovery process. In this work, a bitumen-water-quartz system was applied to study the effect of sodium citrate (Na_3Cit) and calcium ions (Ca^{2+}) on the dynamic displacement of bitumen from quartz surfaces. It was found that the addition of Ca^{2+} slowed down the bitumen displacement rate and generated daughter droplets during the receding process. In contrast, the presence of Na_3Cit not only accelerated the displacement of bitumen from quartz surfaces, but also led to a smaller water contact angle at the end of the experiments. Moreover, Ca^{2+} was chelated by the added Na_3Cit, which counterbalanced the detrimental effect of Ca^{2+} on the bitumen displacement. The reduced interfacial tension of the bitumen-water interface and the increased negative charges on both bitumen and silica surfaces by Na_3Cit were considered as the reasons of the improved bitumen displacement process. To better understand the underlying physics, both the hydrodynamic (HD) model and molecular kinetic (MK) model were employed to analyze the dewetting dynamics of heavy oil from quartz surfaces under the effect of Ca^{2+} and Na_3Cit.

5.1 Introduction

Liquid-liquid displacement on a solid surface is an important step in many technologies in industrial processes. Taking the oil recovery industry as an example, the efficiency of both water-based oil sands extraction and enhanced oil recovery methods is highly dependent on the heavy oil liberation process. Once the oil sands are exposed to the aqueous phase, the thinning and rupture of the oil film result in the formation of the three-phase contact line (TPCL). Then, the TPCL evolves until the contact angle reaches equilibrium, which is referred to as the recession process.[2] Meanwhile, under the hydrodynamic forces, the oil droplet can detach from the substrate at the last step of liberation. Obviously, both the displacement rate and formed static contact angles (θ_s) are highly related to the efficiency of liberation. In our previous study, the effect of a secondary process aids (sodium citrate) on bitumen liberation was quantified with a quartz crystal microbalance with dissipation (QCM-D), and the combined addition of sodium citrate (Na_3Cit) with sodium hydroxide (NaOH) enhanced not only the liberation kinetics but also the degree of bitumen liberation.[141] To fully understand the mechanism of Na_3Cit in enhancing the heavy oil liberation process, the dynamic displacement and the static contact angles at the end of the liberation process need to be considered.

The dynamics of the liquid-liquid-solid system can be quantitatively described by two popular models based on different energy dissipation mechanisms.[77] The hydrodynamic (HD) model considers the viscous flow within the fluid bulk near the TPCL as the predominant mode of energy dissipation. The molecular kinetic (MK) model asserts that

the energy is mainly dissipated by the friction within the immediate three-phase contact region due to the molecular interaction between the solid and the fluid. Individually or in combination, these two models have been applied to investigate the conditions that influence the wetting dynamics, including the wettability, liquid viscosity, droplet size, water chemistry, and so on.[80, 82, 83, 85, 142] By investigating the influence from substrate wettability and heterogeneity, it was suggested that increasing the hydrophobicity of substrates increased the contact line resistance and hindered the liquid-liquid displacement.[80, 85] Also, increasing the liquid viscosity was shown to have an adverse effect on the TPCL motion, which decreased the jumping frequency in the MK model.[82, 83] Studies related to the influence of solution pH indicates that a higher solution pH improved the dynamic displacement of bitumen.[23] To our knowledge, little work has been done to illustrate the dynamic displacement of heavy oil under the effect of chemicals from industrial operations, such as Na_3Cit and calcium ions (Ca^{2+}).

The current research investigated the underlying physics of the heavy oil dewetting process using the bitumen-water-quartz system under the influence of Na_3Cit and Ca^{2+}. Both HD and MK models are applied to analyze the displacement of heavy oil from the quartz surface. The fitting parameters, the static contact angles, and their interplays to the interfacial properties shed light on the fundamental mechanisms of heavy oil displacement from the quartz surface by Na_3Cit and Ca^{2+}.

5.2 Materials and methods

5.2.1 Materials

In this study, Coker-feed bitumen supplied by Syncrude Canada Ltd. (viscosity of 36.7 Pa·s at 45 ºC) was employed as the representative of heavy oil, and quartz disks (NanoFAB, CA) were used as solid substrates. Sodium citrate (99.8%, Sigma Aldrich), sodium chloride (99%, Sigma Aldrich) and calcium chloride (97%, Fisher Scientific) were used to prepare solutions, and sodium hydroxide solution (1N) and hydrochloride acid (1N, Fisher Scientific) were applied to adjust the solution pH. To clean the quartz slides and optical cells, the piranha solution was prepared with sulfuric acid (LabChem) and hydrogen peroxide (30%, Fisher Scientific). Organic solvents such as n-decane (≥ 99%), heptane (≥ 99%) and toluene (99.8%) were purchased from Fisher Scientific. Milli-Q water was used throughout this study.

5.2.2 Bitumen displacement tests

The displacement of heavy oil from the solid substrate in aqueous ambient was estimated by measuring the dynamic contact angle of water phase (θ_d) versus time. A quartz wafer cut into 15×15 mm^2 pieces was used to simulate the sand grains in oil sands. Before each experiment, the quartz slides were immersed in piranha solution ($V_{98\% \ H2SO4}:V_{30\% \ H2O2}$ = 3:1) overnight to remove contaminants, then rinsed with Milli-Q water and dried with pure nitrogen gas before use. A schematic view of the experimental procedures is illustrated in Figure 5.1. Bitumen was preheated to 80 ºC, and one drop of bitumen (15.5 ± 2 mm^3) was placed on the quartz slide, then gradually cooled. The spreading of bitumen over the quartz slide led to a flat and smooth surface. To avoid the aging effect, each bitumen coated slide was prepared five minutes before the recording started. Five conditions were studied in this

experiment: no chemical addition, 1 mM Na_3Cit, 10 mM Na_3Cit, 1 mM calcium chloride ($CaCl_2$), and a mixture of 1 mM $CaCl_2$ and 1 mM Na_3Cit. All the sample solutions contained 10 mM sodium chloride (NaCl) as a background salinity, and the pH was adjusted to 8.5 before starting the experiment. In order to simulate the industrial processes, sample solutions were preheated to 45 °C and immediately injected into an optical cell containing the bitumen coated quartz slide. During the experiment, the optical cell was placed in a thermal chamber connected with a water bath to maintain the temperature at 45 °C. The dynamic contact angle was recorded and analyzed by Attention Tensiometer (Theta).
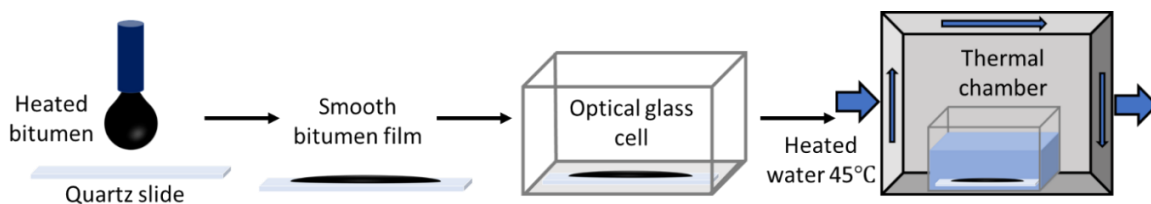
Figure 5.1. Schematics of the bitumen contact angle measurement procedures.

5.2.3 Zeta potential measurements

The zeta potentials of bitumen and quartz in the above conditions were measured with Brookhaven ZetaPALS at 22 °C. To obtain the bitumen stock suspension, 1 mL of diluted bitumen (mass ratio of bitumen:heptane:toluene = 1:3:1) together with 40 mL of 10 mM NaCl was heated to evaporate the organic solvent and emulsified by a model 550 Sonic Dismembrator (Fisher) at 70 amplitude for 15 minutes. The quartz stock suspension was prepared by adding 1 g of quartz particles into 500 mL of 10 mM NaCl. The method for preparing stock suspensions was detailed in our previous work.[141] The sample solutions

were prepared with 2 vol. % of the stock suspension of bitumen or quartz with the chemicals and conditioned for 10 mins. For each sample, the data was averaged from 10 runs (10 cycles for each run).

5.2.4 Interfacial tension measurements

The effect of sodium citrate on the interfacial tension (IFT) of bitumen-water was studied by the reversed pendant drop method with an Attention tensiometer (Theta). Interfacial tension of the bitumen-water interface ($\gamma_{b/w}$) is hard to measure because of the high viscosity of the bitumen. The small density difference between bitumen and water also hinders the drop formation. In order to reduce the impact of these two issues, a 30 wt. % of n-decane was added into the bitumen for dilution. According to the study by Schramm et al., $\gamma_{b/w}$ for diluted bitumen (30 wt. % n-decane) is similar to the raw bitumen.[34, 143] The test conditions were consistent with previous contact angle measurements. The volume of bitumen droplets was controlled at 26 ± 1 μL, and each measurement lasted for 2 hours under room temperature at 22 ºC. It was revealed that the IFT of the bitumen-water interface varied little with the temperature at this pH; thus the IFT for the model analysis was estimated by a linear correlation with a temperature coefficient of –0.013 mN/(m·deg).[31, 144]

5.3 Theoretical models

5.3.1 Hydrodynamic model
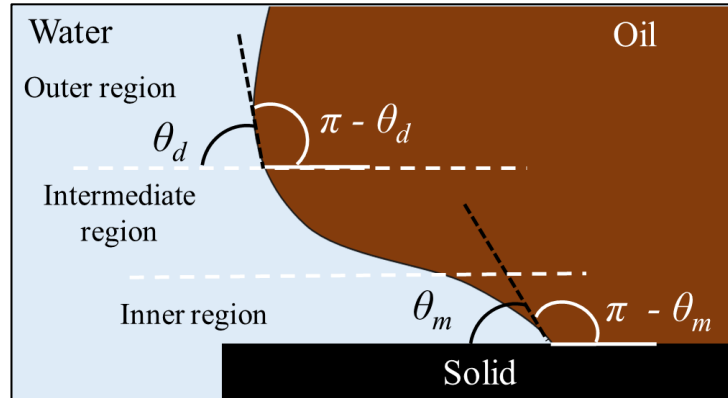
Figure 5.2. Schematic of the three hypothetical regions for the current system. The contact angle captured from the outer region is θ_d, while θ_m is the hypothesized microscopic contact angle in the inner region. (Note: The scale in this schematic does not reflect the real length scale for our system.)

The commonly used form of the HD model was proposed by Cox[86], who derived it by assuming three hypothetical regions around the TPCL: the outer region, where the interface is considered to be static and forms a macroscopic contact angle with the solid surface; the intermediate region, where significant viscous stress arising from the TPCL motion results in the interface deviating from a static-like shape; and finally, the inner region with a microscopic scale, where the interface is governed by intermolecular forces.[145] An illustration of these three hypothetical regions is shown in Figure 5.2, where θ_d and θ_m are the dynamic contact angle captured at the outer region and the hypothesized microscopic contact angle in the inner region; therefore, $(\pi - \theta_d)$ and $(\pi - \theta_m)$ are the corresponding contact angle of the oil phase respectively. The viscous dissipation is considered as the predominant energy dissipation for HD model. In our system, the viscosity of bitumen is

larger than that of water by a factor 6×10^4 at the operation temperature. Therefore, the contact angle of oil phase (receding liquid) was applied in the Cox's solution.

$$U = \frac{\gamma_{b/w}[g(\pi - \theta_m, \mu_w/\mu) - g(\pi - \theta_d, \mu_w/\mu)]}{\mu \, ln \, (L/L_s)} \qquad (5.1)$$

where μ_w/μ represents the viscosity ratio of the water to heavy oil in this study. Since the viscosity of bitumen is much higher than water ($\mu_w/\mu \sim 0$), the integral function $g(\pi - \theta, \mu_w/\mu)$ can be written as[87]

$$g \, (\pi - \theta, 0) = \int_0^{\pi-\theta} \frac{\epsilon - sin \, \epsilon \, cos \, \epsilon}{2 \, sin \, \epsilon} \, d\epsilon \qquad (5.2)$$

In Eq. 5.1, U is the moving velocity of the TPCL, $\gamma_{b/w}$ is the IFT between bitumen and water, μ is the viscosity of bitumen in this case. The L is a macroscopic length scale of the system and L_s is the microscopic cut-off distance.

5.3.2 Molecular kinetic model

As for the MK model, Blake and Haynes proposed that the TPCL motion was controlled by thermally activated adsorption and desorption processes of microscopic elements at the three phase contact zone.[79] By defining the frequency of the random microscopic displacement at the equilibrium state as K_0 and the average distance between two adsorption sites as λ, the relationship between the TPCL velocity and the dynamic contact angle is written as

$$U = 2K_0\lambda \, sinh \left(\frac{\gamma_{b/w}[cos(\pi-\theta_d) - cos(\pi-\theta_s)]\lambda^2}{2k_BT} \right) \qquad (5.3)$$

In order to ensure consistency, the contact angles of the oil phase were also applied in the MK model. If the argument of the hyperbolic sine function is small, Eq. 5.3 can be linearized as

$$U = \frac{\gamma_{b/w}}{\xi} \left[cos(\pi - \theta_d) - cos(\pi - \theta_s) \right] \tag{5.4}$$

By defining θ_s as the static contact angle of the water phase, $(\pi - \theta_s)$ is the static contact angle of the oil phase. The contact line friction coefficient is given as $\xi = \frac{k_B T}{K_0 \lambda^3}$, which quantifies the energy dissipation at the immediate TPCL zone. Here, k_B is the Boltzmann constant, and T is the absolute temperature.

5.4 Results and discussion

5.4.1 Bitumen displacement over time

The temporal evolution of the recession of bitumen from quartz surfaces was investigated under different water chemistry. To illustrate the shape changes of the bitumen film over time, the micrographs of bitumen displacement on the quartz surface are shown in Figure 5.3. At the beginning of the displacement, there was a shape change at the margin of the bitumen film, which was followed by a fast TPCL motion. Then, the bitumen receded to form a drop shape on the substrate with a gradually decreased receding velocity. It was found that increasing the concentration of Na₃Cit greatly accelerated the displacement process, and a complete dewetting of bitumen was observed within three minutes in the presence of 10 mM Na₃Cit at pH 8.5.

No addition
1 mm

1 mM Na₃Cit

10 mM Na₃Cit

0 s   60 s   180 s   5 min   10 min
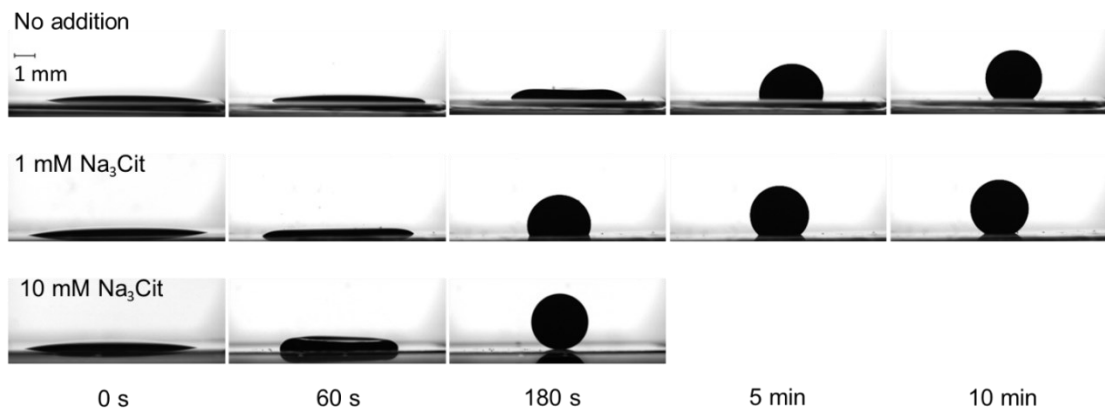
Figure 5.3. Micrographs of bitumen film receding from the quartz surface. The experiments were carried out at 45 ºC, all solutions contained 10 mM NaCl, and the pH was adjusted to 8.5.

The contact angle of the water phase was analyzed from recorded images. To compare the effect of Na₃Cit and Ca^{2+} on bitumen recession, the representative evolution of θ_d over time are plotted in Figure 5.4. The solution that contains only 10 mM NaCl as a background electrolyte (termed 'No addition' in Figures 5.4a and 5.4b) is shown as the standard condition. In Figure 5.4a, increasing the concentration of Na₃Cit not only generated a lower contact angle at the end of displacement, but also accelerated the rate of bitumen receding. Previous studies concluded that the smaller the θ_d, the less energy was needed for bitumen recession and detachment.[1] Therefore, our results suggest that the addition of Na₃Cit is favorable for bitumen liberation at pH 8.5.
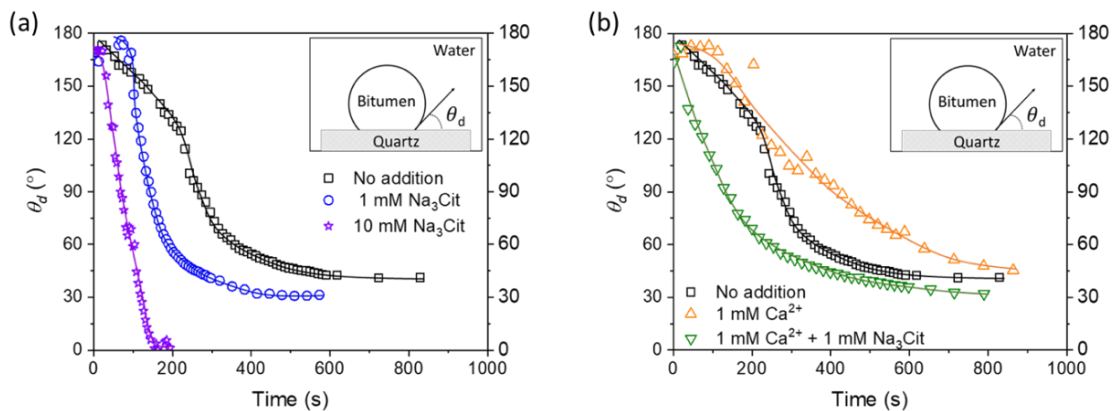
Figure 5.4. The dynamic contact angle of bitumen receding from the quartz surface: (a) Effect of Na_3Cit (b) effect of $CaCl_2$ and Na_3Cit. Experiments were carried out at 45 °C, all solutions contained 10 mM NaCl, and pH was adjusted to 8.5.

On the contrary, adding $CaCl_2$ showed a negative impact on the bitumen receding process. Although the final contact angle was insensitive to Ca^{2+}, the receding rate significantly slowed down under 1 mM Ca^{2+}. Similar results were published by Basu et al., who pointed out that increasing the amount of Ca^{2+} decreased the bitumen displacement rate on glass slides.[48] Meanwhile, the pinning of the TPCL and the formation of daughter droplets frequently occurred in the cases with Ca^{2+}. This phenomenon is possibly caused by the Ca^{2+} bridging between quartz surfaces and natural surfactants adsorbed on the bitumen-water interface at the TPCL, which increases the adhesion between bitumen and quartz surfaces.[1] In general, the detachment of bitumen droplets from solids during bitumen recovery mainly relies on mechanical energies, such as fluid drag force, buoyancy force and aeration of bitumen, and most of them increase as the diameter of bitumen droplets increases. Therefore, the formation of small bitumen droplets is detrimental to bitumen

detachment. Interestingly, when Na_3Cit was added together with Ca^{2+}, the TPCL pinning and the daughter droplets all vanished. Moreover, the final contact angle decreased from 42° to 30° and the displacement rate increased.

5.4.2 Static and dynamics of bitumen dewetting

5.4.2.1 Dynamic dewetting

Captured images were analyzed by using the One Attension software, the contact angle and the contact radius were extracted from the captured images for fitting analysis. The velocity of the TPCL was first calculated by the time derivative of the contact radius for all the collected data. Then, in order to remove some deviations caused by software auto-analysis, the TPCL velocities were smoothed by using cubic spline method in MATLAB software. The least-squares method was applied to obtain the best fit for the HD model. As for MK model, some experiments did not reach a steady-state, and the TPCL speed was not exactly zero. In these cases, accessing the static contact angle from the fitting was suggested as a reliable alternative.[146] Equation 5.4 was employed to obtain ξ and θ_s through least-squares method.

The relationship between the contact angle and the displacement velocity of the TPCL is illustrated in Figure 5.5 with both experimental (symbols) and theoretically fitted (curves) results. Experimentally, the addition of chemicals was found to play a part in determining the initial velocity of bitumen displacement. Previously, the liquid-liquid displacement rate was found to be proportional to the ratio of the oil-water IFT to the viscosity.[147] In the current research, the dynamics of bitumen displacement is dominated by the added

chemicals. For the same oil viscosity, our results suggest that the addition of Na₃Cit reduced the IFT while it accelerated the displacement rate. Meanwhile, a slower initial displacement velocity was captured with the presence of Ca^{2+}.
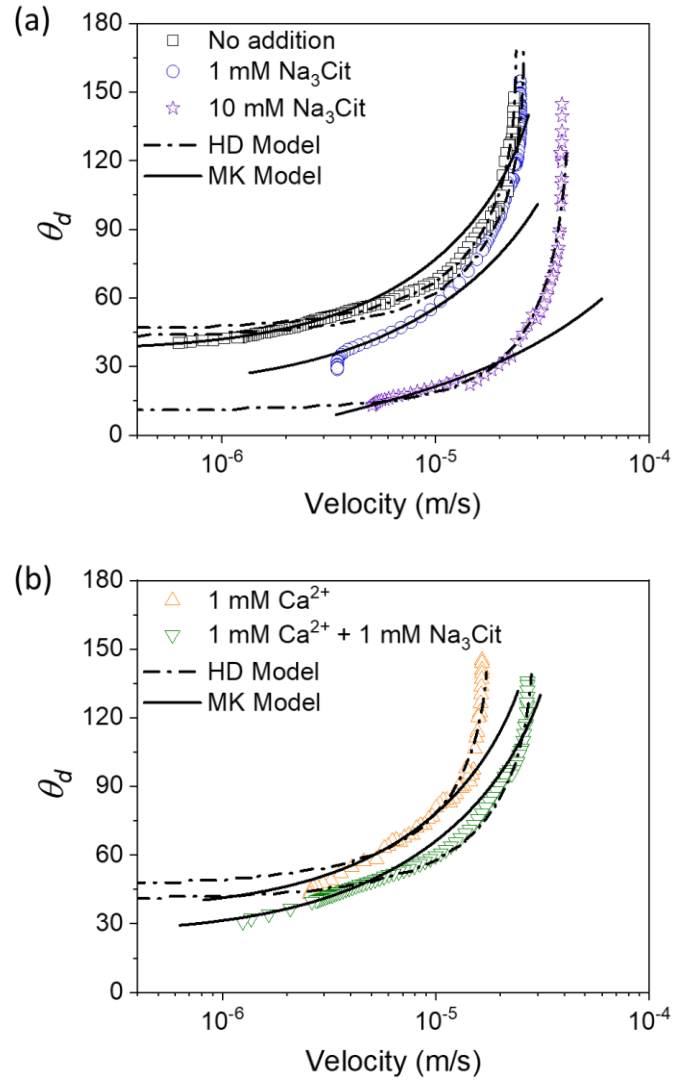
Figure 5.5. Comparison between experiments (symbols) and HD (dash line) or MK models (solid lines) to explain the relationship between the dynamic contact angle and the TPCL speed under different water chemistry: (a) Effect of Na₃Cit; (b) effect of Ca^{2+} and Na₃Cit.

Results with a fast TPCL motion were well predicted by the HD model (dashed line in Figure 5.5), which is consistent with previous findings reported in the literature.[80] Parameters of the best fit are summarized in Table 5.1. Two fitting parameters from the HD model are θ_m and $\ln(L/L_S)$. According to the literature, the microscopic cut-off length (L_S) is around the scale of molecular size (nanometer scale). Considering the droplet radius in our system (~1.5 mm) as L, the calculated L_S from our results are 5 to 9 orders of magnitude smaller than the regular molecular size. In this case, the values of L_S are not physically reasonable. Moreover, the microscopic contact angles of the water phase are systematically larger than the measured contact angles at the final stage, which suggests that the dynamics of the TPCL are not purely dominated by viscous dissipation.[80, 85] Despite those indications, a clear trend of θ_m and $\ln(L/L_S)$ was observed with different chemical additions. The presence of Ca^{2+} resulted in a larger θ_m, while the presence of Na_3Cit provoked the opposite response which resulted in a smaller θ_m. This could be attributed to the ability of chemical additions to modify the solid-oil interactions at the molecular level in the inner region.[77, 145, 148] It has been shown that the presence of Ca^{2+} significantly reduced the long-range electrostatic repulsion and increased the adhesion between bitumen and silica surfaces.[63] Oppositely, Na_3Cit was able to reduce the adhesive force between bitumen and silica.[141] Although the microscopic contact angle is assumed to be governed by the intermolecular interactions between the fluid and substrate, there is no direct experimental evidence to prove the exact relationship between them. The value of the fitting parameter $\ln(L/L_S)$ in the HD model was inversely correlated to the concentration of Na_3Cit, but increased when Ca^{2+} was added. Due to the controlled temperature, the viscosity can be assumed mostly

constant so that the viscous resistance $\mu \ln(L/L_S)$ varied identically to $\ln(L/L_S)$. In other words, the presence of Ca^{2+} resisted the bitumen displacement, while Na_3Cit promoted the liberation of bitumen from quartz surfaces.

For the final stage of bitumen displacement, the linear form of the MK model was employed because of the very small difference between the dynamic contact angle and the static contact angle. Similar to other works related to the MK model[23], a good agreement was obtained in our research (represented by the solid line in Figure 5.5). The fitted static contact angle θ_s from the MK model showed a similar trend with the measured contact angle at the end of displacement, which decreased with the addition of Na_3Cit and barely changed with the presence of Ca^{2+}. It has been proven that the variation of the parameter ξ depended on the viscosity of oil and the solid wettability.[83, 147] In the current work, with the controlled viscosity and solid wettability, ξ appeared to change according to the chemical additions. Specifically, it showed a downward trend with the increase of the concentration of Na_3Cit, and an upward trend with the addition of Ca^{2+}. The work of adhesion (W_a) between bitumen and quartz can be estimated by $W_a = \gamma_{b/w}(1 + \cos(\pi - \theta_s))$ based on the Young-Dupre's equation[149]. The calculated adhesion values in Table 5.1 were found to be consistent with our previous results of colloidal force measurements[141], which showed that the adhesion between bitumen and silica decreased with the addition of Na_3Cit. It is worth mentioning that the value of $\ln(\xi/\mu)$ displayed similar trend with the W_a. This finding is also supported by Blake and De Coninck, who suggested that $\ln(\xi/\mu)$ should vary proportionally to W_a according to the following correlation[150],

$$\xi = \frac{\mu V_L}{\lambda^3} \exp\left(\frac{W_a \lambda^2}{k_B T}\right) \tag{5.5}$$

where V_L is the volume of the unit flow. Therefore, based on theoretical and experimental results, the bitumen displacement process in the current research is highly dependent on the work of adhesion. Specifically, the presence of Ca^{2+} increased the adhesion between bitumen and quartz which consequently hindered bitumen displacement by increasing the contact line friction. In contrast, the role of Na_3Cit in improving the dewetting dynamics was attributed to the reduced adhesion between bitumen and quartz.

Table 5.1. Key parameters for model fitting and discussion.

Experiment condition	θ_m [º]	$\ln(L/L_S)$	θ_S [º]	$\ln(\xi/\mu)$	W_a [mJ/m²]
No addition	42 ± 5	32.9 ± 3.6	35 ± 3	3.3 ± 0.5	3.5 ± 0.006
1 mM Na_3Cit	41 ± 5	26.9 ± 2.2	23 ± 3	3.0 ± 0.3	1.45 ± 0.01
10 mM Na_3Cit	9 ± 4	25.3 ± 1.6	0 ± 0	0.8 ± 0.3	0
1 mM Ca^{2+}	46 ± 2	34.7 ± 1.7	34 ± 5	3.4 ± 0.1	2.9 ± 0.1
1 mM Ca^{2+} + 1 mM Na_3Cit	40 ± 2	26.4 ± 1.6	25 ± 5	3.1 ± 0.1	1.6 ± 0.05

5.4.2.2 Static contact angles and their relations to the interfacial properties.

The static contact angle is an important parameter for the bitumen liberation process. It is related to the driving force of the TPCL movement[77] and is also critical to the final bitumen detachment[1]. From Table 5.1, θ_s from the MK model varied accordingly to the added chemicals. In this study, the quartz surfaces are clean and homogeneous, thus we consider the θ_s is equivalent to the equilibrium contact angle. Therefore, the influences of chemicals

on the θ_s can be addressed based on the famous Young's equation[35] considering the IFT of the bitumen-water interface ($\gamma_{b/w}$), bitumen-solid interface ($\gamma_{b/s}$) and solid-water interface ($\gamma_{s/w}$) at their equilibrium state:

$$cos(\theta) = \frac{\gamma_{b/s} - \gamma_{s/w}}{\gamma_{b/w}} \tag{5.6}$$

In general, a smaller $\gamma_{b/w}$ is beneficial to bitumen liberation. In Figure 5.6a, increasing the concentration of Na$_3$Cit resulted in a decrease of $\gamma_{b/w}$ coupled with a decrease of θ_s, which enhances bitumen liberation. Moreover, when the fitted θ_s is plotted against $\gamma_{b/w}$ (circles in Figure 5.6b), the overall trend shows that θ_s decreases with $\gamma_{b/w}$. However, it is inaccurate to conclude that $\gamma_{b/w}$ is the only contribution to θ_s. The variation of θ_s is also attributed to $\gamma_{s/w}$ and $\gamma_{b/s}$. To clarify this assumption, we plot a reference curve by using Eq. 5.6 and assuming $\gamma_{b/s}$ and $\gamma_{s/w}$ are unchanged with the added Na$_3$Cit and Ca^{2+}, the value of $(\gamma_{b/s} - \gamma_{s/w})$ are calculated from the no addition condition (line in Figure 5.6b). If $(\gamma_{b/s} - \gamma_{s/w})$ remains constant under different conditions, the experimental data points should follow the theoretical solid line plotted in Figure 5.6b. However, the slight deviation in Figure 5.6b indicates that $(\gamma_{b/s} - \gamma_{s/w})$ has been altered by the addition of Na$_3$Cit and Ca^{2+}.
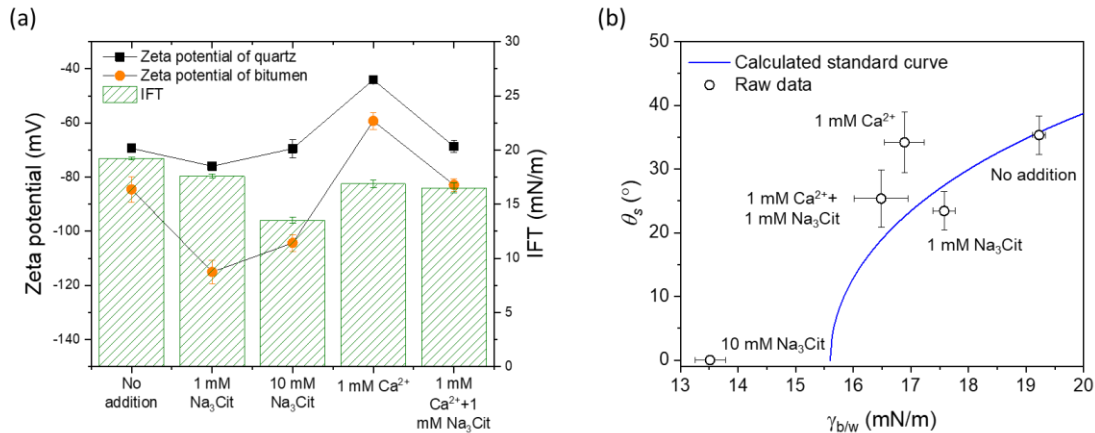
Figure 5.6. Interfacial properties of bitumen and quartz in different conditions. (a) Measured $\gamma_{b/w}$ and zeta potentials of bitumen and quartz, (b) fitted static contact angle θ_s plotted vs the $\gamma_{b/w}$ (circles), the relation between θ_s and $\gamma_{b/w}$ according to Young's equation at a constant $(\gamma_{b/s} - \gamma_{s/w})$ at the no addition case (solid line).

Unlike $\gamma_{b/w}$, $\gamma_{s/w}$ and $\gamma_{b/s}$ are hard to quantify with experimental methods. Theoretically, the alternation of $\gamma_{s/w}$ can be induced by the energy of electrical double layer (EDL) formation on the solid-water interface[45], while $\gamma_{b/s}$ can be changed by the interactions between the bitumen and quartz at the TPCL[46]. Both mechanisms are highly dependent on the zeta potential of quartz and/or bitumen surfaces. Therefore, the zeta potential of quartz and bitumen surfaces were measured and plotted in Figure 5.6a. Clearly, we observed a correlation between the alternation of $(\gamma_{b/s} - \gamma_{s/w})$ and the changes of zeta potential. For example, the data of 1 mM Na$_3$Cit from Figure 5.6b is on the right side of the standard curve, indicating a larger $(\gamma_{b/s} - \gamma_{s/w})$ compared to the no addition case. Meanwhile, the more negatively charged bitumen and quartz surfaces were found in Figure 6a with the presence of 1 mM Na$_3$Cit. In contrast, the 1 mM Ca^{2+} greatly reduced the negative charges on both surfaces compared to the no addition case, which showed at the left side on the standard curve in Figure 5.6b with a smaller $(\gamma_{b/s} - \gamma_{s/w})$. Although quantitative analysis of the relationship between surface charges and $(\gamma_{b/s} - \gamma_{s/w})$ is beyond the scope of this study, it is reasonable to believe that variation of $\gamma_{b/w}$ and zeta potential by the addition of Na$_3$Cit and Ca^{2+} are critical to the static contact angle and the dynamic displacement process of bitumen.

5.5 Summary

In this work, we investigated the effects of chemical additions on the dynamic process and the static contact angle of heavy oil displacement from solid surfaces. Results showed that calcium ions slowed down the bitumen receding process and led to the formation of daughter droplets. In contrast, sodium citrate not only generated a smaller contact angle at the final stage of displacement but also counterbalanced the detrimental effects of calcium ions. The hydrodynamic and molecular kinetic models were successfully applied to describe the dynamic displacement of bitumen. Although the fitted microscopic cut-off distances were considered to be unphysical, a strong dependence between the viscous resistance parameters and the chemical additives was observed. It increased with the presence of calcium ions, which indicates a stronger resistance to bitumen receding from quartz surfaces. However, adding sodium citrate reduced the viscous resistance and compensated the adverse effect of calcium ions. Furthermore, the decreased wetting line friction was dominated by the decreased adhesion between bitumen and quartz in the presence of sodium citrate. Through manipulating the bitumen-water interfacial tension and zeta potential, both calcium ions and sodium citrate are expected to change the intermolecular interactions between bitumen and quartz at the three-phase contact line, and consequently influence the static contact angle and bitumen displacement process.

Chapter 6

Role of Sodium Citrate in the Adsorption of Naphthenic Acids on Inorganic Mineral Surfaces

Abstract

Hypothesis

Both delayed crude oil displacement and coagulation between bitumen and clay minerals are related to the wettability of solid surfaces, which is induced by the adsorption of natural surfactants from bitumen (i.e. naphthenic acid). Sodium citrate (Na$_3$Cit) is expected to strongly coordinate with metal cations and mineral surfaces due to the functionality of three carboxyl groups. Therefore, the addition of Na$_3$Cit prevents the adsorption of naphthenic acid (NAs) on mineral surfaces.

Experiments

A quartz crystal microbalance with dissipation (QCM-D) was applied to study the adsorption of NAs on alumina sensors in the presence and absence of calcium ions (Ca^{2+}), and Na$_3$Cit. Zeta potential distributions of alumina particles were measured to fundamentally understand the adsorption mechanisms. The wetting transition of mineral surfaces was attributed to the adsorption of naphthenic acids as indicated by contact angle measurements.

Findings

The hydrophobicity of the alumina sensor surface increased after adsorption of NAs in both cases with and without Ca^{2+} at pH 8. However, Na$_3$Cit not only competitively adsorbed on the alumina surface but also chelated with Ca^{2+}, which created a negatively charged surface

and prevented the adsorption of naphthenates. Therefore, in the presence of Na_3Cit the mineral surfaces remained hydrophilic.

6.1 Introduction

Natural surfactants in crude oil have shown to play multiple roles in the oil recovery industry. An optimal concentration of natural surfactants modifies the oil-water interfacial properties (zeta potential and interfacial tension) and increases the stability of bubbles, which are beneficial to the oil recovery.[2, 37] However, the adsorption of those surfactants on the mineral clays was found to alter the surface wettability[70] and consequently depresses the crude oil displacement process and froth quality.

Naphthenic acids (NAs) and their metal salts are the major component of the carboxylic surfactants contained in crude oil. The concentration of NAs from industrial process water in tailing ponds ranges from 30 ppm to 100 ppm.[74] It was found that the naturally hydrophilic clay minerals became oil-wet (hydrophobic) due to the adsorption of naphthenates.[70] Moreover, the slime coatings of mineral solids on crude oil was induced by the divalent cations bridging between the natural surfactants at the oil-water interface and solid surfaces.[43, 44, 62] In summary, NAs adsorbed on the mineral surfaces at an alkaline condition through two mechanisms: 1). direct adsorption of carboxyl groups on positively charged surface sites; 2). adsorption through cation bridge (polyvalent cations from process water) on negatively/neutrally charged sites.[1] Thus, a possible approach to prevent the interaction between NAs and minerals is to interfere with these two adsorption mechanisms.

In recent years, the applications of a secondary process aid, sodium citrate (Na_3Cit), together with caustic, have shown significant enhancement on the bitumen recovery and froth quality in the industrial oil sands extraction process.[11] It was found that the improved

bitumen liberation was related to the changes of the surface properties of heavy oil and mineral solid by sodium citrate.[141] Moreover, citric acid has been proven to effectively inhibit the coagulation of bitumen with kaolinite.[62] Therefore, it is important to understand the role of Na$_3$Cit in the interactions between NAs and clay minerals. Most of the clay minerals from oil sands are aluminum phyllosilicates, with silicon tetrahedral sheet and aluminum octahedral sheet.[151] The silicon tetrahedral sheet exhibits a permanent negative charge; thus, it is expected to repel the NAs at alkaline conditions in the absence of multivalent cations (i.e. calcium ions). However, the isoelectric point (IEP) of the aluminum sheet was found ranges from 6 to 7[152], and the IEP of the edge of kaolinite ranges from 5 to 9[153]. Therefore, the alumina components from clay minerals shown the potential to interact with NAs when the solution pH is lower than the IEP. In this study, the aluminum oxide was used as the substrate to mimic the alumina components in clay minerals (i.e. kaolinite, montmorillonite, and illite). The roles of Na$_3$Cit in the adsorption of NAs on alumina surfaces in the presence and absence of calcium ions (Ca^{2+}) were investigated. Meanwhile, the wetting transition of mica surfaces was measured to provide an implication of the effect of Na$_3$Cit in bitumen liberation.

6.2 Materials and methods

6.2.1 Materials

The sodium 3-(3-ethylcyclopentyl) propanoate (Fisher Scientific) was used as a typical naphthenic acid sodium salt (NaN) for QCM-D experiments. Its molecular structure is

illustrated in Figure 6.1. Citric acid trisodium salt (99.8% purity) and calcium chloride (97% purity) were purchased from Fisher Scientific to prepare the sample solutions. Solution pHs were adjusted by the sodium hydroxide solution (1 N, Fisher Scientific) and hydrochloric acid solution (1 N, Fisher Scientific). Aluminum oxide sensors (QSX 309, Nanoscience) were used as the substrate for adsorption tests, and aluminum oxide nano-powders (99.8% purity, Sigma Aldrich) were applied for zeta potential measurements. Mica sheets were purchased from Ted Pella. Sodium dodecyl sulfate (SDS, 99% purity), sodium chloride (NaCl, 99% purity), naphthenic acid (commercial mixture), decane (99.5%) and ethanol (> 99% purity) were purchased from Sigma Aldrich. Milli-Q water was used in all experiments throughout this study.

(a) sodium 3-(3-ethylcyclopentyl)propanoate (b) trisodium 2-hydroxypropane-1,2,3-tricarboxylate
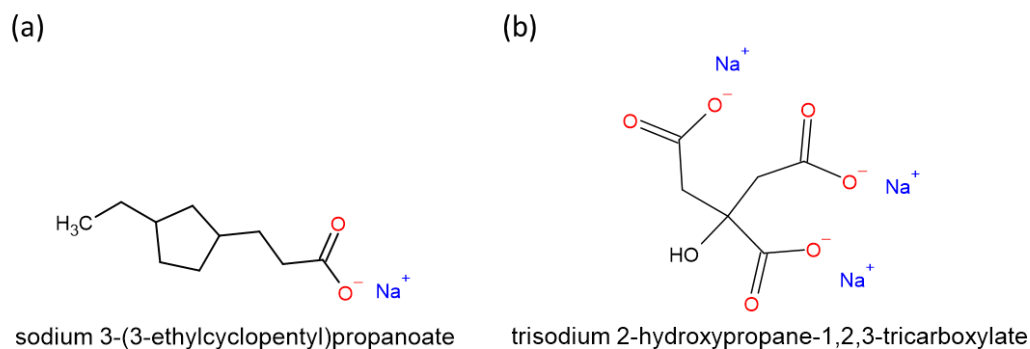
Figure 6.1. The molecular structure of (a) sodium naphthenate and (b) trisodium citrate.

6.2.2 QCM-D theory and procedures

The application of QCM-D enables the real-time surface characterization, including the mass adsorption and desorption process, the thickness and viscoelasticity determination, and the structural conformations of adsorbed molecules. The aluminum oxide sensor is a thin quartz crystal disk covered with gold electrodes on each side and coated with alumina

on the top of the surface. The QCM-D working principle mainly relies on the piezoelectric properties of the quartz crystals. During the operation, the sensor is excited by the applied voltage and oscillates in the thickness-shear mode.[101] The change in resonance frequency (Δf) and energy dissipation (ΔD) of sensor oscillation were recorded at various overtones (n=1, 3, 5,...). According to the Sauerbrey relation[100], the mass change (Δm) is proportional to Δf and can be calculated by the following equation:

$$\Delta m = -C\,\Delta f_n / n \tag{6.1}$$

where C is the mass sensitivity constant, which is equal to 17.7 ng/(cm^{2}Hz) for 5 MHz crystal, and Δf_n is the change of resonance frequency at n overtone. The measurement of ΔD enables the characterization of the viscoelastic properties of the deposited layer on the sensor surface. A small ΔD indicates the adsorbed layer is rigid, while a significant change in ΔD indicates a loose and soft adsorbed layer. The Sauerbrey relation (Eq. 6.1) is only valid at the condition of a rigid and firmly distributed layer.[154] When the shift in dissipation is significant ($\Delta D/\Delta f > \sim 0.2\times10^{-6}$), the mass and film thickness need to be calculated by a viscoelastic model.[102, 155, 156]

The current study was conducted with a Q-sense Analyzer (E4 system, Biolin Scientific). Prior to each experiment, QCM-D flow modules and tubes were immersed in 2 wt. % SDS solution and sonicated for 30 mins. After rinsing with Milli-Q water, these accessories were dried with nitrogen gas. The alumina sensors were immersed in ethanol and sonicated for 15 mins. Then, the sensor was rinsed with Milli-Q water and blow-dried with nitrogen gas.

Before mounting the sensor into QCM-D flow modules, the dried sensors were further treated with UV/ozone for 10 mins.

Two sample solutions, 100 ppm NaN, 100 ppm NaN + 1 mM of Ca^{2+}, were prepared, and each of them was separated into two parts. To evaluate the effect of Na_3Cit, 1 mM Na_3Cit was introduced into one part of the prepared solution. All the solution pHs were adjusted to 8 ~ 8.1 before performing the experiments. The QCM-D measurements were started by introducing Milli-Q water into the system to establish a baseline. For the experiments containing Ca^{2+}, 1 mM of Ca^{2+} was introduced after Milli-Q water to establish the second baseline. Then, the sensors were exposed to the prepared sample solutions. At the end of the experiments, a rinse cycle by Milli-Q water was applied to remove the loosely attached materials. All the experiments were conducted at 22 ºC with a flow rate at 100 μL/min.

6.2.3 Contact angle measurements

The wettability of the alumina sensor was characterized by an Attension Optical Tensiometer using the sessile drop method. Before and after each QCM-D experiment, the sensors were rinsed with Milli-Q water and blow-dried with nitrogen gas. A water droplet with a controlled size (2 ± 0.2 μL) was placed at the top of the sensor at room temperature (22 ºC) for contact angle measurements.

The same equipment was applied to characterize the relative wettability of oil and water on mica surfaces. Milli-Q water and 1 mM Na_3Cit were adjusted to pH 8 prior to each experiment. During the experiment, a fresh and smooth mica surface was immersed in decane containing 10000 ppm NAs, and a drop of sample solution (2 ± 0.5 μL) was placed

on the basal cleavage of the mica surface in the oil phase. The contact angles of the droplet were recorded over time at room temperature.

6.2.4 Zeta potential measurements

The zeta potential distributions of alumina particles were measured with ZetaPhoremeter IV (CAD Instrumentation). An alumina particle stock suspension was prepared by adding 1 g alumina particles (~13 nm) into 1 mM NaCl. Sample solutions were prepared using 1 mM NaCl as background electrolytes at the conditions applied in QCM-D experiments. Before the measurements, 0.2 ml stock suspension was introduced into the sample solution and conditioned by stirring for 5 mins. All tests were conducted at room temperature (22 ºC), and each condition was repeated three times. The zeta potential was obtained by the mobility of tracked particles using the Smoluchowski equation.

6.3 Results and discussion

6.3.1 Adsorption of naphthenates and surface wettability

The effects of Na_3Cit on the adsorption of NAs on alumina surfaces were investigated by QCM-D in the presence and absence of Ca^{2+}. The representative results of frequency and dissipation changes at three different overtones (n=3, 5, 7) were normalized by their overtone number and plotted versus time in Figure 6.2. All the adsorption tests were started with the establishment of an experimental baseline, which is shown as step I (Milli-Q water) in Figure 6.2, and step II is the secondary baseline (1 mM Ca^{2+}) in Figure 6.2c and Figure

6.2d. Then sample solution containing NaN and/or Na₃Cit and Ca^{2+} was injected, followed by a rinse cycle with Milli-Q water (last step).
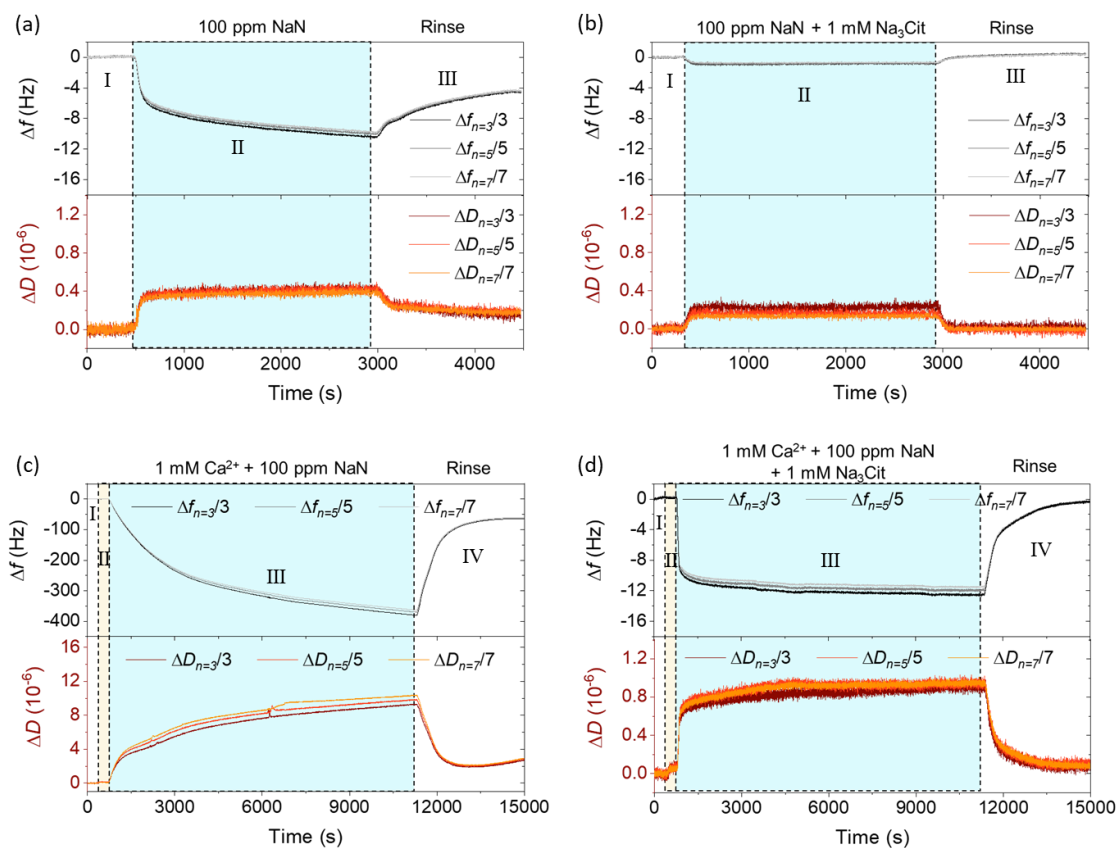
Figure 6.2. Change in frequency and dissipation of the alumina sensor under the presence of (a) 100 ppm NaN, (b) 100 ppm NaN and 1 mM of Na₃Cit, (c) 1 mM of Ca^{2+} and 100 ppm NaN and (d) 1 mM of Ca^{2+}, 100 ppm NaN and 1 mM of Na₃Cit. The ΔD and Δf at 3, 5 and 7 overtone are normalized by the overtone number. The step I represents the injection of Milli-Q water, step II in Figure 6.2c and Figure 6.2d indicates the second baseline of 1 mM of Ca^{2+}, and followed with an injection of the sample solution, which represented by step II in Figure 6.2a and Figure 6.2b; step III in Figure 6.2c and Figure 6.2d.

At pH 8, the injection of 100 ppm of NaN led to a decrease of frequency and an increase in dissipation (stage II in Figure 6.2a). After rinsing with water, the frequency and dissipation stabilized at - 4 Hz and 0.2×10^{-6}, respectively, which can be considered as a thin layer of naphthenates tightly adsorbed on the alumina surface. Surprisingly, when 1 mM Na_3Cit was injected together with 100 ppm NaN into the system, the frequency only dropped to around -1 Hz while the dissipation increased to 0.3×10^{-6} (stage II in Figure 6.2b). Both Δf and ΔD gradually returned to zero after a rinse cycle, indicating a trace amount or no adsorption of naphthenates. A similar function of Na_3Cit was observed at the scenarios with the addition of Ca^{2+}. Although the presence of Ca^{2+} significantly increased the naphthenates adsorption with Δf stabilized at -60 Hz (Figure 6.2c) after rinse, the change in frequency and dissipation was barely observed when Na_3Cit was added together with Ca^{2+} and NaN (Figure 6.2d). The fact that Δf remained stable at -0.5 Hz after the rinsing step suggests that adding Na_3Cit prevented almost all of the adsorption of naphthenates.

The adsorption of NAs on the alumina sensor at pH 8 was found to increase the hydrophobicity of the surface. Before experiments, the clean alumina sensor has a contact angle around 15° (Figure 6.3a), which is consistent with the value reported in the literature.[157] However, it increased to 63° after exposure to 100 ppm NaN. Such effect was magnified by adding Ca^{2+} together with NaN, which led to an even higher contact angle of 87° (Figure 6.3d). It is interesting to note that the presence of Na_3Cit prevented the adsorption of naphthenates in both cases with and without Ca^{2+} and consequently

maintained the wettability of alumina surfaces, as illustrated in Figures 6.3c and 6.3e, respectively.
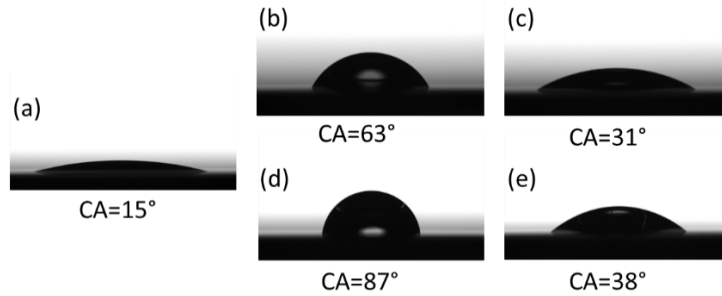
Figure 6.3. Contact angle (CA) of the alumina sensor: (a) before QCM-D experiments, (b) after exposure to 100 ppm NaN, (c) after exposure to 100 ppm NaN and 1 mM of Na_3Cit, (d) after exposure to 1 mM of Ca^{2+} and 100 ppm NaN and (e) after exposure to 1 mM of Ca^{2+}, 100 ppm NaN and 1 mM of Na_3Cit.

6.3.2 The viscoelastic and electrokinetic properties of adsorbed layers

To characterize the adsorbed layers under different conditions, the ΔD-Δf plots from QCM-D experiments are summarized in Figure 6.4; the details of the highlighted area (red box) are plotted on the right side. Meanwhile, the zeta potential distributions of alumina particles under selected conditions are shown in Figure 6.5.
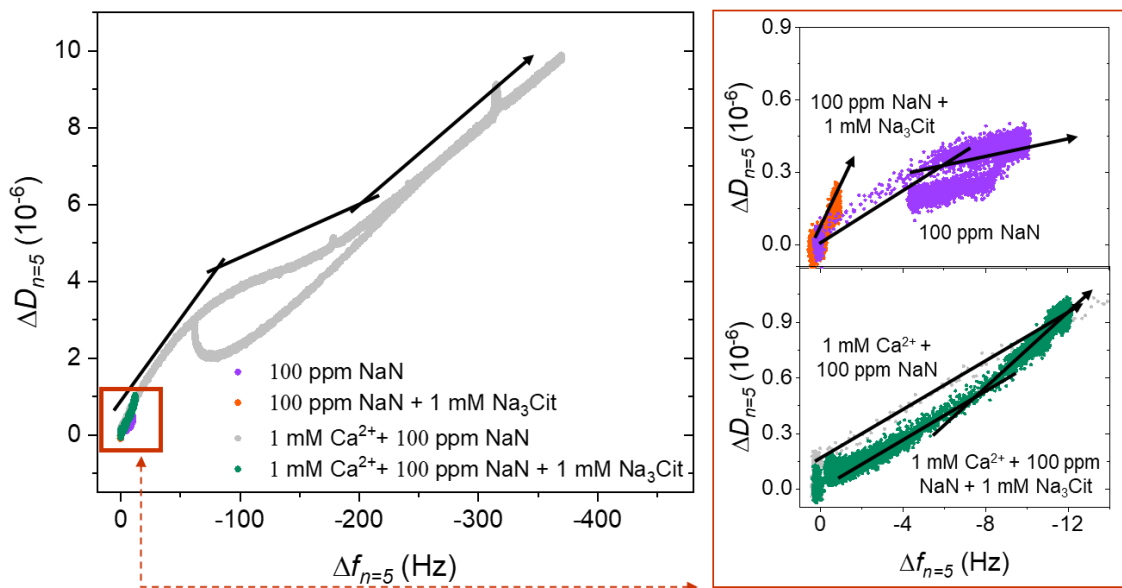
Figure 6.4. ΔD versus Δf plots of naphthenates adsorption at 5th overtone. Experimental data are presented by dots, and solid lines indicate the approximate trend of ΔD-Δf curves.

The plot of ΔD versus Δf provides information on the viscoelasticity of the adsorbed layer.[158] A larger value of ΔD/Δf indicates that the adsorbed layer has a looser structure, while a lower value represents a rigid and compact attached layer.[159] Moreover, the slope variation of the ΔD-Δf curve can explain the conformation changes of the adsorbed layer during the experiment. In Figure 6.4, the change in the slope of the ΔD-Δf curve under 100 ppm NaN (purple dots) indicates that this adsorption process undergoes two stages: (1) a loose and soft layer of naphthenate spontaneously formed on the alumina surface, which is represented by the initial region with a higher slope; (2) With more naphthenates injected into the QCM-D flow module, the conformation of adsorbed naphthenates changes to a more compact structure which is represented by the second region with a lower slope. For a monolayer adsorbed naphthenates, the negative charge of the carboxyl group is supposed

to be eliminated by the interaction with alumina surfaces. However, the alumina surfaces carry high negative charges under this condition based on the measured zeta potential (Figure 6.5a). In this case, bilayer adsorption of naphthenates induced by the hydrophobic interactions is suggested to explain the layer conformation changes. Meanwhile, the outer layer exposes their carboxyl groups to the environment, which increases the negative charges of alumina surfaces.

Compared with adding NaN alone, the ΔD-Δf curve is much steeper in the presence of Na$_3$Cit (red dots in Figure 6.4). This is an indicator of either the adsorbed naphthenates became looser in the presence of Na$_3$Cit, or different materials other than naphthenates adsorbed on the alumina surface. Comparing the zeta potential distribution of alumina particle in Figure 6.5a, the mixture of NaN and Na$_3$Cit shows a similar trend with the solution that only contains Na$_3$Cit, which strongly indicates that alumina surfaces were dominated by Na$_3$Cit.

The alumina surface became more positively charged in the presence of 1 mM Ca^{2+} (Figure 6.5b). This is consistent with previous studies which suggested Ca^{2+} increases positive charges on the alumina surface by interacting with AlO$^-$ or AlOH.[160-162] Therefore, more naphthenates are attracted to the alumina surfaces. Moreover, the interaction between naphthenates and Ca^{2+} assisted the adsorption of naphthenates on alumina surfaces.[163] Obviously, the layer structure became more complicated when Ca^{2+} was introduced into the system (grey dots in Figure 6.4). It changed twice over time, with a more compact structure at first and less rigid structure at the end. The initial decreased slope is similar to

the case that only contains NaN. A reorientation of adsorbed naphthenates from parallel

adsorption to perpendicular adsorption and hydrophobic interactions between the

hydrophobic tails of naphthenate led to a more compact structure. Later, the accumulation

of Ca-naphthenate complexes led to a significant drop in frequency, and resulted in a loose

and soft structure, which was illustrated by the third region of the ΔD-Δf curve. When

citrate was added together (green dots), the decrease in frequency was much smaller, and

the adsorbed layer become less rigid over time.
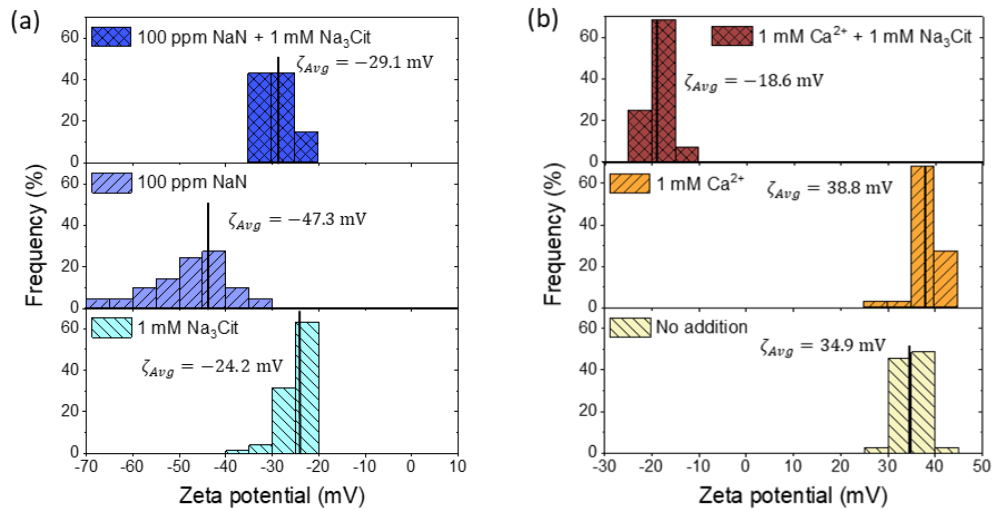
Figure 6.5. Zeta potential distribution of alumina particle under different conditions at pH

8: (a) Zeta potential distribution of alumina particle in the presence of Na$_3$Cit and NaN

respectively and in combination, (b) zeta potential distribution of alumina particle in the

presence of Ca^{2+} and Na$_3$Cit together with Ca^{2+}.

6.3.3 Possible mechanism of sodium citrate in preventing naphthenates from

adsorption on solid surfaces

Previous studies showed that the point of zero charge of alumina is around pH 9 ± 0.5.[164-166] In this study, the pH of all sample solutions was adjusted to around 8, which resulted in a positively charged alumina surface. Meanwhile, the NaN fully dissociated at this pH because the pKa for most of the naphthenic acids is around 4 to 5.[72] Based on this information and the experimental results, a competitive adsorption mechanism between naphthenic acid and sodium citrate on the alumina surface can be proposed. A schematic diagram of the role of Na_3Cit on naphthenate adsorption in the presence and absence of Ca^{2+} is illustrated in Figure 6.6.
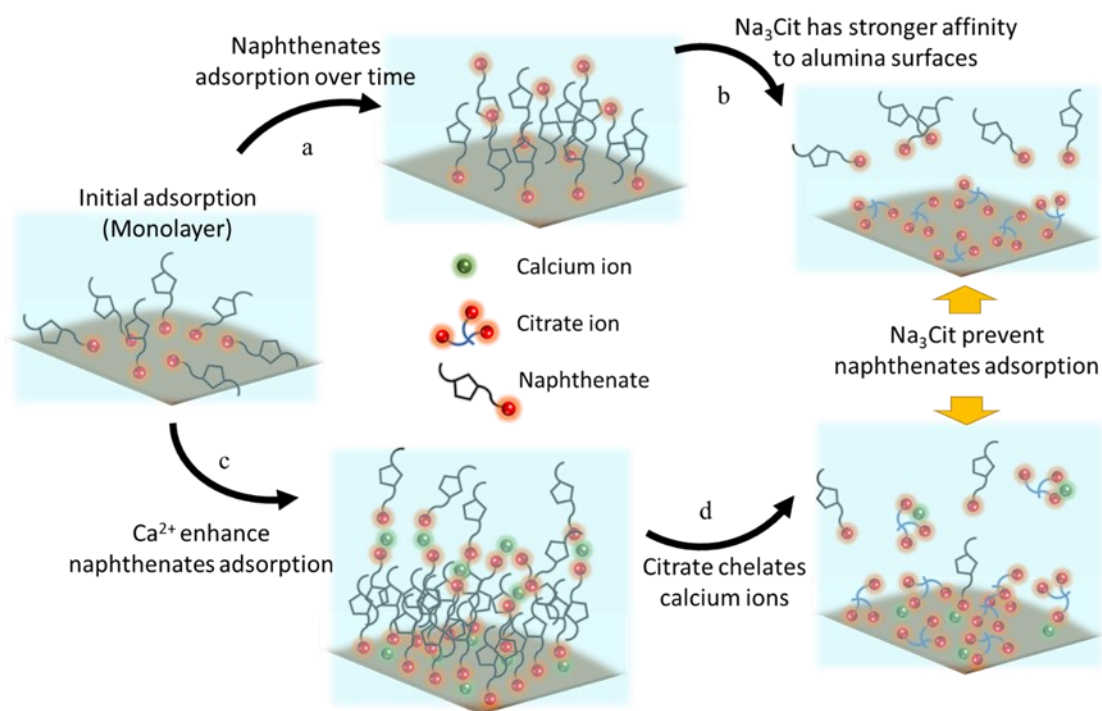
Figure 6.6. Mechanism of naphthenates adsorption on alumina surfaces in the presence and absence of Ca^{2+} and the role of Na_3Cit. At pH 8, the initial adsorption of naphthenates on alumina surfaces is driven by electrostatic attractions. (a) Carboxyl groups from naphthenates coordinate with alumina surfaces and form bilayer adsorption through

hydrophobic interaction. (b) The presence of Na₃Cit prevents adsorption of naphthenates since it has a stronger affinity to alumina surfaces. (c) Adding Ca^{2+} significantly increases the adsorption of naphthenates. (d) Na₃Cit not only pre-adsorb on alumina surfaces but also chelates Ca^{2+}, which prevents naphthenates adsorption.

Once the aluminum oxide is exposed to the sample solution at pH 8, the formed hydroxide on the surface undergoes a protonation process and results in a positively charged surface. Thus, the adsorption of naphthenates on the alumina sensor was initiated by electrostatic attraction. To prove this mechanism, the adsorption of naphthenates was repeated at a more alkaline condition (solution pH ≥ 9) and no adsorption was observed since the alumina surface exhibited neutral or negative charges and naphthenates were repelled from the alumina surface (Figure 6.7).
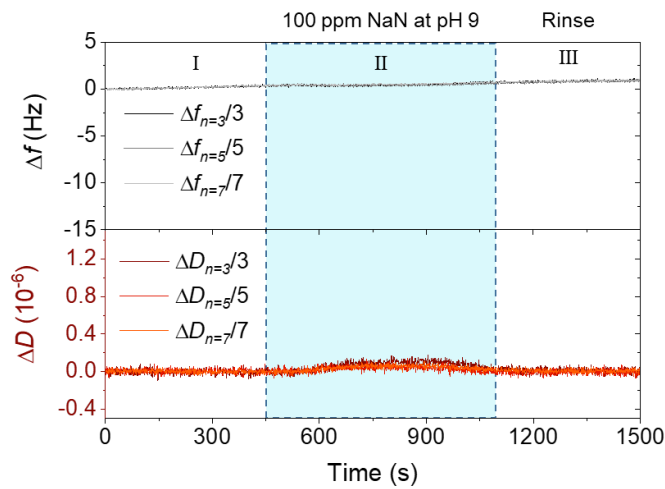
Figure 6.7: Change in frequency and dissipation of the alumina sensor in the presence of 100 ppm sodium naphthenate at pH 9. The ΔD and Δf at 3, 5 and 7 overtone have been normalized by the overtone number. Step I represents an injection of Milli-Q water; step II indicates the injection of the sample solution, and step III is the rinse step.

The carboxyl groups from naphthenic acid are capable of coordinating with the alumina surface[167, 168] and lead to a loosely attached monolayer at the beginning. More naphthenates adsorb on alumina surfaces over time and lead to a reorientation of the naphthenates and the formation of a second layer. The outer layer can be rinsed off by water, which leaves a stable monolayer with hydrophobic tails exposed to the environment. Therefore, even though the alumina surface is highly negatively charged in NaN solution, the alumina sensor became hydrophobic after adsorption experiments.

The presence of Na_3Cit preventing the adsorption of naphthenates can be explained by a competitive adsorption mechanism. Sodium citrate is a well-known chelating agent with three carboxyl groups that fully dissociates at pH 8. In general, the affinity of complexants for the metal oxides depends on their pKa values, molecular structures, and functional groups and their relative position, etc. Compared with naphthenate, citrate is a smaller molecule with three carboxyl groups and one hydroxyl group. Although the exact structures of Alumina-Cit surface complexes have not been proved yet, it was suggested that the tendency of forming surface complex is similar to forming a complex with the corresponding metal ions.[168-170] Thus three carboxyl groups and the hydroxyl group can participate in complexing with alumina surfaces, indicating that Na_3Cit has a stronger affinity to alumina surfaces than naphthenates. Moreover, it is not necessary for all the functional groups to coordinate with the surface, and the rest of the uncoordinated groups will contribute to the surface charges. According to the zeta potential results, the adsorption of Na_3Cit shifted the surface charge of alumina from positive to negative at pH 8, which

forms a barrier and repels the naphthenates from the surfaces. Therefore, citrate not only has a stronger affinity to alumina surface, which competes with naphthenates, but also creates a negative charge barrier to prevent the adsorption of naphthenates.

Similarly, in the presence of Ca^{2+}, the adsorption of naphthenates on alumina surface experiences conformation changes to form a bilayer structure. Later, a continually increasing in naphthenates adsorption is caused by the synergistic effect of the formation of Ca-Naphthenate complex and hydrophobic interactions between naphthenates. Therefore, most of the adsorbed naphthenates can be rinsed off by water. In this case, Na_3Cit preventing the adsorption of naphthenates is mainly attributed to its ability to chelate metal cations. The coordination strength between citrate and polyvalent metal cations is very strong. At pH 8, Ca^{2+} and citrate exist mainly as the bidentate complex shown as Ca-Cit⁻.[171] Therefore, adding Na_3Cit together with Ca^{2+} created negatively charged alumina surfaces (see Figure 6.5b). The adsorption of naphthenates in the presence of Ca^{2+} can be prevented by Na_3Cit through two ways: removing free Ca^{2+} in bulk and blocking the alumina surfaces by citrate molecules.

6.4 Implications of solid wettability to bitumen liberation

According to the above discussion, Na_3Cit is capable of forming complexes with Ca^{2+} and aluminum oxides, which interfere with the naphthenates adsorption on alumina surfaces. To figure out the implications of such benefits in the crude oil recovery process, the wetting transitions through competitive adsorption of NAs and Na_3Cit on mica surfaces were measured. Mica has a 2:1 layer structure with an aluminum octahedral sheet sandwiched

between two silicon tetrahedral sheets, which has an atomic smoothness at its basal cleavage. The basal cleavage of mica was applied to mimic the hydrophilic clay minerals contained in oil sands. The experimental set up for the relative wettability of oil and water on mica surfaces is illustrated in Figure 6.8. A mica sheet with freshly exposed basal cleavage was placed in pure decane oil, and a Milli-Q water droplet was generated in the oil phase. Once the water droplet was in contact with mica, it spread on the mica surface immediately and formed a negligible contact angle. This result indicates that the mica basal cleavage is very hydrophilic, which can be fully wetted by water in the oil without NAs inside.
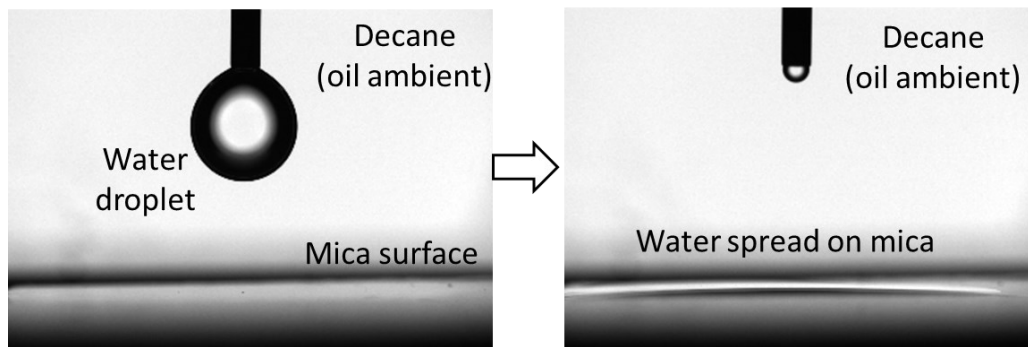
Figure 6.8. Experimental setup of measuring water contact on mica surfaces in an oil ambient.

Later, 10000 ppm NAs was dissolved into decane to simulate the natural surfactant from bitumen, and the contact angle of the aqueous phase was recorded over time (Figure 6.9). The water droplets were found to spread on the mica surface at the beginning until the contact angle reached 40°. Later, the contact angle gradually increased to 52° after 1 hr (Figure 6.9a). Obviously, the presence of NAs in decane triggered an in situ wettability transition on mica surfaces and inhibited the spreading of water. It is interesting to note the

addition of 1 mM Na₃Cit into the water phase promoted the spreading of water and resulted

in a contact angle of 12° (Figure 6.9b). It further proved the role of Na₃Cit in maintaining

the wettability of mineral surfaces.
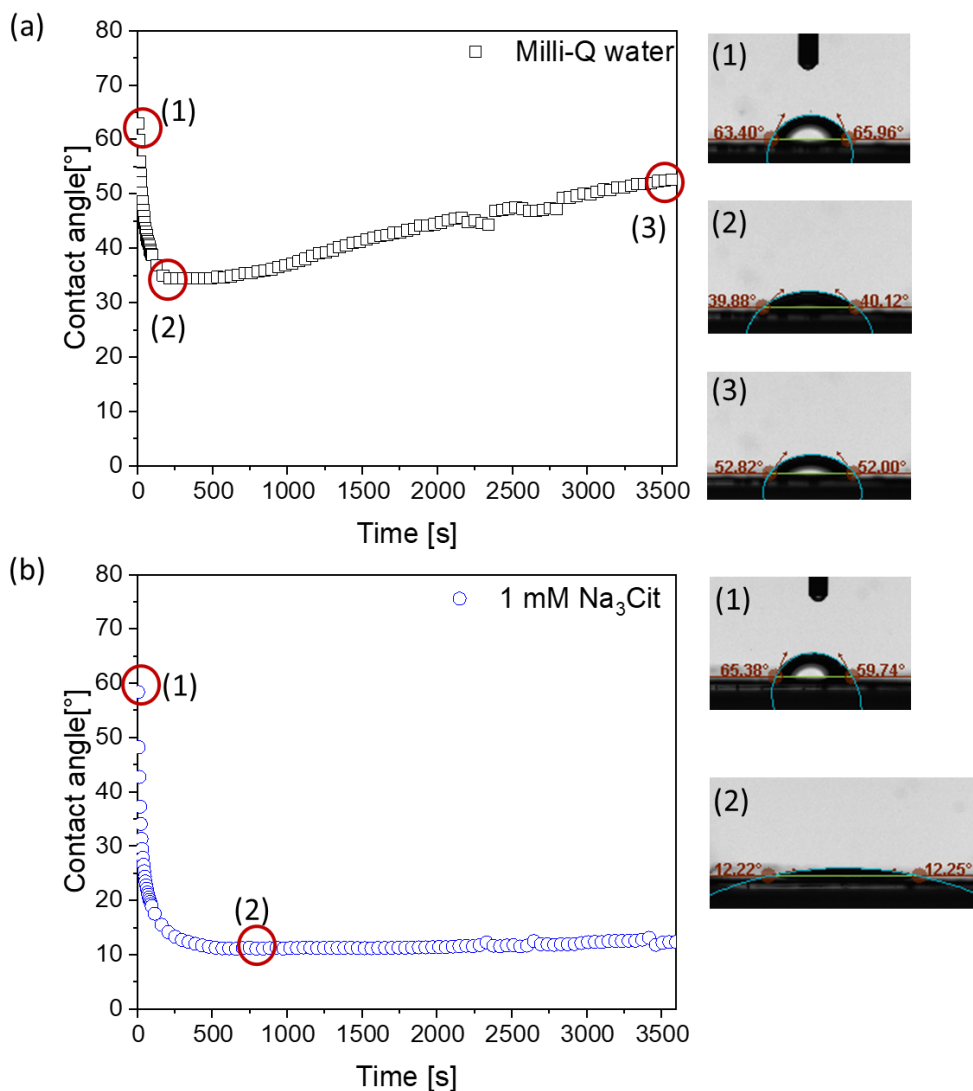
Figure 6.9. Water wetting on mica surfaces in ambient decane containing naphthenic acids, side views of droplets are illustrated at the right side of each graph. (a) Milli-Q water at pH 8 (squares), (b) 1 mM Na₃Cit at pH 8 (circles).

These results provide an implication to the enhanced bitumen recovery process. The presence of NAs in crude oil inhibits the spreading of the water phase which is detrimental to bitumen displacement. Adding Na_3Cit in the aqueous phase prevents the adsorption of dissociated NAs on alumina surfaces, and it is expected to promote the water phase displacing the bitumen phase. Based on the above discussions, the role of Na_3Cit in preventing naphthenates adsorption and its implication to bitumen recovery is illustrated in Figure 6.10. At the bitumen-solid-water three-phase contact line (TPCL), Na_3Cit adsorbs on positively charged solid surfaces (i.e. alumina basal plane and the edge of clay minerals) which prevents the adsorption of naphthenates from the bitumen-water interface to solid surfaces. On the other hand, Na_3Cit removes cation bridges between negatively charged solid surfaces (sand grains and silica basal plane), promoting the TPCL movement by increasing the repulsion between bitumen and solid surfaces. According to the same mechanism, Na_3Cit maintains the hydrophilicity of solid surfaces, which inhibits coagulation between bitumen and mineral solid. Therefore, it is reasonable to observe an improved bitumen recovery and froth quality during oil sands extraction by adding Na_3Cit.[11]
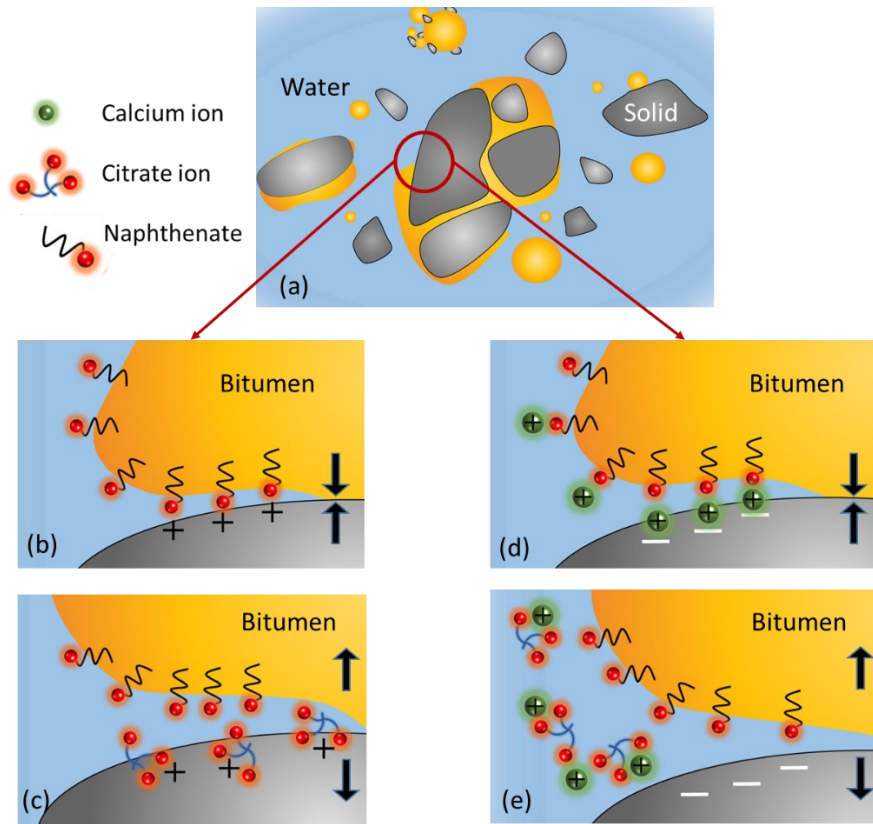
Figure 6.10. Implications of solid wettability alternation to bitumen liberation under the effect of sodium citrate. (a) Schematics of oil sands lumps present in the aqueous solution. The red circle highlights the bitumen-solid-water TPCL. (b) Microscopic view of the TPCL pinning caused by NAs adsorption at positively charged solid surfaces. (c) The microscopic view of the TPCL, Na_3Cit prevents NAs adsorption and increases repulsion between solid and bitumen. (d) The microscopic view of the TPCL pinning caused by cation bridged between NAs and solid surfaces. (e) Microscopic view of the TPCL, Na_3Cit breaks cation bridges and increases repulsion between solid and bitumen.

6.5 Conclusion

126

The effects of sodium citrate and calcium ions on the adsorption of naphthenic acid on alumina surfaces were investigated at an alkaline condition. It was found that the negatively charged naphthenates adsorbed on the positively charged sites of alumina surfaces and increased its hydrophobicity. A significant increase in naphthenates adsorption was observed when calcium ions were added together, which consequently generated a higher contact angle of alumina surfaces. Interestingly, the presence of sodium citrate prevented the adsorption of naphthenates in both cases with and without calcium ions. By analyzing the layer conformation and zeta potential distribution, possible mechanisms were proposed to explain the effect of sodium citrate in preventing naphthenic acid adsorption on the alumina surface. Calcium ions enhanced the adsorption of naphthenates through increasing the positive charges on alumina surfaces, and also it interacted with naphthenates on alumina surfaces and in bulk. However, since sodium citrate has a stronger affinity to both alumina surfaces and calcium ions, it not only removed the free calcium ions but also competitively adsorbed on the alumina surfaces. Accordingly, sodium citrate prevents the wetting transition of alumina and mica, which is beneficial to the crude oil displacement process and inhibits bitumen-solid coagulations.

Chapter 7 Conclusions and Future work

7.1 Conclusions

A new method to quantifying the liberation process with quartz crystal microbalance with dissipation (QCM-D) was developed in this work. By applying this method, the roles of sodium citrate in bitumen liberation and solid wettability alternation were fundamentally understood.

The feasibility of applying QCM-D in bitumen liberation was validated by using a bitumen spin-coated silica sensor. Results indicated that a high solution pH and/or a high temperature was beneficial to bitumen liberation, which is consistent with previously published research. Meanwhile, the fundamental mechanisms for bitumen film thinning and rupture were proposed based on the measured frequency and dissipation variation. It was found that the bitumen liberation was significantly depressed if the silica sensor surface was hydrophobized before bitumen coating. Since the hydrophobic surface cannot form H-bonding with water molecules, thus, it is hard for water to form water channels in the bitumen film and destroy it. In general, the QCM-D is a reliable technique to measure both the DBL and kinetics of the bitumen liberation process under various operation conditions.

According to the QCM-D results, the mixture of Na_3Cit and NaOH generated the highest DBL of all tested concentrations. In addition, the benefit of Na_3Cit on the sub-step of bitumen liberation, the dynamic displacement of bitumen from the quartz surface, was

verified experimentally and theoretically. At pH 8 and 45 ºC, increasing the concentration of Na$_3$Cit not only accelerated the bitumen displacement rate but also generated a smaller contact angle at the end of the experiment. Moreover, the addition of 10 mM Na$_3$Cit resulted in a complete dewetting of bitumen within 3 mins. In contrast, the addition of Ca^{2+} slowed down the displacement rate and generated daughter droplets during displacement. Modelling results from the hydrodynamic model and the molecular kinetic model indicated both the viscous resistance and contact line friction decreased in the presence of Na$_3$Cit, which explained the enhanced displacement dynamics. However, these two parameters were increased in the presence of Ca^{2+}.

The effects of Na$_3$Cit in naphthenic acids (NAs) adsorption induced solid wettability alternation were investigated by QCM-D. The alumina sensor was applied to mimic the alumina components of clay minerals. It was found that the adsorption of NAs at pH 8 increased the hydrophobicity of the alumina surface, and the presence of Ca^{2+} magnified this effect. Surprisingly, the addition of Na$_3$Cit together with NAs prevented the adsorption of naphthenates on alumina surface with and without Ca^{2+}.

The effects of Na$_3$Cit in enhancing bitumen liberation and inhibiting NAs adsorption are related to its chelating ability and modifying the interfacial properties in this system. It was found that both the bitumen surface and solid surface (silica and alumina) became more negatively charged in the presence of Na$_3$Cit. Therefore, the stronger electrostatic repulsion between bitumen and solids enhances the bitumen recession from solid surfaces. The adhesion force between bitumen and silica decreased in the presence of sodium citrate as

measured by AFM, which is beneficial to bitumen detachment. The reduction in adhesion force between bitumen and silica also explained the enhanced bitumen displacement dynamics. Besides, Na_3Cit was preferentially adsorbed on alumina surfaces, preventing the adsorption of naphthenates. The Ca^{2+} contained in the solution were chelated by Na_3Cit so that the detrimental effects of Ca^{2+} were eliminated.

7.2 Future work

Based on the developed experimental method and findings, several research areas are suggested for future study.

- In Chapter 3, the QCM-D was successfully employed to study the bitumen liberation from a silica sensor surface. However, in addition to silica, mineral clays such as kaolinite, illite and montmorillonite are frequently found in the oil sands ores. The sensor surface can be manufactured with different mineral surfaces. It is worth investigating the bitumen liberation process on different mineral clays and its efficiency under various conditions using QCM-D.

- The presence of Na_3Cit reduces the adhesion and increases the long-range repulsion between bitumen and silica. In addition, the interactions between different clays and bitumen in the presence of Na_3Cit should be studied in the future.

- In this thesis, the silica surfaces became more negatively charged in the presence of Na_3Cit. The increased negative charges are possibly attributed to the dissolution of silicon

ions from the silica surfaces. The origin of a more negatively charged silica-water interface in the presence of sodium citrate should be explored in the future.

- It is worth to experimentally confirm the competitive chelation ability to metal cations between citrate ions and organic acids from bitumen.

- During bitumen displacement, daughter droplets were frequently observed in the presence of Ca^{2+} while disappeared as Na_3Cit was added. The underlying mechanisms remain unclear. It was assumed that this phenomenon was related to the intermolecular interactions at the TPCL, which is worth investigating both experimentally and theoretically.

References

1.   Masliyah, J.; Czarnecki, J.; Xu, Z., Handbook on theory and practice of bitumen recovery from Athabasca oil sands. *Theoretical Basis* **2011,** 1.

2.   Masliyah, J.; Zhou, Z. J.; Xu, Z.; Czarnecki, J.; Hamza, H., Understanding water-based bitumen extraction from Athabasca oil sands. *The Canadian Journal of Chemical Engineering* **2004,** 82, (4), 628-654.

3.   Clark, K., Hot water Separation of Bitumen from Alberta Bituminous Sand. *Research Council of Alberta,Edmonton, Alberta, Canad* **1923**.

4.   Clark, K.; Pasternack, D., Hot water seperation of bitumen from Alberta bituminous sand. *Industrial & Engineering Chemistry* **1932,** 24, (12), 1410-1416.

5.   Dai, Q.; Chung, K.; Czarnecki, J., Formation of calcium carbonate in the bitumen/aqueous sodium hydroxide system. *AOSTRA Journal of Research* **1992,** 8, 95-95.

6.   Schramm, L. L.; Smith, R. G., Two classes of anionic surfactants and their significance in hot water processing of oil sands. *The Canadian Journal of Chemical Engineering* **1987,** 65, (5), 799-811.

7.   Li, H.; Long, J.; Xu, Z.; Masliyah, J., Synergetic role of polymer flocculant in low-temperature bitumen extraction and tailings treatment. *Energy & fuels* **2005,** 19, (3), 936-943.

8.   Li, H.; Zhou, Z.; Xu, Z.; Masliyah, J., Role of acidified sodium silicate in low temperature bitumen extraction from poor-processing oil sand ores. *Industrial & engineering chemistry research* **2005,** 44, (13), 4753-4761.

9.   Flury, C.; Afacan, A.; Tamiz Bakhtiari, M.; Sjoblom, J.; Xu, Z., Effect of caustic type on bitumen extraction from Canadian oil sands. *Energy & Fuels* **2013,** 28, (1), 431-438.

10.   Long, J.; Gu, Y., Sodium triphosphate and caustic as process aids for the extraction of bitumen from mined oil sands. In Google Patents: 2014.

11.   Long, J.; Gu, Y. J. Sodium citrate and caustic as process aids for the extraction of bitumen from mined oil sands. 2016.

12.   Clark, K., Hot water separation of Alberta bituminous sand. *Trans. Can. Inst. Min. Metall* **1944,** 47, 257-274.

13.   Wallwork, V.; Xu, Z.; Masliyah, J., Processibility of Athabasca Oil Sand Using a Laboratory Hyd ro t ransport Extraction System (LHES). *The Canadian Journal of Chemical Engineering* **2004,** 82, (4), 687-695.

14.   Takamura, K.; Wallace, D., The physical chemistry of the hot water process. *Journal of Canadian Petroleum Technology* **1988,** 27, (06).

15.   Basu, S.; Nandakumar, K.; Masliyah, J. H., A study of oil displacement on model surfaces. *Journal of colloid and interface science* **1996,** 182, (1), 82-94.

16.	Basu, S.; Nandakumar, K.; Masliyah, J. H., On bitumen liberation from oil sands. *The Canadian Journal of Chemical Engineering* **1997,** 75, (2), 476-479.

17.	Srinivasa, S.; Flury, C.; Afacan, A.; Masliyah, J.; Xu, Z., Study of bitumen liberation from oil sands ores by online visualization. *Energy & Fuels* **2012,** 26, (5), 2883-2890.

18.	Sauerbrey, G., The use of quarts oscillators for weighing thin layers and for microweighing. *Z. Phys.* **1959,** 155, 206-222.

19.	Voinova, M. V.; Rodahl, M.; Jonson, M.; Kasemo, B., Viscoelastic acoustic response of layered polymer films at fluid-solid interfaces: continuum mechanics approach. *Physica Scripta* **1999,** 59, (5), 391.

20.	Dixon, M. C., Quartz crystal microbalance with dissipation monitoring: enabling real-time characterization of biological materials and their interactions. *Journal of biomolecular techniques: JBT* **2008,** 19, (3), 151.

21.	Abudu, A.; Goual, L., Adsorption of crude oil on surfaces using quartz crystal microbalance with dissipation (QCM-D) under flow conditions. *Energy & Fuels* **2009,** 23, (3), 1237-1248.

22.	Rudrake, A.; Karan, K.; Horton, J. H., A combined QCM and XPS investigation of asphaltene adsorption on metal surfaces. *Journal of colloid and interface science* **2009,** 332, (1), 22-31.

23.	Primkulov, B. K.; Lin, F.; Xu, Z., Microscale liquid-liquid displacement dynamics: Molecular kinetic or hydrodynamic control. *Colloids and Surfaces A: Physicochemical and Engineering Aspects* **2016,** 497, 336-343.

24.	Energy, A., Oil Sands Facts. *Alberta Department of Energy* **2002**.

25.	Shin, H.; Polikar, M. In *Optimizing the SAGD process in three major Canadian oil-sands areas*, SPE Annual Technical Conference and Exhibition, 2005; Society of Petroleum Engineers: 2005.

26.	Teare, M.; Cruickshank, R.; Miller, S.; Overland, S.; Marsh, R. *Alberta's energy reserves 2013 and supply/demand outlook 2014-2023*; Alberta Energy Regulator, Calgary, Alberta.: 2014.

27.	Camp, F. W., *The tar sands of Alberta*. Cameron Engineers: 1976.

28.	Madge, D.; Romero, J.; Strand, W., Hydrocarbon cyclones in hydrophilic oil sand environments. *Minerals engineering* **2004,** 17, (5), 625-636.

29.	Mossop, G. D., Geology of the Athabasca oil sands. *Science* **1980,** 207, (4427), 145-152.

30.	Takamura, K., Microscopic structure of Athabasca oil sand. *The Canadian Journal of Chemical Engineering* **1982,** 60, (4), 538-545.

31.	Long, J.; Drelich, J.; Xu, Z.; Masliyah, J. H., Effect of Operating Temperature on Water-Based Oil Sands Processing. *The Canadian Journal of Chemical Engineering* **2007,** 85, (5), 726-738.

32.   Sury, K. N., Low temperature bitumen recovery process. In Google Patents: 1990.

33.   Takamura, K.; Wallace, D., Experimental and theoretical studies of the hot water processability of different grades of Athabasca oil sands. *Flocculation in Biotechnology and Separation Systems", YA Attia, Ed., Elsevier Science Publ., Amsterdam, The Netherlands* **1987**, 579-597.

34.   Schramm, L. L.; Stasiuk, E. N.; Turner, D., The influence of interfacial tension in the recovery of bitumen by water-based conditioning and flotation of Athabasca oil sands. *Fuel Processing Technology* **2003,** 80, (2), 101-118.

35.   Young, T., III. An essay on the cohesion of fluids. *Philosophical transactions of the royal society of London* **1805**, (95), 65-87.

36.   Sanford, E.; Seyer, F., Processibility of Athabasca tar sand using a batch extraction unit: the role of NaOH. *CIM Bull* **1979,** 72, (803), 164-169.

37.   Schramm, L. L.; Stone, J. A., A surface-tension method for the determination of anionic surfactants in hot water processing of athabasca oil sands. *Colloids and surfaces* **1984,** 11, (3-4), 247-263.

38.   Park, S.-J.; Seo, M.-K., Intermolecular force. In *Interface Science and Technology*, Elsevier: 2011; Vol. 18, pp 1-57.

39.   Takamura, K.; Chow, R. S., The electric properties of the bitumen/water interface Part II. Application of the ionizable surface-group model. *Colloids and surfaces* **1985,** 15, 35-48.

40.   Dai, Q.; Chung, K. H., Bitumen—sand interaction in oil sand processing. *Fuel* **1995,** 74, (12), 1858-1864.

41.   Liu, J.; Zhou, Z.; Xu, Z.; Masliyah, J., Bitumen–clay interactions in aqueous media studied by zeta potential distribution measurement. *Journal of colloid and interface science* **2002,** 252, (2), 409-418.

42.   Liu, J.; Xu, Z.; Masliyah, J., Studies on bitumen− silica interaction in aqueous solutions by atomic force microscopy. *Langmuir* **2003,** 19, (9), 3911-3920.

43.   Zhou, Z.; Xu, Z.; Masliyah, J. H.; Czarnecki, J., Coagulation of bitumen with fine silica in model systems. *Colloids and Surfaces A: Physicochemical and Engineering Aspects* **1999,** 148, (3), 199-211.

44.   Gan, W.; Crozier, B.; Liu, Q., Effect of citric acid on inhibiting hexadecane–quartz coagulation in aqueous solutions containing Ca2+, Mg2+ and Fe3+ ions. *International Journal of Mineral Processing* **2009,** 92, (1-2), 84-91.

45.   Hanly, G.; Fornasiero, D.; Ralston, J.; Sedev, R., Electrostatics and metal oxide wettability. *The Journal of Physical Chemistry C* **2011,** 115, (30), 14914-14921.

46.   Mugele, F.; Bera, B.; Cavalli, A.; Siretanu, I.; Maestro, A.; Duits, M.; Cohen-Stuart, M.; Van Den Ende, D.; Stocker, I.; Collins, I., Ion adsorption-induced wetting transition in oil-water-mineral systems. *Scientific reports* **2015,** 5, 10519.

47.   Dehghan Monfared, A.; Ghazanfari, M. H.; Kazemeini, M.; Jamialahmadi, M.; Helalizadeh, A., Wettability alteration modeling for oil-wet Calcite/Silica nanoparticle

system using surface forces analysis: contribution of DLVO versus Non-DLVO interactions. *Industrial & Engineering Chemistry Research* **2018,** 57, (43), 14482-14492.

48.   Basu, S.; Nandakumar, K.; Lawrence, S.; Masliyah, J., Effect of calcium ion and montmorillonite clay on bitumen displacement by water on a glass surface. *Fuel* **2004,** 83, (1), 17-22.

49.   Luthra, M., A visualization technique for estimating bitumen recovery from oil sands. **2003**.

50.   Long, J.; Zhang, L.; Xu, Z.; Masliyah, J. H., Colloidal interactions between Langmuir− Blodgett bitumen films and fine solid particles. *Langmuir* **2006,** 22, (21), 8831-8839.

51.   He, L.; Lin, F.; Li, X.; Xu, Z.; Sui, H., Enhancing bitumen liberation by controlling the interfacial tension and viscosity ratio through solvent addition. *Energy & fuels* **2014,** 28, (12), 7403-7410.

52.   Ren, S.; Dang-Vu, T.; Zhao, H.; Long, J.; Xu, Z.; Masliyah, J., Effect of weathering on surface characteristics of solids and bitumen from oil sands. *Energy & fuels* **2009,** 23, (1), 334-341.

53.   Dang-Vu, T.; Jha, R.; Wu, S.-Y.; Tannant, D. D.; Masliyah, J.; Xu, Z., Effect of solid wettability on processability of oil sands ores. *Energy & fuels* **2009,** 23, (5), 2628-2636.

54.   Ren, S.; Zhao, H.; Dang-Vu, T.; Xu, Z.; Masliyah, J. H., Effect of weathering on oil sands processability. *The Canadian Journal of Chemical Engineering* **2009,** 87, (6), 879-886.

55.   Liu, J.; Xu, Z.; Masliyah, J., Interaction forces in bitumen extraction from oil sands. *Journal of colloid and interface science* **2005,** 287, (2), 507-520.

56.   Sanford, E., Processibility of Athabasca oil sand: Interrelationship between oil sand fine solids, process aids, mechanical energy and oil sand age after mining. *The Canadian Journal of Chemical Engineering* **1983,** 61, (4), 554-567.

57.   Schramm, L. L.; Smith, R. G., The influence of natural surfactants on interfacial charges in the hot-water process for recovering bitumen from the Athabasca oil sands. *Colloids and surfaces* **1985,** 14, (1), 67-85.

58.   Takamura, K.; Chow, R. S., A mechanism for initiation of bitumen displacement from oil sand. *Journal of Canadian Petroleum Technology* **1983,** 22, (06).

59.   Qin, R.; Lillico, D.; How, Z. T.; Huang, R.; Belosevic, M.; Stafford, J.; El-Din, M. G., Separation of oil sands process water organics and inorganics and examination of their acute toxicity using standard in-vitro bioassays. *Science of The Total Environment* **2019,** 695, 133532.

60.   Tamiz Bakhtiari, M.; Harbottle, D.; Curran, M.; Ng, S.; Spence, J.; Siy, R.; Liu, Q.; Masliyah, J.; Xu, Z., Role of Caustic Addition in Bitumen–Clay Interactions. *Energy & Fuels* **2015,** 29, (1), 58-69.

61.   Chen, T.; Lin, F.; Primkulov, B.; He, L.; Xu, Z., Impact of salinity on warm water-based mineable oil sands processing. *The Canadian Journal of Chemical Engineering* **2017,** 95, (2), 281-289.

62.   Gan, W.; Liu, Q., Coagulation of bitumen with kaolinite in aqueous solutions containing Ca2+, Mg2+ and Fe3+: Effect of citric acid. *Journal of colloid and interface science* **2008,** 324, (1-2), 85-91.

63.   Zhao, H.; Long, J.; Masliyah, J. H.; Xu, Z., Effect of divalent cations and surfactants on silica− bitumen interactions. *Industrial & engineering chemistry research* **2006,** 45, (22), 7482-7490.

64.   Harjai, S. K.; Flury, C.; Masliyah, J.; Drelich, J.; Xu, Z., Robust aqueous–nonaqueous hybrid process for bitumen extraction from mineable Athabasca oil sands. *Energy & fuels* **2012,** 26, (5), 2920-2927.

65.   Lin, F.; He, L.; Hou, J.; Masliyah, J.; Xu, Z., Role of ethyl cellulose in bitumen extraction from oil sands ores using an aqueous–nonaqueous hybrid process. *Energy & Fuels* **2016,** 30, (1), 121-129.

66.   Glusker, J. P., Citrate conformation and chelation: enzymic implications. *Accounts of Chemical Research* **1980,** 13, (10), 345-352.

67.   Goldberg, R. N.; Kishore, N.; Lennen, R. M., Thermodynamic quantities for the ionization reactions of buffers. *Journal of physical and chemical reference data* **2002,** 31, (2), 231-370.

68.   Rosen, M. J.; Kunjappu, J., Surfactants and Interfacial Phenomena, John Willey and Sons. *Inc., Hoboken, New Jersey* **2012**, 150-225.

69.   Chen, F.; Finch, J.; Xu, Z.; Czarnecki, J., Wettability of fine solids extracted from bitumen froth. *Journal of adhesion science and technology* **1999,** 13, (10), 1209-1224.

70.   Jiang, T.; Hirasaki, G. J.; Miller, C. A.; Ng, S., Wettability alteration of clay in solid-stabilized emulsions. *Energy & fuels* **2011,** 25, (6), 2551-2558.

71.   Lebedeva, E. V.; Fogden, A., Wettability alteration of kaolinite exposed to crude oil in salt solutions. *Colloids and Surfaces A: Physicochemical and Engineering Aspects* **2011,** 377, (1-3), 115-122.

72.   Havre, T. E.; Sjöblom, J.; Vindstad, J. E., Oil/water-partitioning and interfacial behavior of naphthenic acids. *Journal of dispersion science and technology* **2003,** 24, (6), 789-801.

73.   Headley, J. V.; McMartin, D. W., A review of the occurrence and fate of naphthenic acids in aquatic environments. *Journal of Environmental Science and Health, Part A* **2004,** 39, (8), 1989-2010.

74.   Wu, C.; De Visscher, A.; Gates, I. D., On naphthenic acids removal from crude oil and oil sands process-affected water. *Fuel* **2019,** 253, 1229-1246.

75.   Gomari, K. R.; Denoyel, R.; Hamouda, A., Wettability of calcite and mica modified by different long-chain fatty acids (C18 acids). *Journal of colloid and interface science* **2006,** 297, (2), 470-479.

76.   Xiang, B.; Liu, Q.; Long, J., Probing Bitumen Liberation by a Quartz Crystal Microbalance with Dissipation. *Energy & Fuels* **2018,** 32, (7), 7451-7457.

77.   Blake, T. D., The physics of moving wetting lines. *Journal of colloid and interface science* **2006,** 299, (1), 1-13.

78.   Huh, C.; Scriven, L. E., Hydrodynamic model of steady movement of a solid/liquid/fluid contact line. *Journal of colloid and interface science* **1971,** 35, (1), 85-101.

79.   Blake, T.; Haynes, J., Kinetics of liquidliquid displacement. *Journal of colloid and interface science* **1969,** 30, (3), 421-423.

80.   Fetzer, R.; Ralston, J., Dynamic dewetting regimes explored. *The Journal of Physical Chemistry C* **2009,** 113, (20), 8888-8894.

81.   Zhang, Y.; Fuentes, C. A.; Koekoekx, R.; Clasen, C.; Van Vuure, A. W.; De Coninck, J. l.; Seveno, D., Spreading dynamics of molten polymer drops on glass substrates. *Langmuir* **2017,** 33, (34), 8447-8454.

82.   Duvivier, D.; Seveno, D.; Rioboo, R.; Blake, T.; De Coninck, J., Experimental evidence of the role of viscosity in the molecular kinetic theory of dynamic wetting. *Langmuir* **2011,** 27, (21), 13015-13021.

83.   Li, R.; Manica, R.; Yeung, A.; Xu, Z., Spontaneous Displacement of High Viscosity Micrometer Size Oil Droplets from a Curved Solid in Aqueous Solutions. *Langmuir* **2018,** 35, (3), 615-627.

84.   Ramiasa, M.; Ralston, J.; Fetzer, R.; Sedev, R., Contact line friction in liquid–liquid displacement on hydrophobic surfaces. *The Journal of Physical Chemistry C* **2011,** 115, (50), 24975-24986.

85.   Fetzer, R.; Ramiasa, M.; Ralston, J., Dynamics of liquid− liquid displacement. *Langmuir* **2009,** 25, (14), 8069-8074.

86.   Cox, R., The dynamics of the spreading of liquids on a solid surface. Part 1. Viscous flow. *Journal of fluid mechanics* **1986,** 168, 169-194.

87.   Voinov, O., Hydrodynamics of wetting. *Fluid dynamics* **1976,** 11, (5), 714-721.

88.   Eyring, H., The Activated Complex and the Absolute Rate of Chemical Reactions. *Chemical Reviews* **1935,** 17, (1), 65-77.

89.   Jaiswal, A.; Smoukov, S.; Poggi, M.; Grzybowski, B., Quartz crystal microbalance with dissipation monitoring (QCM-D): real-time characterization of nano-scale interactions at surfaces. *Nsti Nanotech 2008* **2008,** 1, 855-858.

90.   Farooq, U.; Sjöblom, J.; Øye, G., Desorption of asphaltenes from silica-coated quartz crystal surfaces in low saline aqueous solutions. *Journal of dispersion science and technology* **2011,** 32, (10), 1388-1395.

91.   Nourani, M.; Tichelkamp, T.; Gaweł, B.; Øye, G., Method for determining the amount of crude oil desorbed from silica and aluminosilica surfaces upon exposure to combined low-salinity water and surfactant solutions. *Energy & Fuels* **2014,** 28, (3), 1884-1889.

92.   Li, X.; Bai, Y.; Sui, H.; He, L., Understanding desorption of oil fractions from mineral surfaces. *Fuel* **2018,** 232, 257-266.

93.   Cho, N.-J.; Frank, C. W.; Kasemo, B.; Höök, F., Quartz crystal microbalance with dissipation monitoring of supported lipid bilayers on various substrates. *nature protocols* **2010,** 5, (6), 1096-1106.

94.   Kelesoglu, S.; Volden, S.; Kes, M.; Sjoblom, J., Adsorption of naphthenic acids onto mineral surfaces studied by quartz crystal microbalance with dissipation monitoring (QCM-D). *Energy & Fuels* **2012,** 26, (8), 5060-5068.

95.   Wang, L.; Siretanu, I.; Duits, M. H.; Stuart, M. A. C.; Mugele, F., Ion effects in the adsorption of carboxylate on oxide surfaces, studied with quartz crystal microbalance. *Colloids and surfaces A: Physicochemical and engineering aspects* **2016,** 494, 30-38.

96.   Abudu, A.; Goual, L., Adsorption of crude oil on surfaces using quartz crystal microbalance with dissipation (QCM-D) under flow conditions. *Energy & Fuels* **2008,** 23, (3), 1237-1248.

97.   Chen, I.-C.; Akbulut, M., Nanoscale dynamics of heavy oil recovery using surfactant floods. *Energy & Fuels* **2012,** 26, (12), 7176-7182.

98.   Li, X.; Xue, Q.; Wu, T.; Jin, Y.; Ling, C.; Lu, S., Oil detachment from silica surface modified by carboxy groups in aqueous cetyltriethylammonium bromide solution. *Applied Surface Science* **2015,** 353, 1103-1111.

99.   Farooq, U.; Asif, N.; Tweheyo, M. T.; Sjöblom, J.; Øye, G., Effect of low-saline aqueous solutions and pH on the desorption of crude oil fractions from silica surfaces. *Energy & Fuels* **2011,** 25, (5), 2058-2064.

100.   Sauerbrey, G., The use of quartz oscillators for weighing thin layers and for microweighing. *Z. Phys.* **1955,** 155, 206-222.

101.   Rodahl, M.; Höök, F.; Krozer, A.; Brzezinski, P.; Kasemo, B., Quartz crystal microbalance setup for frequency and Q-factor measurements in gaseous and liquid environments. *Review of Scientific Instruments* **1995,** 66, (7), 3924-3930.

102.   Cho, N.-J.; Kanazawa, K. K.; Glenn, J. S.; Frank, C. W., Employing two different quartz crystal microbalance models to study changes in viscoelastic behavior upon transformation of lipid vesicles to a bilayer on a gold surface. *Analytical chemistry* **2007,** 79, (18), 7027-7035.

103.   Wallace, D.; Henry, D.; Miadonye, A.; Puttagunta, V., Viscosity and solubility of mixtures of bitumen and solvent. *Fuel Science and Technology International* **1996,** 14, (3), 465-478.

104.   Dai, Q.; Chung, K. H., Hot water extraction process mechanism using model oil sands. *Fuel* **1996,** 75, (2), 220-226.

105.   Dang-Vu, T.; Jha, R.; Wu, S.-Y.; Tannant, D. D.; Masliyah, J.; Xu, Z., Wettability determination of solids isolated from oil sands. *Colloids and Surfaces A: Physicochemical and Engineering Aspects* **2009,** 337, (1-3), 80-90.

106.   Liu, Q.; Yuan, S.; Yan, H.; Zhao, X., Mechanism of oil detachment from a silica surface in aqueous surfactant solutions: molecular dynamics simulations. *The Journal of Physical Chemistry B* **2012,** 116, (9), 2867-2875.

107.   Zhang, P.; Xu, Z.; Liu, Q.; Yuan, S., Mechanism of oil detachment from hybrid hydrophobic and hydrophilic surface in aqueous solution. *The Journal of chemical physics* **2014,** 140, (16), 164702.

108.   Kolev, V.; Kochijashky, I.; Danov, K.; Kralchevsky, P.; Broze, G.; Mehreteab, A., Spontaneous detachment of oil drops from solid substrates: governing factors. *Journal of colloid and interface science* **2003,** 257, (2), 357-363.

109.   Liu, J.; Xu, Z.; Masliyah, J., Processability of oil sand ores in Alberta. *Energy & fuels* **2005,** 19, (5), 2056-2063.

110.   He, L.; Lin, F.; Li, X.; Sui, H.; Xu, Z., Interfacial sciences in unconventional petroleum production: from fundamentals to applications. *Chemical Society Reviews* **2015,** 44, (15), 5446-5494.

111.   Long, J.; Xu, Z.; Masliyah, J., On the role of temperature in oil sands processing. *Energy & fuels* **2005,** 19, (4), 1440-1446.

112.   Seyer, F.; Gyte, G., Viscosity. *AOSTRA technical handbook on oil sands, bitumens and heavy oils. AOSTRA Technical Publication Series* **1989,** 6.

113.   Hepler, L. G., Alberta oil sands: Industrial procedures for extraction and some recent fundamental research. **1994**.

114. Hupka, J.; Miller, J.; Cortez, A., Importance of bitumen viscosity in the hot water processing of domestic tar sands. *Mining engineering* **1983,** 35, (12), 1635-1641.

115. Schramm, L.; Stasiuk, E.; Yarranton, H.; Maini, B.; Shelfantook, B., Temperature effects from the conditioning and flotation of bitumen from oil sands in terms of oil recovery and physical properties. *Journal of Canadian Petroleum Technology* **2003,** 42, (08).

116. Hupka, J.; Oblad, A. G.; Miller, J. D., Diluent-assisted hot-water processing of tar sands. **2007**.

117. Hupka, J.; Budzich, M.; Miller, J. *Preliminary examination of oil bonding at sand surfaces and its influence on hot water separation*; Utah Univ., Salt Lake City, UT (United States). Dept. of Fuels Engineering: 1991.

118. Farooq, U.; Asif, N.; Tweheyo, M. T.; Sjöblom, J.; Øye, G., Effect of Low-Saline Aqueous Solutions and pH on the Desorption of Crude Oil Fractions from Silica Surfaces. *Energy & Fuels* **2011,** 25, (5), 2058-2064.

119. Vakarelski, I. U.; Ishimura, K.; Higashitani, K., Adhesion between Silica Particle and Mica Surfaces in Water and Electrolyte Solutions. *Journal of Colloid and Interface Science* **2000,** 227, (1), 111-118.

120. Tabor, R. F.; Grieser, F.; Dagastine, R. R.; Chan, D. Y. C., Measurement and analysis of forces in bubble and droplet systems using AFM. *Journal of Colloid and Interface Science* **2012,** 371, (1), 1-14.

121.   Ren, S.; Dang-Vu, T.; Zhao, H.; Long, J.; Xu, Z.; Masliyah, J., Effect of weathering on surface characteristics of solids and bitumen from oil sands. *Energy & Fuels* **2008,** 23, (1), 334-341.

122.   Hogshead, C. G.; Manias, E.; Williams, P.; Lupinsky, A.; Painter, P., Studies of bitumen− silica and oil− silica interactions in ionic liquids. *Energy & Fuels* **2010,** 25, (1), 293-299.

123.   Júnior, J. A. A.; Baldo, J. B., The behavior of zeta potential of silica suspensions. *New Journal of Glass and Ceramics* **2014,** 4, (02), 29.

124.   Jacobs, F.; Filby, R., Solvent extraction of oil-sand components for determination of trace elements by neutron activation analysis. *Analytical Chemistry* **1983,** 55, (1), 74-77.

125.   Strausz, O. P.; Lown, E. M., *The chemistry of Alberta oil sands, bitumens and heavy oils*. Alberta Energy Research Institute Calgary, Alberta, Canada: 2003.

126.   Bensebaa, F.; Kotlyar, L. S.; Sparks, B. D.; Chung, K. H., Organic coated solids in Athabasca bitumen: Characterization and process implications. *The Canadian Journal of Chemical Engineering* **2000,** 78, (4), 610-616.

127.   Kotlyar, L.; Sparks, B.; Woods, J.; Raymond, S.; Le Page, Y.; Shelfantook, W., Distribution and types of solids associated with bitumen. *Petroleum science and technology* **1998,** 16, (1-2), 1-19.

128.   Sparks, B.; Kotlyar, L.; O'Carroll, J.; Chung, K., Athabasca oil sands: effect of organic coated solids on bitumen recovery and quality. *Journal of Petroleum Science and Engineering* **2003,** 39, (3-4), 417-430.

129.   Zhao, S.; Kotlyar, L. S.; Sparks, B. D.; Woods, J. R.; Gao, J.; Chung, K. H., Solids contents, properties and molecular structures of asphaltenes from different oilsands. *Fuel* **2001,** 80, (13), 1907-1914.

130.   Rosen, M. J.; Kunjappu, J. T., *Surfactants and interfacial phenomena*. John Wiley & Sons: 2012.

131.   Dean, J. A., *Lange's handbook of chemistry*. New york; London: McGraw-Hill, Inc.: 1999.

132.   Crundwell, F., The mechanism of dissolution of minerals in acidic and alkaline solutions: Part V surface charge and zeta potential. *Hydrometallurgy* **2016,** 161, 174-184.

133.   Crundwell, F., The mechanism of dissolution of minerals in acidic and alkaline solutions: Part II Application of a new theory to silicates, aluminosilicates and quartz. *Hydrometallurgy* **2014,** 149, 265-275.

134.   Takahashi, R.; Sato, S.; Sodesawa, T.; Kawakita, M.; Ogura, K., High surface-area silica with controlled pore size prepared from nanocomposite of silica and citric acid. *The Journal of Physical Chemistry B* **2000,** 104, (51), 12184-12191.

135.   Wang, L.; Tomura, S.; Ohashi, F.; Maeda, M.; Suzuki, M.; Inukai, K., Synthesis of single silica nanotubes in thepresence of citric acid. *Journal of Materials Chemistry* **2001,** 11, (5), 1465-1468.

136.   Liu, J.; Huang, W.; Xing, Y.; Li, R.; Dai, J., Preparation of durable superhydrophobic surface by sol–gel method with water glass and citric acid. *Journal of Sol-Gel Science and Technology* **2011,** 58, (1), 18-23.

137.   Bacon, F. R.; Raggon, F. C., Promotion of attack on glass and silica by citrate and other anions in neutral solution. *Journal of the American Ceramic Society* **1959,** 42, (4), 199-205.

138.   Bennett, P.; Melcer, M.; Siegel, D.; Hassett, J., The dissolution of quartz in dilute aqueous solutions of organic acids at 25 C. *Geochimica et Cosmochimica Acta* **1988,** 52, (6), 1521-1530.

139.   Herting, G.; Jiang, T.; Sjöstedt, C.; Wallinder, I. O., Release of Si from Silicon, a Ferrosilicon (FeSi) Alloy and a Synthetic Silicate Mineral in Simulated Biological Media. *PloS one* **2014,** 9, (9), e107668.

140.   Pokrovski, G. S.; Schott, J., Experimental study of the complexation of silicon and germanium with aqueous organic species: implications for germanium and silicon transport and Ge/Si ratio in natural waters. *Geochimica et Cosmochimica Acta* **1998,** 62, (21-22), 3413-3428.

141.   Xiang, B.; Truong, N. T. V.; Feng, L.; Bai, T.; Qi, C.; Liu, Q., Study of the Role of Sodium Citrate in Bitumen Liberation. *Energy & Fuels* **2019,** 33, (9), 8271-8278.

142.   Li, R.; Manica, R.; Lu, Y.; Xu, Z., Role of surfactants in spontaneous displacement of high viscosity oil droplets from solid surfaces in aqueous solutions. *Journal of Colloid and Interface Science* **2020**.

143.   Stasiuk, E.; Schramm, L., An absolute droplet pressure interfacial tensiometer and its application to bituminous systems of vanishing density contrast. *Colloid and Polymer Science* **2000,** 278, (12), 1172-1179.

144.   Drelich, J., *The role of wetting phenomena in the hot water process for bitumen recovery from tar sand*. University of Utah, Department of Metallurgical Engineering: 1993.

145.   De Gennes, P.-G., Wetting: statics and dynamics. *Reviews of modern physics* **1985,** 57, (3), 827.

146.   Ramiasa, M.; Ralston, J.; Fetzer, R.; Sedev, R., Nanoroughness impact on liquid–liquid displacement. *The Journal of Physical Chemistry C* **2012,** 116, (20), 10934-10943.

147.   Lin, F.; He, L.; Primkulov, B.; Xu, Z., Dewetting dynamics of a solid microsphere by emulsion drops. *The Journal of Physical Chemistry C* **2014,** 118, (25), 13552-13562.

148.   Li, R., A study of high viscosity oil displacement from a curved solid in aqueous solutions. **2019**.

149. Vega, M.; Gouttiere, C.; Seveno, D.; Blake, T.; Voue, M.; De Coninck, J.; Clarke, A., Experimental investigation of the link between static and dynamic wetting by forced wetting of nylon filament. *Langmuir* **2007,** 23, (21), 10628-10634.

150. Blake, T.; De Coninck, J., The influence of solid–liquid interactions on dynamic wetting. *Advances in colloid and interface science* **2002,** 96, (1-3), 21-36.

151. Chen, Q.; Liu, Q., Bitumen Coating on Oil Sands Clay Minerals: A Review. *Energy & Fuels* **2019,** 33, (7), 5933-5943.

152. Kumar, N.; Andersson, M. P.; Van den Ende, D.; Mugele, F.; Sîretanu, I., Probing the surface charge on the basal planes of kaolinite particles with high-resolution atomic force microscopy. *Langmuir* **2017,** 33, (50), 14226-14237.

153. Wang, Y.-H.; Siu, W.-K., Structure characteristics and mechanical properties of kaolinite soils. I. Surface charges and structural characterizations. *Canadian Geotechnical Journal* **2006,** 43, (6), 587-600.

154. Rodahl, M.; Höök, F.; Fredriksson, C.; Keller, C. A.; Krozer, A.; Brzezinski, P.; Voinova, M.; Kasemo, B., Simultaneous frequency and dissipation factor QCM measurements of biomolecular adsorption and cell adhesion. *Faraday discussions* **1997,** 107, 229-246.

155. Medina, S. C.; Farinha, A. S.; Emwas, A.-H.; Tabatabai, A.; Leiknes, T., A fundamental study of adsorption kinetics of surfactants onto metal oxides using quartz

crystal microbalance with dissipation (QCM-D). *Colloids and Surfaces A: Physicochemical and Engineering Aspects* **2020,** 586, 124237.

156.   Wang, S.; Segin, N.; Wang, K.; Masliyah, J. H.; Xu, Z., Wettability control mechanism of highly contaminated hydrophilic silica/alumina surfaces by ethyl cellulose. *The Journal of Physical Chemistry C* **2011,** 115, (21), 10576-10587.

157.   Leese, H.; Bhurtun, V.; Lee, K. P.; Mattia, D., Wetting behaviour of hydrophilic and hydrophobic nanostructured porous anodic alumina. *Colloids and Surfaces A: Physicochemical and Engineering Aspects* **2013,** 420, 53-58.

158.   Eita, M., In situ study of the adsorption of humic acid on the surface of aluminium oxide by QCM-D reveals novel features. *Soft Matter* **2011,** 7, (2), 709-715.

159.   Yan, M.; Liu, C.; Wang, D.; Ni, J.; Cheng, J., Characterization of adsorption of humic acid onto alumina using quartz crystal microbalance with dissipation. *Langmuir* **2011,** 27, (16), 9860-9865.

160.   Huang, C.-P.; Stumm, W., Specific adsorption of cations on hydrous γ-Al2O3. *Journal of Colloid and Interface Science* **1973,** 43, (2), 409-420.

161.   de Lint, W. S.; Benes, N. E.; Lyklema, J.; Bouwmeester, H. J.; van der Linde, A. J.; Wessling, M., Ion adsorption parameters determined from zeta potential and titration data for a γ-alumina nanofiltration membrane. *Langmuir* **2003,** 19, (14), 5861-5868.

162.   Coreño-Alonso, J.; Coreño-Alonso, O.; Martínez-Rosales, J. M., Apatite formation on alumina: the role of the initial adsorption of calcium and phosphate ions. *Ceramics International* **2014,** 40, (3), 4909-4915.

163.   Havre, T. E., Near-IR spectroscopy as a method for studying the formation of calcium naphthenate. *Colloid and Polymer Science* **2004,** 282, (3), 270-279.

164.   Hiemstra, T.; Yong, H.; Van Riemsdijk, W. H., Interfacial charging phenomena of aluminum (hydr) oxides. *Langmuir* **1999,** 15, (18), 5942-5955.

165.   Singh, B. P.; Menchavez, R.; Takai, C.; Fuji, M.; Takahashi, M., Stability of dispersions of colloidal alumina particles in aqueous suspensions. *Journal of colloid and interface science* **2005,** 291, (1), 181-186.

166.   Wu, C.; Wang, L.; Harbottle, D.; Masliyah, J.; Xu, Z., Studying bubble–particle interactions by zeta potential distribution analysis. *Journal of colloid and interface science* **2015,** 449, 399-408.

167.   Megias-Alguacil, D.; Tervoort, E.; Cattin, C.; Gauckler, L. J., Contact angle and adsorption behavior of carboxylic acids on α-Al2O3 surfaces. *Journal of colloid and interface science* **2011,** 353, (2), 512-518.

168.   Hidber, P. C.; Graule, T. J.; Gauckler, L. J., Influence of the dispersant structure on properties of electrostatically stabilized aqueous alumina suspensions. *Journal of the European Ceramic Society* **1997,** 17, (2-3), 239-249.

169.   Desset-Brèthes, S.; Cabane, B.; Spalla, O., Competition between ligands for Al2O3 in aqueous solution. *The Journal of Physical Chemistry A* **2012,** 116, (25), 6511-6518.

170.   Hidber, P. C.; Graule, T. J.; Gauckler, L. J., Citric acid—a dispersant for aqueous alumina suspensions. *Journal of the American Ceramic Society* **1996,** 79, (7), 1857-1867.

171.   Rice, G.; Barber, A.; O'Connor, A.; Stevens, G.; Kentish, S., A theoretical and experimental analysis of calcium speciation and precipitation in dairy ultrafiltration permeate. *International dairy journal* **2010,** 20, (10), 694-706.

172.   Bulmer, J.; Starr, J., Syncrude analytical methods for oil sand and bitumen processing. *AOSTRA, Edmonton* **1979**.

Appendix A：Synergetic effect of Sodium Citrate and Sodium Hydroxide on Oil Sands Recovery

A.1 Materials and Methods

A.1.1 Materials

Process water and oil sands ores were supplied by Syncrude Canada Ltd. Citric acid trisodium salt (99.8% purity) and sodium hydroxide solution (1 N) were purchased from Fisher Scientific. Toluene (99.8% purity) and ethanol (>99% purity) were purchased from Sigma Aldrich. Milli-Q water with a resistivity of 18.2 MΩ cm^{-1} was used throughout this study.

A.1.2 Bitumen extraction experiments

A modified Denver cell was used for the bitumen extraction experiment. The thermal water bath connected with the Denver cell was preheated to 50°C and kept constant during the entire experiments. Sample solutions were prepared by adding different amounts of sodium hydroxide (NaOH) and Na$_3$Cit into 250ml of process water and heated to 80°C. Then, mixing 500g of smashed oil sands ore with heated process water and agitated at 600 rpm with an airflow rate at 150 ml/min for 10 mins (slurry conditioning). After conditioning, turned off the air supply and introduced 800 ml of heated process water (50°C) into the cell. Agitation was controlled at 600 rpm for 10 mins, and the primary froth was collected

with a thimble during this 10 mins. Later, the agitation speed was increased to 800 rpm and the airflow rate was controlled at 50 ml/min for 5 mins, which is referred to secondary flotation and secondary froth was collected after this process. All of the collected froth from primary separation and secondary flotation were weighed with the thimbles and sent for Dean-stark analysis.[172]

A.1.3 Dean-stark analysis

Prior to the Dean-stark analysis, 200 ml of toluene was filled into the distillation flask. The collected froth and thimbles were placed in the flask. Heated the flask to 200°C and last for 3 hours, until the toluene dripping from the thimble became colorless, indicated that all the bitumen from the collected froth was dissolved into toluene and water contained in oil sands already evaporated and condensed in the water trap. After the apparatus cool down to room temperature, 5 ml of the bitumen-toluene mixture was evenly spread on a filter paper with known mass. This filter paper was subsequently dried in a fume hood to evaporate toluene for 1 day, and weighed to calculate the mass of bitumen. Thimbles with remained solid were dried for 3 days in a fume hood for solid weight measurement.

A.1.4 Oil sands ore composition measurements

Replace the bitumen froth by 50 g oil sand ore, the composition of the oil sands ore AS and AT were measured by Dean-Stark analysis described above. Meanwhile, the fines contained in solids were analyzed. Cold solvent wash method was used instead of Dean-Stark to remove the bitumen and water content in oil sands. The solvent was prepared with ethanol and toluene (24 Vol % and 76 Vol %) and mixed with oil sands to wash off the

bitumen and water. Then, the solids from the solvent were separated by centrifuge, which were further dried in the fume hood for one day. Dried solids were disaggregated and pour into 2000 micron sieve to remove the rocks. The size distribution of the solids was measured by the Mastersizer 2000 laser particle size analyzer to determine the fines content.

A.2 Results and discussion

Oil sands ore and process water were supplied by Syncrude Canada Ltd. The composition of the ore (AT and AS) for bitumen extraction is shown in Table A.1. The ore AS and AT are considered as the low-grade ore (<10%) with high fine content (> 20%).

Table A.1. Composition of oil sands ore used for Bitumen extraction experiments

|	Ore Composition (wt. %)			
	Bitumen	Water	Solid	Fine(wt.% of solid)
AS	9.3%	84.1%	6.5%	39.6%
AT	9.2%	83.1%	7.7%	30.2%

The total chemical dosage for each extraction test is ranging from 0% to 0.05%. The calculation method of bitumen recovery is listed below.

$$Bitumen\ recovery = \frac{Weight\ of\ bitumen\ from\ froth(g) \times 100\%}{Weight\ of\ oil\ sands\ used\ for\ extraction(g) \times Ore\ grade} \quad (A.1)$$

$$Total\ recovery = Primary\ Recovery + Secondary\ Recovery \quad (A.2)$$

Results were summarized in Figure A.1. Without chemical addition, the lowest total recovery was found at 40.2% and 27.9% for AS and AT, respectively, which is reasonable for poor processing ore. The addition of chemical aids largely improved processability. Comparing the best performance with the lowest recovery, there were 38% and 35%

increases on AS and AT. Moreover, it is worth to be mentioned that the combination of Na$_3$Cit and NaOH conducted the highest recovery at each test compare to the using Na$_3$Cit and NaOH separately. Take ore AS as an example, the combined addition of Na$_3$Cit (0.005 wt. %) and NaOH (0.025 wt. %) at a total dosage 0.03 wt.%, which generated a total recovery at 69.2%. This value is much higher than applying Na$_3$Cit (0.03 wt. %) and NaOH (0.03 wt. %) separately, which are 59.7% and 60.9%. It confirmed the synergetic effect of NaOH and Na$_3$Cit in bitumen extraction. The details of the bitumen recovery results are listed in Table A2 and Table A3.
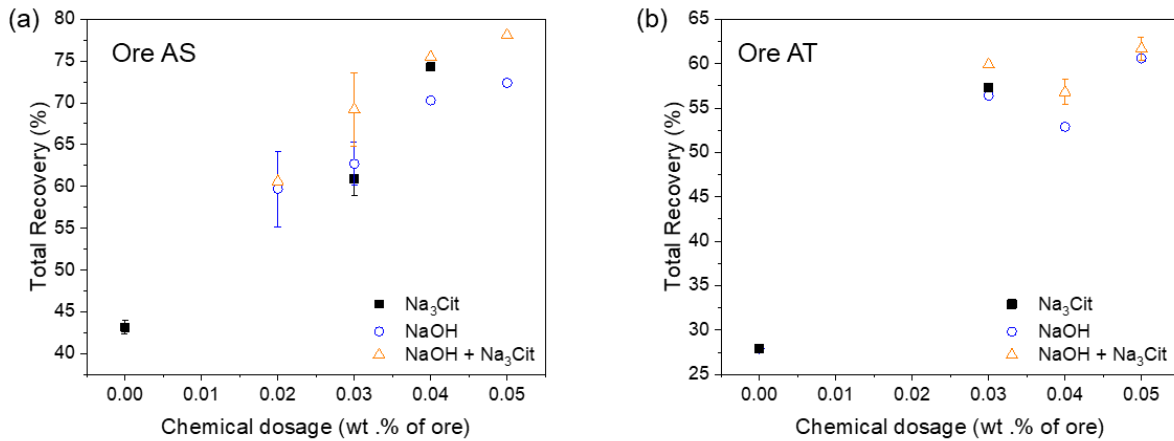
Figure A.1. Bitumen recovery of ore AS and AT as a function of chemical aids dosage (a) ore AS, (b) ore AT.

Table A.2. Experimental details of ore AS extraction.

Chemical dosage				
AS	wt. %	wt. %	wt. %	Total recovery
Wt (g)	Caustic	Sodium citrate	Total	

500	0	0	0	43.2%
500	0.02	0	0.02	56.5%
500	0.03	0	0.03	59.7%
500	0.04	0	0.04	70.3%
500	0.05	0	0.05	72.4%
500	0	0.03	0.03	60.9%
500	0	0.04	0.04	74.3%
500	0.015	0.005	0.02	60.6%
500	0.025	0.005	0.03	69.2%
500	0.03	0.01	0.04	75.5%
500	0.04	0.01	0.05	78.1%

Table A.3. Experimental details of ore AT extraction.

Chemical dosage				
AT	wt. %	wt. %	wt. %	Total
Wt (g)	Caustic	Sodium citrate	Total	recovery
500	0	0	0	27.93%
500	0.03	0	0.03	56.40%
500	0.4	0	0.03	52.90%
500	0.5	0	0.03	60.60%
Test 2				
500	0	0.03	0.03	57.3%
Test 3				
500	0.025	0.005	0.03	59.9%
500	0.03	0.01	0.04	56.8%
500	0.04	0.01	0.05	61.7%